

# NATIONAL AIR INTELLIGENCE CENTER



COMPILED OF SATELLITE NAVIGATION SYSTEMS  
(Selected Chapters)



DTIC QUALITY INSPECTED 5

Approved for public release:  
distribution unlimited

19951108 001

Accesion For	
NTIS	CRA&I <input checked="" type="checkbox"/>
DTIC	TAB <input type="checkbox"/>
Unannounced <input type="checkbox"/>	
Justification _____	
By _____	
Distribution / _____	
Availability Codes	
Dist	Avail and / or Special
A-1	

**HUMAN TRANSLATION**

NAIC-ID(RS)T-0326-95 17 October 1995

MICROFICHE NR: 95C000649

COMPILED OF SATELLITE NAVIGATION SYSTEMS  
(Selected Chapters)

English pages: 190

Source: Astronautics, Vol. 1, Nr. 3, 1994; pp. I-III;  
1-26; 73-152.

Country of origin: China

Translated by: Leo Kanner Associates  
F33657-88-D-2188

Requester: NAIC/TASS/Scott Feairheller

Approved for public release: distribution unlimited.

THIS TRANSLATION IS A RENDITION OF THE ORIGINAL  
FOREIGN TEXT WITHOUT ANY ANALYTICAL OR EDITO-  
RIAL COMMENT STATEMENTS OR THEORIES ADVO-  
CATED OR IMPLIED ARE THOSE OF THE SOURCE AND  
DO NOT NECESSARILY REFLECT THE POSITION OR  
OPINION OF THE NATIONAL AIR INTELLIGENCE CENTER.

PREPARED BY:

TRANSLATION SERVICES  
NATIONAL AIR INTELLIGENCE CENTER  
WPAFB, OHIO

**GRAPHICS DISCLAIMER**

**All figures, graphics, tables, equations, etc. merged into this  
translation were extracted from the best quality copy available.**

## CIVIL SATELLITE NAVIGATION SYSTEMS

Translated by Wang Jianping, and edited by Wang Weilian

ABSTRACT: The military satellite navigation systems GPS and GLONASS show that satellite navigation systems have vast superiority over the traditional land-based systems. Although these satellite systems will undoubtedly replace other systems, yet these systems are unable to be transferred to civilian use without any barriers. Civilian requirements are often different from military use since civilian management and technical details known publicly should be required. These requirements lead to considerations of many military authorities before the approval of the establishment of a civil satellite navigation system. In particular, these considerations include how to carry out the international civilian administration, and several schemes proposed some years ago are undergoing gradual selection. However, in another aspect, the actual experiments have begun to prove that military systems can be applied to some civilian use. This article briefly presents some major proposals on civilian systems.

## I. Foreword

Approximately 80% of the costs of GPS (possibly also including GLONASS) are used in military purposes. There are many requirements in military systems: antijamming, counter-counter electronic measures, and active operations, among others. However, there are no such requirements on civilian systems. Perhaps a civilian system is not required to be designed according to such strict accuracy indicators. This is not to denigrate civilian systems as the civilian systems are an excellent proof of high-tech applications. Unfortunately, however, an overall impression given to observers is that a civilian navigation system is very expensive. Although they have undoubtedly technical superiorities, yet conventional civilian use is unable to be considered. The article aims at presenting the superiorities of satellite navigation systems, and explains this feasibility by referring to some proposed system and other systems under practical applications.

## II. Reasons for Adopting Satellite Navigation Systems

Designers of radio navigation systems consistently have struggled between two contradictory requirements, as between accuracy and acting distance. Table 1 lists the radio frequencies of the main present-day systems with nearly accurate corresponding data among radio frequencies, distances, and accuracy. Generally speaking, very high frequencies can be applied to obtain very high accuracy, but the acting distance is

TABLE 1. Comparison of Navigation Systems

1系统	距离(公里) 2	精度(米) 3	频率(兆赫) 4
奥米伽 (Omega)	15,000	2000~1,000m	.0102
劳兰-C (Loran-C)	1,500	200~100	.100
台卡 (Decca)	350	50~200	.085
脉冲/8 (Pulse / 8)	800	15~50	.100
道兰 (Toran)	400	50~250	1.4~1.8
劳拉克 (Lorac)	400	50~250	1.6~1.8
雷迪斯特 N (Raydist N)	400	50~250	1.6~2.4
雷迪斯特 DRS (Raydist DRS)	300	25~75	1.6~4.0
海班-菲克斯 (Hyper-Fix)	600	5~30	1.8~3.0
海德罗特拉克 (Hydrotrac)	400	10~50	1.6~2.4
南船星座 (Argo)	300	10~50	1.6~1.8
斯波特 (Spot)	500	5~25	1.6~2.4(s)
吉奥劳克 (Geoloc)	500	5~25	1.6~2.4(s)
三叉戟 (Trident)	50	5~20	220
子午仪 (Transit)	15,000	50	150 / 400
马克希兰 (Maxiran)	150	10~30	420~450
西勒迪斯 (Syledis)	150	5~20	420~450(s)
阿蒂米斯 (Artemis)	30	2~25	1,000
全球定位系统 (GPS)	15,000	15~50	1,500
小型测距仪 (Miniranger)	50	4~12	5,000
米克罗菲克斯 (Micro-Fix)	80	3~10	5,000
特里斯邦德 (Trisponder)	80	5~15	10,000
微波测距仪 (Telluroneter)	20	1~3	10,000
经纬仪 (Theodolite)	5	1~5	(flight)

KEY: 1 - system 2 - distance (km) 3 - accuracy (m)  
4 - frequency (MHz)

very short, but low frequencies are used to obtain low precision at remote distances. There is not a single system without a satellite that can simultaneously obtain high accuracy and remote distances. The reason is very simple. As a navigator, one should know his position. Therefore, only some instruments can be used to determine how far and in what direction from a known point or points. In radio systems, this is achieved by ranging of some type (or even through orientation determination). In these surveys, time is used as the analog quantity. Time can be measured very accurately, so it is easy to have the ranging accuracy corresponding to several millimeters. However, the difficulty is to convert into distance. Since radio waves are likely to be jammed by various kind of propagation, thus noise, time lags, and so on are induced. The final result is that there is very vague corresponding relationship between time and distance. The ideal state is a radio wave without any jamming, however, this is impossible at any frequencies. Since the extent of jamming rapidly decreases with rise in frequency, therefore applications requiring very high accuracy should adopt very high frequencies. Thus, the line-of-sight distance is also restricted. This factor is not very significant for an aircraft, although it should be remembered that even at the altitudes of modern jet aircraft, the line-of-sight distance is only about 200 miles. This corresponds to a flight time of only 20min. In the case of steamships, they often navigate on the seas for more than 30 to 50 miles from the coast. As a result, steamships have to

use the low frequency that can provide adequate distance of ground wave propagation. With the adoption of sky waves, these problems should be considered in interference due to rainfall and electrostatic charges, as well as noise from thunder and lightning. Besides, the only way of obtaining adequate accuracy in using these frequencies is to adopt phase surveying method. To solve the problem of inherent vagueness in this survey method, the only approach that can be adopted is to have noise and sky waves to determine the accuracy, but not the phase surveying itself. The only radio surveying system without a satellite and without distance limitations is the OMEGA long-distance navigation system, which operates at frequencies of nearly 12kHz. However, this can give only an accuracy of several miles. The above-mentioned situations compelled previous researchers to develop some quite different radio navigation systems for ships and aircraft. But the results are only a repetition and waste.

The fundamental laws of physics will not change because of different designs. Before satellites came into the picture, nothing could be done with this problem. However, once satellites appeared, most problems have been abruptly solved. From a single satellite operating in earth orbit at not too-low altitudes, the emitted radio waves can very easily cover most areas over half a globe, and such propagation of radio waves requires only such frequencies in the line of sight. All problems of sky waves, electrostatic charges, thunder, lightning, and noises are solved. Other infrequent problems such as

capturing, operating and the maintenance problem in remote sites of transmitters are also abruptly solved. Technically speaking, satellite communication is without any competitor. However, there are some disputes. Comparing the traditional land-based systems and the satellite navigation systems, only the repairing of a land-based transmitter is somewhat easier than repairing the satellite. But there are no other technical superiorities. At this point we must mention that several Transit instruments onboard navigation satellites have operated successfully in orbits for two decades without any maintenance or repair.

The Transit instruments onboard satellite navigation systems represent the first satellite navigation system. The limitation is only that one positioning can be made only after 2h. Notwithstanding this limitation, the system has become a standard shipboard navigation system, not only used in high-seas navigation, but also in navigation on entering a port.

### III. Definitions

Strict technical terms have to be used to describe radio navigation systems. This is related to life safety in navigation as acknowledged internationally. This is the greatest possible protection in other related systems. When radio navigation communication is lost onboard a ship or an aircraft so that passengers are unable to talk with family members over the phone, this is only inconvenient, but not a life-or-death problem such as the loss of a main navigation system, possibly resulting in

the ship being grounded or airliners crashing into mountains.

There have been such incidents. This line of philosophy leads to very precise technical terms.

Generally speaking, radio-determination is defined as follows in the International Communication Laws and Regulations:

Use is made of the properties of radio wave propagation to determine the position, speed, and or other features of an object, or to capture the related information of these parameters.

Radio-navigation is the radio navigation used for navigational purposes, including forewarning of approaching barriers.

Radiolocation is defined as the radio determination, other than radio navigation.

Therefore, there are two entirely different patterns, and they have different priorities. Radio navigation has its specific exclusive radio frequency bands, which are not allowed to be used in other traffic. Therefore, freedom from jamming can be guaranteed. However, radiolocation does not have such exclusive frequencies, therefore freedom from jamming is not guaranteed. Which category a system is in depends on the position in the radio-frequency spectrum and the status of users that the system serves.

What is navigation? In the broad sense, this includes the motion of a ship, or other means of transportation moving from a location to another location, and the continuous position

derivation as the vehicle proceeds. Conversely, location is not related to motion and continuity, and it is also not required to accomplish the positioning in the transportation vehicle.

We have to remember that there are entirely different designs, operations, and implementations of these two applied systems.

#### IV. Civilian Usage of Military Systems

Military systems obviously can be provided for free use by civilian users; of course, besides the civilian users have to pay finally in some form of taxation. Thus, only with the approval of using military systems, why cannot the cost of buying a receiver for use with these systems be justified? In the current situations, there are some military navigation systems, namely the LORAN-C series, Transit Instrument Series, as well as the first stage satellites of the early GPS versions. All the present-day civilian systems originated from military systems. This is true.

The only problem is that the civilian users are unable to control these military systems. If these systems suspend normal operations due to certain considerations, civilian users will be helpless. Besides, very few civilian users can obtain the information relating to change of plans, malfunctioning, and unscheduled suspension of broadcasting. Of course, sometimes some nonconfidential information is broadcast. But a military department will not make public within a few minutes that the

problems of their major systems arise. Concerning the DECCA navigation system, users often said that, although the system has its problems, still the only superiority of the system for commercial use is that users know the source when it is not operating.

Even at present, military departments repeatedly mention to the civilian users of GPS that any losses are their own responsibility, and no guarantee can be made. In September the entire GPS system was suspended for civilian users for as long as 2 weeks. This incurred much damage to offshore prospecting. Although this incident was made public in advance, yet users were warned that similar incidents in the future may not be prewarned.

With regard to another point, if without partial control on these systems by nations other than the United States and the Soviet Union, legislation cannot be passed on to GPS and GLONASS. According to law, all aircraft and ships should carry some navigation equipment. However, for these nations that are signatories to these laws, actually they also have these obligatory navigation equipment operated by themselves. Therefore, the responsibility of correct operation can be accepted. To a system that is under absolute control by a foreign military authority, of course they cannot operate in this way.

Therefore there are some other technical problems. As we heard in the case for safety protection, the system users of GPS and GLONASS can only have the accuracy not better than 100m.

Although such accuracy is adaptable to conventional navigation, but the accuracy is not sufficient for prospecting, hydrological surveying, and landing approaches by aircraft. Some researchers propose using the local correction stations (difference corrections) to restore the accuracy. This concept raises hope among some of us, but this is not likely to be carried out, because United States military circles are currently also concerned with the possibility of accuracy revision. They are also attempting to put such civilian systems under their control, even to put correction stations outside the United States and not under United States management also under their control.

These suspicious points made people unable to rely on these navigation systems. All this is because these systems basically are not operated for civilian users.

#### V. Costs

It is estimated that approximately 110 million U.S. dollars should be spent for Block-2 satellites. Therefore, a total of 1.98 billion U.S. dollars should be spent for launching 18 such satellites. Up to the year 1992, it was estimated that the total system costs will be about 4 billion U.S. dollars when the system is still operating with expenditures including ground support, maintenance and repair, command and control. Each year the operating and management costs are about 120 million U.S. dollars. These figures are quite high. When compared with land-based systems, less than 100 million U.S. dollars can build an

entire LORAN-C system covering all of Europe, and management and operating expenditures each year are only 15 million U.S. dollars. These comparisons prevent the real discussion on using satellite navigation as a substitute for civilian land-based systems in the selection schemes.

However, let us look over another set of figures. The civilian navigation does not require an entire satellite, but only a very simple exclusive transponder. As estimated by the International Maritime Communications Satellite Organization, eight such transponders can cover 86 percent of the entire globe. The costs of these transponders, with the addition of partial expenditures for launching a standard geostationary satellite, the shared launch costs do not exceed 54 million U.S. dollars. By using four main earth stations for remote control and the entire monitoring network of the system, this will require additional 17 million U.S. dollars. Therefore, the total cost is about 71 million U.S. dollars. If the current communication technique standard equipment of the International Maritime Communications Satellite Organization is used as much as possible, it is estimated that the annual management and operational expenditures are 7 million U.S. dollars. Each year, 24 million dollars should be recovered for the satellite and maintenance cost of 13-year operating life in orbit. Therefore, only by requiring the cost of lower than a single Loran-C system, a civilian navigation satellite system covering the entire globe can be built.

There are perhaps two extreme cases. However, this can illustrate that the civilian satellite navigation system is not always expensive. The following facts further explain this point. At present, the only nonmilitary-used satellite navigation system, the STARFIX system, is used by the United States. The system provides an accuracy better than the accuracy required by navigation in the area of the entire United States and outside the United States. Although the number of users is less than 50, yet this is a case of commercial success.

## VI. System Designs

As a civilian system, cost is the factor to be considered at the outset. The best method of using the minimum number of satellites to obtain the most effective coverage is the use of geostationary orbits. Navigation requires more than one such satellite, but at the minimum, how many satellites are required?

A single satellite is not able to conduct navigation positioning. The only useful measurement is distance. As a result, one can generate a position line on the surface of the globe.

Two satellites can generate two such position lines. Although these lines can intersect at two locations, as shown in Fig. 1, but generally these locations are quite far apart. It is very easy to find out the correct one. The key to the problem is the distance determination. A user can transmit a timing signal through the satellite; however, this approach limits the number

of users and user equipment becomes complicated. In another approach, satellites can transmit their own timing signals, not

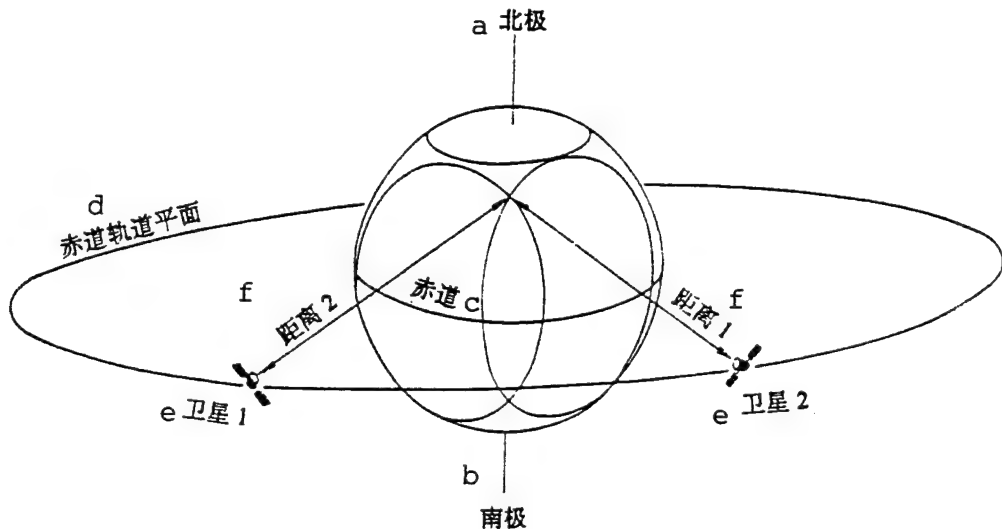


Fig. 1

KEY: a - north pole    b - south pole  
c - equator    d - equatorial orbital plane  
e - satellite    f - distance

requiring users to initiate the interrogation signals, but requiring users very precisely to know the timing datum used by the satellites. Therefore the only feasible method is to let a third satellite operate on the same time datum as that on both satellites, thus having the function of datum signals. However, if a user has a very stable timing datum in his receiver, such as the atomic clock standard, then the third satellite can [illegible] align the time with that of the third satellite. After the third satellite leaves the scene, by relying on the stability two satellites can be used to continuously and effectively operate.

As was mentioned in the above, three satellites can give

independent positioning. This positioning is obtained from two location lines. Any navigator understands this is not a very geometric solution, especially when these two location lines intersect at an acute angle.

Four satellites can solve this problem. One satellite is used as the timing datum and three other satellites can provide three location lines. The result is the formation of the classical positioning triangulation method.

From most navigation usage, other than when used as reserve information during malfunctioning, it is excessive to have more than four satellites. However, this approach is useful when used in very accurate prospecting operations.

In the satellite system, another factor requires to be considered. We should consider the three-dimensional problem, and solve the problem from two-dimensional graphs and charts. As mentioned above the location line is actually not a line, but a portion of the spherical surface. When the line intersects the earth's surface, then the location line is formed. The position of the earth's surface should be very accurate. Besides, if all these satellites operate in the same orbital plane, the effect is very poor. We should input the earth surface data. If we are not on the earth's surface, it is required to input the altitude from the earth's surface. To a steamship, it is not difficult to estimate the distance between the sea surface and the earth's center, but what is the distance of an airplane from the earth's center? In many areas, unless we can accurately know the

distance to the earth's center, otherwise the final positioning will not be very satisfactory. When the line of intersection with the earth's surface and the local north-south direction forms an angle of very small degrees, this problem becomes very serious. Then, any altitude error will generate great latitude errors. To the zone under the satellite (equatorial zone), this system almost cannot be used. This problem can be solved by adding another satellite on different orbital planes. This is the reason for merging the GPS/GLONASS into their system as proposed by the International Maritime Communications Satellite Organization.

If due to nontechnical reasons this merger proposal is not accepted, then another three or four satellites with large orbital elevation angles should be added. To this scheme, a Molniya type (12 hours) and a Tundra type (24 hours in the polar zone) large elliptical orbit satellites are the best. Then the system is very similar to the navigation satellite system of the European Space Agency (refer to the following passages).

## VII. Merger with Land-based Systems

Assuming that all are synchronized with the same time datum, a radio navigation does require that all signals are from the same type of transmitter. Satellite transmitters can very easily be matched with any type of ground transmitters. Many proposals expect to be carried out in this manner. One proposal is to install similar small GPS transmitters in areas requiring

enhancement of GPS accuracy. For example, for use in landing approach of aircraft the transmitter can emit similar signals (except for coding) as that of a GPS satellite. A conventional GPS receiver can receive this kind of signals without any modification. This is called the Pseudolites.

Another proposal is to directly use transmitters of Loran-C, Decca, or other navigation systems. By proper selection of these transmitters, accuracy can be enhanced by using the method of changing the geometric relationship; in addition, certain types of local control can be reestablished. Of course, this method gives rise to old problems, such as interference and sky waves, for the satellite system. Thus, the entire system can be used only in that the ground transmitters can function; however, this system has some attraction in areas that have been heavily invested in.

## VIII. Present-day Systems

The GPS and the GLONASS navigation systems are well known; they are all military systems. Only with civil administration, can both systems be considered for civilian use.

The Transit satellite systems have been used for many years. This is a reliable system with sufficient verification. However, the systems are unable to provide continuous positioning and also cannot be used by aircraft.

So is the case for the Tsicada system of the former Soviet Union.

The STARFIX navigation system of the John Chance Corporation in the United States is the only currently-operating civilian satellite navigation system.

### 1. STARFIX system

The system is operating in the Gulf of Mexico, mainly provided services for offshore prospecting requiring very high accuracy around the clock. The system requires at least three geostationary orbiting satellites. In practice, four satellites are used. The satellites are used only as transponders. That is, the satellites receive signals from earth stations and these signals are converted to another frequency, then to be transmitted. These signals do not require formatting, therefore the operation can be very simple. The system is very suitable for standard transponders designed for communications, and is also used in the STARFIX system to operate together with the conventional commercial uplink stations. Systems such as these can be built in any areas of the world. Only with three or four satellites operating at suitable positions as well as a suitable uplink station can a system be operated.

### 2. Operating method (refer to Fig. 2)

Four satellites in operation: the Milky Way-II satellite, (made by the Hughes Corporation) operating at  $286^{\circ}$ ; Western Union-IV satellite (Western Union Corporation) operating at  $261^{\circ}$ ; SPACENET-I satellite (of the GTE Corporation) operating at  $240^{\circ}$ ;

and the first replacement satellite for SYNCOM (of RCA Corporation) operating at 221°.

The uplink frequency is in the 6GHz band, and the downlink frequency is 4GHz. The Houston Main Control Station generates a

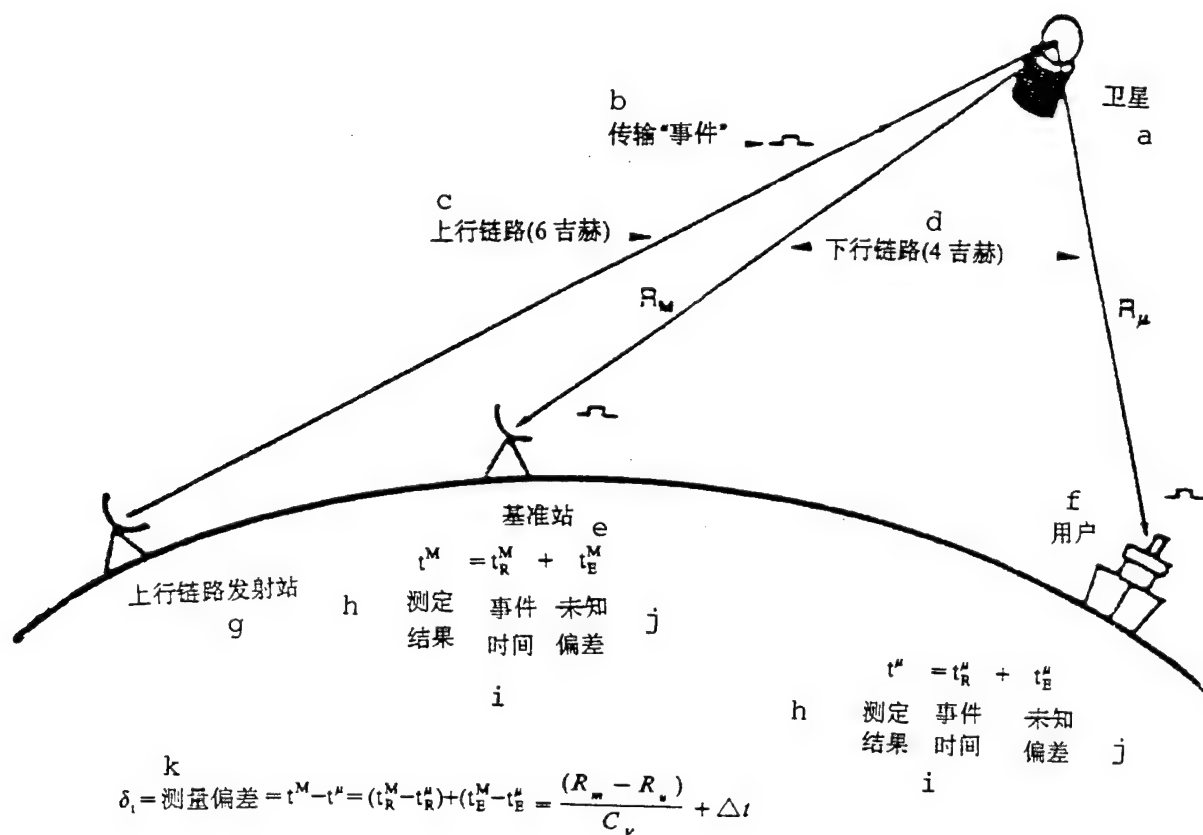


Fig. 2.  
 KEY: a - satellite b - transmission of events  
 c - uplink (6GHz) d - downlink (4GHz)  
 e - datum station f - user  
 g - transmitting station of uplink  
 h - determination results i - time of event  
 j - unknown deviation k - deviation of measurement

rectangular frequency expanded signal and transmits into the

uplink for relaying. Users and monitor control stations receive these signals, and relay the timing signal via the satellite to the Main control station, which superimposes the detected time-delay data on a data signal of the main transmission for users. At the same time, adjustment and timing are applied to maintain a fixed time delay. Users conduct all computations at their receivers and record all data for reanalysis. The key to the entire system is to maintain a constant time delay. Thus, the alignment by the Main Control Station can cause a delay of several seconds in each timing. Distributed throughout the United States, these monitoring control stations are quite small, unattended with almost complete automation. Since the system operates only with satellites in the geostationary orbital plane, the fundamental problem is the determination problem as mentioned above. However, to their service objects, this is not repetitive, because ships on the ocean can very accurately determine their distance from the earth's center.

Another advantage of this system is the simultaneous transmission of differential information for the GPS system.

### 3. Accuracy

As revealed from results analyzed from more than three years of records, the inherent accuracy is 2 or 3m. However, as revealed with the unique maritime inspection with the currently most accurate conventional system, the actual accuracy is maintained at about 5m. This is better than the positioning accuracy of

using GPS precise code.

#### 4. Equipment

With the simultaneous reception of signals from four geostationary orbiting satellites on a small ship, if the conventional parabolic antenna used for this reception is not employed, then a semistable platform is required to carry four small horn antennas as shown in Fig. 3. Each horn is permanently aimed at a satellite with constant orientation angle and elevation angle. The entire platform is gyroscopically driven, to be stabilized in one orientation. The bandwidth of the horn antenna is determined by the general situation of the ship's pitching and rolling. The signal gain should be limited to about 12dB, thus requiring a certain amount of satellite power (24dBW). However, the progress achieved in designing low-noise amplified antennas is gradually reducing such power requirements. Perhaps in the near future, directional antennas will not be required.

### IX. Proposed Systems

#### 1. GEOSTAR/LOCSTAR (Fig. 4)

The original GEOSTAR system was proposed in 1984 in the United States. However, a consortium under the direction of the European and French Space Research Centers is speeding up the development of the LOCSTAR system with similar technology.

This requires a cooperative system launched by users. The system does not require continuous positioning, and positioning

is not done in moving vehicles. Therefore the system is not a

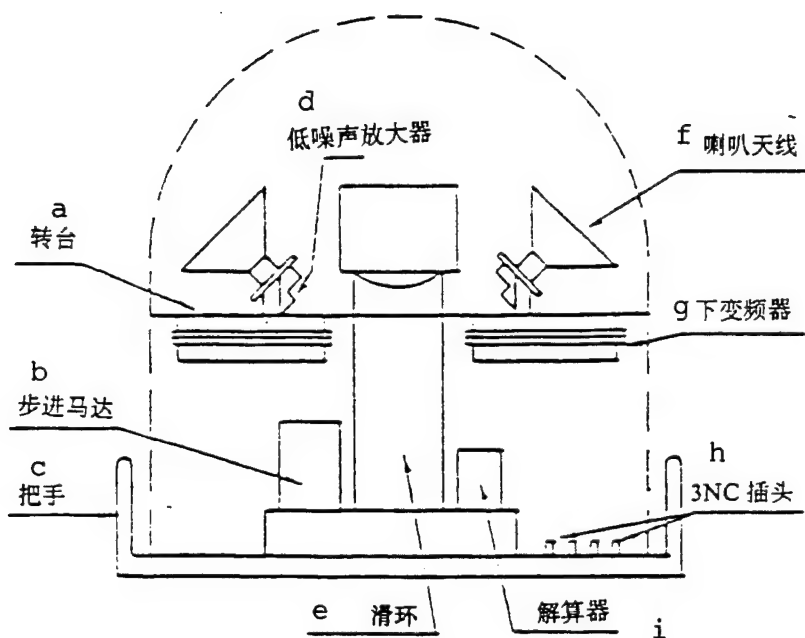


Fig. 3.

KEY: a - turntable    b - stepper motor  
c - handle    d - low-noise amplifier  
e - slip ring    f - horn antenna  
g - lowering-frequency variator  
h - plug    i - calculator

navigation system and so the operating frequency is not within the wavebands allocated to navigation.

### 1.1. Operational Method

The simplest form is to adopt two geostationary satellites, or dedicated satellites, or satellites installed with appropriate payload. Through a satellite, a main control station can continuously send signals supplemented with appropriate timing

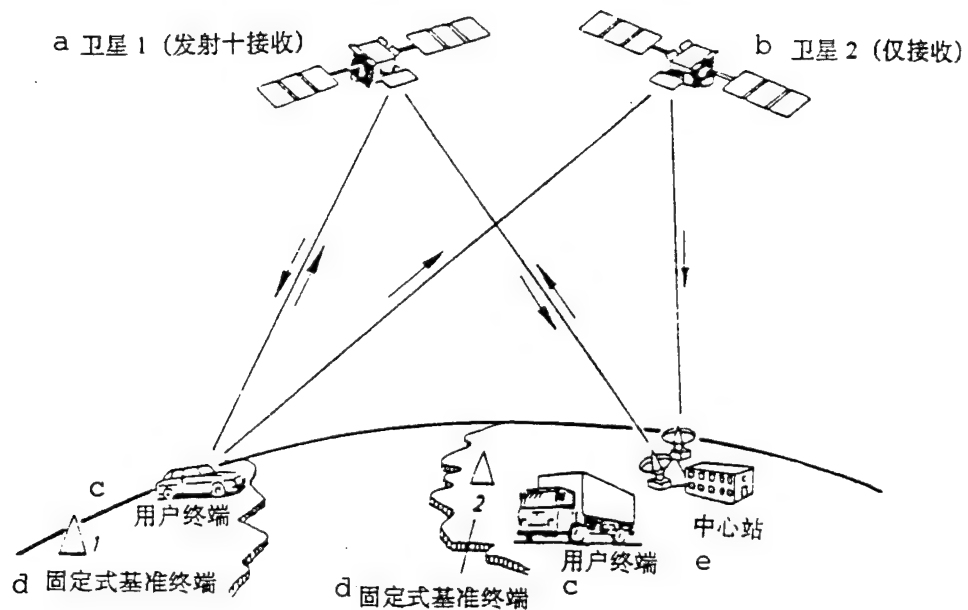


Fig. 4.

KEY: a - satellite 1 (transmission + receiving) b - satellite 2 (receiving only) c - user terminal d - fixed type datum terminal e - central station

marks. After a user's receiver receives these signals and employs them to control his response, a telegram message is transmitted for the timing signal and a discrimination symbol. Both satellites relay this signal to the main control station, which calculates the user's position with the conventional ranging location algorithm of the two stations. Thus, the user does not have to carry accurate timing equipment. The user's equipment can be quite simple; however, the equipment should have sufficient transmitting power capable of reaching both satellites. This is a constraint on the size.

If it is required, the user location can be sent back to him by employing the same circuitry. However, a primary application of this system is to let the fleet owner consistently track his mobile vehicles. Mainly, the office of these vehicles must know their location signals, but not these mobile vehicles. As to other messages, such as the type of cargo and the sending of new destination order to the drivers, these can also be relayed.

Such calculated locations are not required to be very accurate. If high accuracy is required, some serious obstacle should be overcome. For example, the user's distance from the earth's center is absolutely necessary as an input quantity. In the dual-satellite positioning method, the user is unable to obtain his altitude. When applying the STARFIX system, the altitude of maritime users may be easily obtained, but difficulties of obtaining the altitude for land users are much greater. It is even more difficult for aerial users. Only to obtain an approximate solution, it should be first required to have a preliminary height estimate. Then, more accurate position signals can be obtained, to re-input a better height data. Only then does this algorithm receive an acceptable accuracy. As claimed by the proposer of this system, this problem can be solved by only installing a digital altitude graph for the covering region at the main control station. However, in certain situations the risk of unstable positioning solution will crop up when determining position from altitude, and vice versa. An aircraft has relayed its altitude. Unless the aircraft is

positioned by using a radio altimeter, it only can obtain an altitude based on atmospheric pressure. Then the altitude relative to the earth's surface should be calculated from the datum plane of atmospheric pressure. Theoretically speaking, all this is feasible, but not suitable since sometimes great errors may appear. As these problems have very low data rates, this approach is not very likely to be adopted with aircraft.

### 1.2. Development Situation

Up to the present time (September 1989), the positioning capability has not been certified. As Loran-C has been used for motor vehicles, certification has been made on the relay data through satellite transponders

## II. Guidance Satellite System of the European Space Agency

This is a real navigation system proposed by the European Space Agency. Several years' development was conducted. Other proposals have been absorbed in the development process; however, in the original concept, the aerial portion is kept as simple as possible. All the complicated sectors are placed into the ground control station. Therefore, satellites act only as a simple transponder, without any timing or message format. They relay signals from the ground station, which increases the payload continuously as in the STARFIX system. Thus, dedicated satellites are not required, and transponders can be installed in a communications satellite.

## 2.1. Operational Method (Fig. 5)

Like the STARFIX system, some geostationary satellites are used. However, to solve the above-mentioned problem for a single orbital plane, some large elliptical orbiting satellites are also deployed. This scheme matches with the proposals of communications with high-latitude zones by launching such satellites. These satellites seem to have the feature of quietly (not moving) hovering in the sky for as long as 8h almost each time. These satellites can be designed or remain in high latitudes, therefore, communications with very large elevation angles are feasible as those of equatorial countries, thus

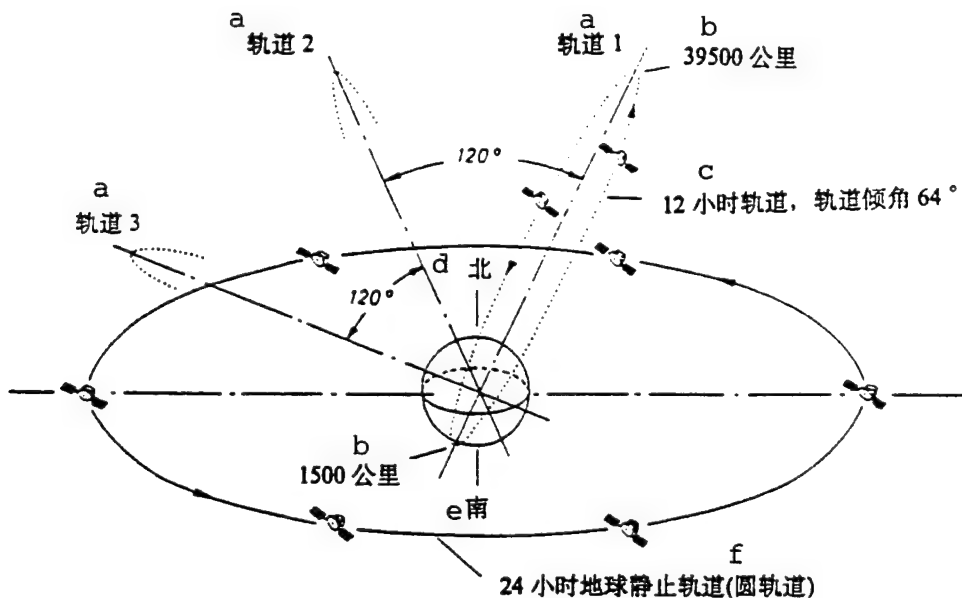


Fig. 5.  
KEY: a - orbit   b - km   c - 12-h orbit  
with  $64^{\circ}$  for dip angle at orbit  
d - north   e - south   f - 24-h geo-  
stationary orbit (circular orbit)

providing communication traffic for countries far from the equator in the southern and northern hemispheres. Of course, several satellites are required to provide the traffic volume as that for a single satellite over the equator. These satellites are distributed in certain phase positions in order to appear in the visible time of the 8-h period.

## 2.2. Present Status

Only when the European Space Agency member-countries concur to provide funds for this development scheme, can it be carried out. At present, efforts are being made in this direction. However, some proposals want to merge with the Inmarsat Organization plan (refer to the following passages).

## III. International Maritime Communications Satellites (Inmarsat)

As specified in the commercial license of the Inmarsat Organization, it consistently has the authority to provide a positioning service. However, until one or two years ago the organization made little of these services. With the appearance of GPS and a dispute over the interest and risk relationship between civilian and military use, the Inmarsat Organization gradually realized that the organization can function internationally as a provider of civil navigation services. Several research projects began to be planned along the related aspects. The present satellites deployed by the organization are not suitable for independent applications. However, with the

launching of the third-stage new satellites in the 1994-1995 period, sufficient reserve can provide such navigation services. This has not been considered as a commercial service (as the problem of not sharing an orbital plane still exists), but is still considered as a method of maintaining civilian control, but at the same time utilizing some capacity of GLONASS. Several years later, the final result may be a civilian-controlled satellite navigation system, while utilizing some features of military systems. When these systems are unable to be used, the fundamental function still can be maintained. As an international organization, Inmarsat has to consider these two satellite navigation systems, GPS and GLONASS. In the following passages, the acronym GPSG will represent these two systems.

### 3.1. Operational Method (Fig. 6)

Navigation equipment will be installed in many geostationary satellites (operating and standby International Maritime Communications Satellites) so that these satellites can simultaneously retransmit on the L-band signals that appear to be similar to GPS and GLONASS signals, with frequencies very close to the GPSG frequency band. Therefore, the conventional GPSG antenna can be used. A receiver only requires considering the signals transmitted by Inmarsat as another set of GPSG signals for corresponding processing. During processing, those signals with coding configuration that is the same as the real signals should be distinguished. The propagated data signals will be adjusted to some extent, in order to adopt the standard GPSG

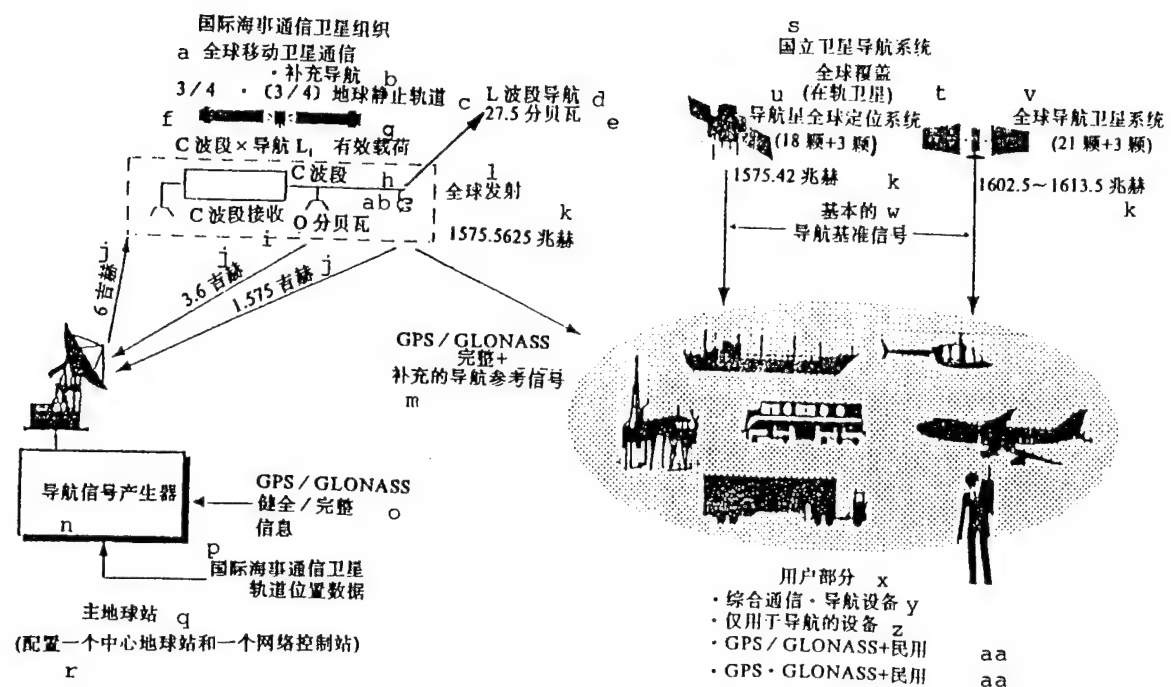


Fig. 6. Scheme of geostationary orbital system

KEY: a - global mobile satellite communication of the Inmarsat Communications Satellite Organization      b - supplementary navigation  
c - geostationary orbit      d - L-band navigation  
e - 27.5dBW      f - C-band x navigation L<sub>1</sub>      g - payload  
h - C-band      i - C-band reception      j - GHz      k - MHz  
l - global transmission      m - hole + supplementary navigation reference signals      n - navigation signal generator  
o - excellent signal/complete signal      p - data of orbital position for International Maritime Communications Satellite  
q - main ground station      r - deployment of a central earth station and a network control station      s - national satellite navigation system      t - global coverage (in-orbit satellite)  
u - global positioning system of navigation satellites (18 satellites + 3 satellites)      v - global navigation satellite system (21 satellites + 3 satellites)      w - fundamental signals of navigation datum      x - for the users      y - comprehensive navigation and communication equipment      z - equipment used only for navigation      aa - civilian      ab - 0dBW

algorithm with as little change as possible. Actually, a user

will obtain many additional GPSG satellites even though the primary users relying on the GPSG system will also improve the geographic positioning relationship relative to the GPS system. However, for primary civilian users relying on signals of the International Maritime Communications Satellite, the GPSG will solve the altitude problem. Even when the GPSG does not operate because of some reasons, the International Maritime Communications Systems will provide appropriate positioning capability for the most conventional navigation.

Other than the conventional data signals related directly to ranging, the signals of the International Maritime Communications Satellites also include the overall and differential data obtained from the ground monitoring stations, which were built and operated as a portion of the same organization.

This system obviously is developing toward the systems of the European Space Agency. Requiring only that several elliptical orbiting satellites be added, thus GPSG is not required to be an entirely independent application system. Those required to be added are possibly Molniya type satellites, or the 24-hour polar region type orbiting communications satellites. These satellites will be used to enhance the maritime communications capability of the International Maritime Communications Satellites.

### 3.2. Current Status

Many preliminary experiments were begun, including the signals similar to GPS as mentioned in the current transmission of the International Maritime Communications Satellites. Extensive international consultation is conducted to install navigation equipment in the third stage of the International Maritime Communications systems; details of engineering technology are under study. This scheme acquires more and more support internationally, therefore it appears that it will most likely be realized.

# PRINCIPLE, METHOD, AND ACCURACY ANALYSIS OF DUAL-SATELLITE POSITIONING

Yang Weilan

## I. Foreword

In the dual-satellite positioning system, two geostationary satellites over the equator with a certain distance between them are used as the datum. With radio-ranging signals, distances between a user and the two satellites are determined in order to locate the user's position. This is a new radio positioning system. The ground central station of this system emits ranging signals to the user at a certain time through these two satellites. The users receive and respond to this signal and transmit it back to the satellites. Based on the round-trip time of the signal thus measured, summation of distances from the central station to the satellites and from the satellites to the user can be calculated. Since the satellite positions are known, the distances between satellites and users can be calculated. If the user's altitude is known, then these two distance measuring data can be used to further determine longitudes and latitudes of the user's position. This is the fundamental principle of the dual satellite positioning system.

If these two distance data are used directly for positioning, the effect on positioning accuracy is relatively significant due to the satellite positioning errors, as well as the time delay errors for the signal passing through the ionosphere and the troposphere. In actual applications, the positioning method based on the difference between the two distances can be applied to reduce this effect as much as possible: if there is a datum station near the user with position accurately determined (200 to 300km), the station transmitter and the receiver can be used to simultaneously determine two different round-trip distances. By subtracting one round-trip distance from the other such that both distances are measured with the same satellite with respect to the user and the datum station, twice the difference of the distances to the satellite from the user and from the datum station can be obtained; one half is the difference between the distances. The difference between these two distances of the satellites can be obtained. User position can be calculated by using the difference between these two distances. Thus, the effect can be greatly reduced from the satellite positioning errors and the signal propagation errors in the ionospheric and troposphere. This is the advantage of the positioning method based on the difference between the two distances. The article presents this positioning calculation method, explains the geometric principle of the method, and analyzes the effect on positioning accuracy due to surveying error, user altitude error, and satellite positioning error.

## III. Positioning Method Based on Difference Between Two Distances and Its Geometric Principle

### 1. Positioning method

$\rho_j$  and  $\rho_{oj}$  indicate, respectively, the distances between the user and the datum station and the  $j$ -th satellite (refer to Fig. 1).  $\Delta\rho_j = \rho_j - \rho_{oj}$  : this difference between the distances is related to the user, datum station, and satellite positions. After obtaining the observation  $\Delta\rho_j^o$  of  $\Delta\rho_j$ , we can list the following two equations

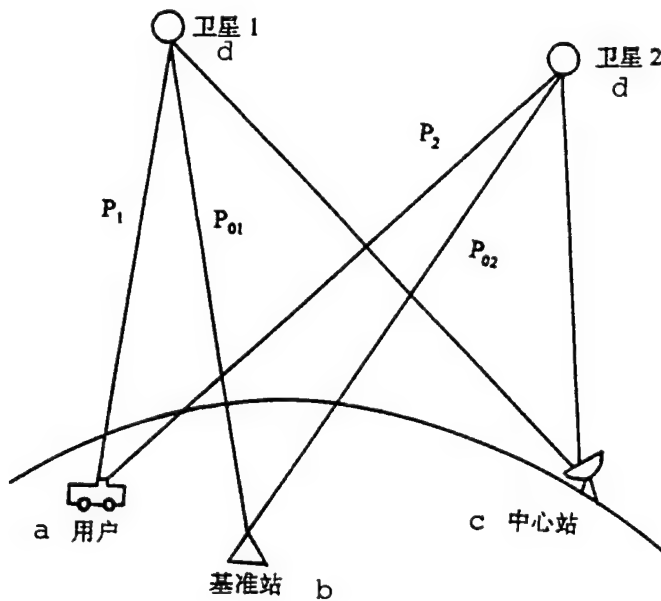


Fig. 1. Schematic Diagram of Dual-Satellite Positioning System

KEY: a - user b - datum station c - central station d - satellite

$$\Delta\rho_1 = \Delta\rho_1^o \quad (1)$$

$$\Delta\rho_2 = \Delta\rho_2^o \quad (2)$$

as the longitude  $\lambda$ , latitude  $\phi$  of the user's position and the

distance between the earth's center and user position (relative to altitude) are the unknowns, so there are three unknowns in the above-mentioned equations. if there is no altitude information, we cannot solve for longitude and latitude. If user altitude is known, then this is equivalent, for a given estimated value  $R^0$ , to user's distance  $R$  from the earth's center, we then derive the third equation:

$$R=R^0 \quad (3)$$

Altogether, there are three equations with three unknowns. With little difficulty, we can see that this set of equations can be separated. In other words,  $R$  is completely determined by  $R^0$ . Substitute Eq. (3) in Eqs. (1) and (2), and then we convert the equation sets into two equations containing two unknowns,  $\lambda$  and  $\phi$ . Generally speaking, these two-element nonlinear algebraic equations can have two sets of solutions:  $\lambda = \hat{\lambda}$ , and  $\phi = \pm \hat{\phi}$ . However, in the actual positioning we always know whether a user is in the southern hemisphere or the northern hemisphere, so the user's real position can always be calculated.

The general method of solving this equation set is the step-by-step iterative method. Assume that we already know the rough positions  $\lambda_0$  and  $\phi_0$  of the user, we can obtain an approximate linear equation set

$$\begin{cases} \frac{\partial(\Delta\rho_1)}{\partial\lambda}(\lambda - \lambda_0) + \frac{\partial(\Delta\rho_1)}{\partial\phi}(\phi - \phi_0) = \Delta\rho_1^0 - \Delta\rho_1 \\ \frac{\partial(\Delta\rho_2)}{\partial\lambda}(\lambda - \lambda_0) + \frac{\partial(\Delta\rho_2)}{\partial\phi}(\phi - \phi_0) = \Delta\rho_2^0 - \Delta\rho_2 \end{cases} \quad (4)$$

In the above-mentioned equation set, the constant terms

$\frac{\partial \Delta \rho_j}{\partial \lambda}$ ,  $\frac{\partial \Delta \rho_j}{\partial \varphi}$  and  $\Delta \rho_j$  are values obtained in calculation by substituting  $\lambda_0$ ,  $\varphi_0$ . After this equation set is solved, a new estimate value of the user's position can be obtained. Then this set of estimated values is considered as new initial values  $\lambda_0$  and  $\varphi_0$  to be substituted into the above-mentioned equation set, and so we can obtain a more accurate estimated values. After several rounds of iterative calculations, we can satisfactorily solve for the user's position.

## 2. Geometric explanation of positioning method by using the difference between two distances

After a user's altitude is known, this is equivalent to the user's distance  $R$  from the earth's center being known. Then we can determine that the user is on a spherical surface with its center at the earth's center and  $R$  is the radius. On the other hand, since the position of the datum station is known accurately, the distance  $\rho_{0j}$  between the datum station and the predicted satellite position (not the actual satellite position) can be accurately calculated. Adding the difference between the distances from the user and from the datum station to the satellite thus measured as the difference between the distance to the predicted satellite position, we obtain the distance between the user and the predicted satellite position. Since the distance between the user and the datum station is much smaller than the distance to the satellite, the difference between the distance of the actual satellite is almost the same as the distance difference of the predicted satellite position. Then

the distance between the user to the predicted satellite position can be accurately calculated. Notwithstanding that the absolute value of the satellite positioning error is greater, this is the reason that the positioning method with the distance difference can greatly reduce the effect of satellite positioning error. After the accurate distances between the user and the two predicted satellite positions are obtained, we can obtain two spherical surfaces with these two satellite positions as the center of a sphere and the two distances as radii. These two spherical surfaces intersect, forming a circle. This circle intersects the spherical surface of the user on the ground at two points. These two points of intersection are symmetric relative to the equator. We can easily determine which point is the user's real position.

By using the positioning method based on the difference between two distances, we can also basically eliminate the error of electric wave propagation, because the distance between user and datum station is very small, and the effect is basically the same for the distance measured with respect to the same satellite, as well as the ionosphere and the troposphere, and after subtraction, the same portions cancel each other out.

### III. Analysis of Positioning Accuracy

#### 1. Calculation Formula

Let us assume that  $\Delta p_j$  is the distance difference between user and datum station, on the one hand, and the  $j$ -th satellite,

on the other.

$$\Delta\rho_j = \Delta\rho_j(R, \lambda, \phi, R_0, \lambda_0, \phi_0, r_j, \lambda_j, \phi_j) \quad (5)$$

In the equation,  $R$ ,  $\lambda$ ,  $\phi$ , as well as  $R_0$ ,  $\lambda_0$ , and  $\phi_0$  are, respectively, the distance to the earth's center, geographic longitude and latitude of the user and the datum station.  $r_j$ ,  $\lambda_j$ , and  $\phi_j$  are, respectively, the distance to the earth's center, longitude and latitude of the  $j$ -th satellite. In the positioning calculation procedures, the estimated values  $\hat{R}$ ,  $\hat{\lambda}$ ,  $\hat{\phi}$  of the user's position can be determined, thus satisfying

$$\Delta\rho_j(\hat{R}, \hat{\lambda}, \hat{\phi}, R_0, \lambda_0, \phi_0, r_j, \lambda_j, \phi_j) = \Delta\rho_j^0 \quad (6)$$

In the equation,  $\Delta\rho_j^0$  is the measured distance difference, then the relationship between the positioning error, on the one hand, and the satellite positioning error, surveying error, and altitude error, on the other, is

$$\begin{aligned} & \frac{\partial(\Delta\rho_j)}{\partial R} \delta R + \frac{\partial(\Delta\rho_j)}{\partial \lambda} \delta \lambda + \frac{\partial(\Delta\rho_j)}{\partial \phi} \delta \phi + \frac{\partial(\Delta\rho_j)}{\partial \lambda_j} \delta \lambda_j \\ & + \frac{\partial(\Delta\rho_j)}{\partial \phi_j} \delta \phi_j + \frac{\partial(\Delta\rho_j)}{\partial r_j} \delta r_j = \delta(\Delta\rho_j) \end{aligned} \quad (7)$$

In the equation  $\delta(\Delta\rho_j)$  is the survey error of the distance difference, and  $\delta r_j$ ,  $\delta \lambda_j$ ,  $\delta \phi_j$  are the satellite positioning error,  $\delta R$  is the user altitude error and  $\delta \lambda$  and  $\delta \phi$  are the longitude and latitude errors of the user's position.

Note

$$\begin{aligned} \delta(\Delta\rho_j) &= \delta(\Delta\rho_j) - \frac{\partial(\Delta\rho_j)}{\partial R} \delta R - \frac{\partial(\Delta\rho_j)}{\partial \lambda_j} \delta \lambda_j \\ & - \frac{\partial(\Delta\rho_j)}{\partial \phi_j} \delta \phi_j - \frac{\partial(\Delta\rho_j)}{\partial r_j} \delta r_j \end{aligned} \quad (8)$$

then we have

$$\frac{\partial(\Delta\rho_j)}{\partial\lambda}\delta\lambda + \frac{\partial(\Delta\rho_j)}{\partial\varphi}\delta\varphi = \delta(\Delta\rho_j). \quad (9)$$

again note  $\delta L_i = R\delta\lambda, \delta L_\varphi = R\delta\varphi$ , then we have

$$\begin{bmatrix} \frac{1}{R} \frac{\partial(\Delta\rho_1)}{\partial\lambda} & \frac{1}{R} \frac{\partial(\Delta\rho_1)}{\partial\varphi} \\ \frac{1}{R} \frac{\partial(\Delta\rho_2)}{\partial\lambda} & \frac{1}{R} \frac{\partial(\Delta\rho_2)}{\partial\varphi} \end{bmatrix} \begin{bmatrix} \delta L_i \\ \delta L_\varphi \end{bmatrix} = \begin{bmatrix} \delta(\Delta\rho_1) \\ \delta(\Delta\rho_2) \end{bmatrix} \quad (10)$$

Then we obtain

$$\begin{cases} \delta L_i = \frac{1}{RD} \left[ \frac{\partial(\Delta\rho_2)}{\partial\varphi} \delta(\Delta\rho_1) - \frac{\partial(\Delta\rho_1)}{\partial\varphi} \delta(\Delta\rho_2) \right] \\ \delta L_\varphi = \frac{1}{RD} \left[ \frac{\partial(\Delta\rho_1)}{\partial\lambda} \delta(\Delta\rho_2) - \frac{\partial(\Delta\rho_2)}{\partial\lambda} \delta(\Delta\rho_1) \right] \end{cases} \quad (11)$$

In the equation

$$D = \frac{1}{R^2} \left[ \frac{\partial(\Delta\rho_1)}{\partial\lambda} \frac{\partial(\Delta\rho_2)}{\partial\varphi} - \frac{\partial(\Delta\rho_1)}{\partial\varphi} \frac{\partial(\Delta\rho_2)}{\partial\lambda} \right] \quad (12)$$

By clearly indicating the effect of altitude error and satellite positioning error, then we have

$$\begin{aligned} \delta L_i &= \frac{1}{RD} \left[ \frac{\partial(\Delta\rho_2)}{\partial\varphi} \delta(\Delta\rho_1) - \frac{\partial(\Delta\rho_1)}{\partial\varphi} \delta(\Delta\rho_2) \right] \\ &\quad - \frac{1}{RD} \left[ \frac{\partial(\Delta\rho_2)}{\partial\varphi} \frac{\partial(\Delta\rho_1)}{\partial R} - \frac{\partial(\Delta\rho_1)}{\partial\varphi} \frac{\partial(\Delta\rho_2)}{\partial R} \right] \delta R \\ &\quad - \frac{1}{RD} \left[ \frac{\partial(\Delta\rho_2)}{\partial\varphi} \frac{\partial(\Delta\rho_1)}{\partial\lambda_1} \delta\lambda_1 - \frac{\partial(\Delta\rho_1)}{\partial\varphi} \frac{\partial(\Delta\rho_2)}{\partial\lambda_2} \delta\lambda_2 \right] \end{aligned} \quad (13)$$

$$\begin{aligned}
& -\frac{1}{R^2 D} \left[ \frac{\partial(\Delta\rho_2)}{\partial\varphi} \frac{\partial(\Delta\rho_1)}{\partial r_1} R\delta r_1 - \frac{\partial(\Delta\rho_1)}{\partial\varphi} \frac{\partial(\Delta\rho_2)}{\partial r_2} R\delta r_2 \right] \\
& -\frac{1}{R^2 D} \left[ \frac{\partial(\Delta\rho_2)}{\partial\varphi} \frac{\partial(\Delta\rho_1)}{\partial\varphi_1} R\delta\varphi_1 - \frac{\partial(\Delta\rho_1)}{\partial\varphi} \frac{\partial(\Delta\rho_2)}{\partial\varphi_2} R\delta\varphi_2 \right] \\
& \delta L = \frac{1}{RD} \left[ \frac{\partial(\Delta\rho_1)}{\partial\lambda} \delta(\Delta\rho_2) - \frac{\partial(\Delta\rho_2)}{\partial\lambda} \delta(\Delta\rho_1) \right] \quad (14) \\
& -\frac{1}{RD} \left[ \frac{\partial(\Delta\rho_1)}{\partial\lambda} \frac{\partial(\Delta\rho_2)}{\partial R} - \frac{\partial(\Delta\rho_2)}{\partial\lambda} \frac{\partial(\Delta\rho_1)}{\partial R} \right] \delta R \\
& -\frac{1}{RD} \left[ \frac{\partial(\Delta\rho_1)}{\partial\lambda} \frac{\partial(\Delta\rho_2)}{\partial r_2} \delta r_2 - \frac{\partial(\Delta\rho_2)}{\partial\lambda} \frac{\partial(\Delta\rho_1)}{\partial r_1} \delta r_1 \right] \\
& -\frac{1}{R^2 D} \left[ \frac{\partial(\Delta\rho_1)}{\partial\lambda} \frac{\partial(\Delta\rho_2)}{\partial\lambda_2} R\delta\lambda_2 - \frac{\partial(\Delta\rho_2)}{\partial\lambda} \frac{\partial(\Delta\rho_1)}{\partial\lambda_1} R\delta\lambda_1 \right] \\
& -\frac{1}{R^2 D} \left[ \frac{\partial(\Delta\rho_1)}{\partial\lambda} \frac{\partial(\Delta\rho_2)}{\partial\varphi_2} R\delta\varphi_2 - \frac{\partial(\Delta\rho_2)}{\partial\lambda} \frac{\partial(\Delta\rho_1)}{\partial\varphi_1} R\delta\varphi_1 \right]
\end{aligned}$$

Assume that the above-mentioned errors are independent, then the relationship between error and variance is

$$\begin{aligned}
\sigma_{L_1}^2 &= \frac{1}{R^2 D^2} \left\{ \left[ \frac{\partial(\Delta\rho_2)}{\partial\varphi} \right]^2 + \left[ \frac{\partial(\Delta\rho_1)}{\partial\varphi} \right]^2 \right\} \sigma_{\Delta\rho}^2 \\
&+ \frac{1}{R^2 D^2} \left[ \frac{\partial(\Delta\rho_2)}{\partial\varphi} \frac{\partial(\Delta\rho_1)}{\partial R} - \frac{\partial(\Delta\rho_1)}{\partial\varphi} \frac{\partial(\Delta\rho_2)}{\partial R} \right]^2 \sigma_R^2 \\
&+ \frac{1}{R^2 D^2} \left\{ \left[ \frac{\partial(\Delta\rho_2)}{\partial\varphi} \frac{\partial(\Delta\rho_1)}{\partial r_1} \right]^2 + \left[ \frac{\partial(\Delta\rho_1)}{\partial\varphi} \frac{\partial(\Delta\rho_2)}{\partial r_2} \right]^2 \right\} \sigma_r^2, \quad (15) \\
&+ \frac{1}{R^4 D^2} \left\{ \left[ \frac{\partial(\Delta\rho_2)}{\partial\varphi} \frac{\partial(\Delta\rho_1)}{\partial\lambda_1} \right]^2 + \left[ \frac{\partial(\Delta\rho_1)}{\partial\varphi} \frac{\partial(\Delta\rho_2)}{\partial\lambda_2} \right]^2 \right\} \sigma_{R\lambda}^2 \\
&+ \frac{1}{R^4 D^2} \left\{ \left[ \frac{\partial(\Delta\rho_2)}{\partial\varphi} \frac{\partial(\Delta\rho_1)}{\partial\varphi_1} \right]^2 + \left[ \frac{\partial(\Delta\rho_1)}{\partial\varphi} \frac{\partial(\Delta\rho_2)}{\partial\varphi_2} \right]^2 \right\} \sigma_{R\varphi}^2
\end{aligned}$$

$$\begin{aligned}
\sigma_{L\alpha}^2 &= \frac{1}{R^2 D^2} \left\{ \left[ \frac{\partial(\Delta\rho_1)}{\partial\lambda} \right]^2 + \left[ \frac{\partial(\Delta\rho_2)}{\partial\lambda} \right]^2 \right\} \sigma_{\Delta\rho}^2 \\
&+ \frac{1}{R^2 D^2} \left[ \frac{\partial(\Delta\rho_1)}{\partial\lambda} \frac{\partial(\Delta\rho_2)}{\partial R} - \frac{\partial(\Delta\rho_2)}{\partial\lambda} \frac{\partial(\Delta\rho_1)}{\partial R} \right]^2 \sigma_R^2 \\
&+ \frac{1}{R^2 D^2} \left\{ \left[ \frac{\partial(\Delta\rho_1)}{\partial\lambda} \frac{\partial(\Delta\rho_2)}{\partial r_2} \right]^2 + \left[ \frac{\partial(\Delta\rho_2)}{\partial\lambda} \frac{\partial(\Delta\rho_1)}{\partial r_1} \right]^2 \right\} \sigma_{r_1}^2 \\
&+ \frac{1}{R^4 D^2} \left\{ \left[ \frac{\partial(\Delta\rho_1)}{\partial\lambda} \frac{\partial(\Delta\rho_2)}{\partial\lambda_2} \right]^2 + \left[ \frac{\partial(\Delta\rho_2)}{\partial\lambda} \frac{\partial(\Delta\rho_1)}{\partial\lambda_1} \right]^2 \right\} \sigma_{\lambda_1}^2 \\
&+ \frac{1}{R^4 D^2} \left\{ \left[ \frac{\partial(\Delta\rho_1)}{\partial\lambda} \frac{\partial(\Delta\rho_2)}{\partial\varphi_2} \right]^2 + \left[ \frac{\partial(\Delta\rho_2)}{\partial\lambda} \frac{\partial(\Delta\rho_1)}{\partial\varphi_1} \right]^2 \right\} \sigma_{\varphi_1}^2
\end{aligned} \tag{16}$$

In the equation  $\sigma_{L\alpha}^2$  and  $\sigma_{L\alpha}^2$ , are, respectively, the variance of the user positioning error in the longitudinal and latitudinal directions; then  $\sigma_R^2$  is the variance of altitude error. Then we have  $\sigma_{R\lambda}^2 = \left(\frac{R}{r}\right)^2 \sigma_{\lambda}^2$  and  $\sigma_{R\varphi}^2 = \left(\frac{R}{r}\right)^2 \sigma_{\varphi}^2$ ;  $\sigma_r^2$ ,  $\sigma_{\lambda_1}^2$ , and  $\sigma_{\varphi_1}^2$  are, respectively, the variances of error of the distance between the satellite and the earth's center, and in the longitudinal and latitudinal directions.

In the following, we further derive the equations expressing the partial derivatives mentioned above. Indicated with rectangular coordinates, we have

$$\begin{aligned}
x &= R \cos \varphi \cos \lambda \\
y &= R \cos \varphi \sin \lambda \\
z &= R \sin \varphi \\
x_0 &= R \cos \varphi_0 \cos \lambda_0 \\
y_0 &= R \cos \varphi_0 \sin \lambda_0 \\
z_0 &= R \sin \varphi_0 \\
x_j &= r_j \cos \varphi_j \cos \lambda_j \\
y_j &= r_j \cos \varphi_j \sin \lambda_j \\
z_j &= r_j \sin \varphi_j
\end{aligned}$$

$$\rho_j = \sqrt{(x - x_j)^2 + (y - y_j)^2 + (z - z_j)^2}$$

$$\rho_{o_j} = \sqrt{(x_0 - x_j)^2 + (y_0 - y_j)^2 + (z_0 - z_j)^2}$$

$$\Delta \rho_j = \rho_j - \rho_{o_j} \quad (17)$$

Based on the above-mentioned fundamental expression equations, we can very easily derive the partial derivatives required:

$$\frac{\partial(\Delta \rho_j)}{\partial R} = \frac{x - x_j}{\rho_j} \frac{x}{R} + \frac{y - y_j}{\rho_j} \frac{y}{R} + \frac{z - z_j}{\rho_j} \frac{z}{R}$$

$$\frac{\partial(\Delta \rho_j)}{\partial \lambda} = -\frac{(x - x_j)y}{\rho_j} + \frac{(y - y_j)x}{\rho_j}$$

$$\frac{\partial(\Delta \rho_j)}{\partial \varphi} = -\frac{x - x_j}{\rho_j} z \cos \lambda - \frac{y - y_j}{\rho_j} z \sin \lambda + \frac{z - z_j}{\rho_j} R \cos \varphi$$

$$\begin{aligned}
\frac{\partial(\Delta\rho_j)}{\partial r_j} &= \frac{x_j}{r_j} \left( \frac{x_o - x_j}{\rho_{oj}} - \frac{x - x_j}{\rho_j} \right) + \frac{y_j}{r_j} \left( \frac{y_o - y_j}{\rho_{oj}} - \frac{y - y_j}{\rho_j} \right) \\
&\quad + \frac{z_j}{r_j} \left( \frac{z_o - z_j}{\rho_{oj}} - \frac{z - z_j}{\rho_j} \right) \\
\frac{\partial(\Delta\rho_j)}{\partial \lambda_j} &= y_j \left( \frac{x - x_j}{\rho_j} - \frac{x_o - x_j}{\rho_{oj}} \right) + x_j \left( \frac{y_o - y_j}{\rho_{oj}} - \frac{y - y_j}{\rho_j} \right) \\
\frac{\partial(\Delta\rho_j)}{\partial \varphi_j} &= z_j \left( \frac{x - x_j}{\rho_j} - \frac{x_o - x_j}{\rho_{oj}} \right) \cos\lambda_j \\
&\quad + z_j \left( \frac{y - y_j}{\rho_j} - \frac{y_o - y_j}{\rho_{oj}} \right) \sin\lambda_j \\
&\quad - r_j \left( \frac{z - z_j}{\rho_j} - \frac{z_o - z_j}{\rho_{oj}} \right) \cos\varphi_j
\end{aligned} \tag{18}$$

To simplify the computations, we can conduct a coordinate transformation. Let us use the center point of the two satellites as the origin of longitude; with respect to two geostationary satellites, we can take  $r_j=r_0$  and  $\varphi_j=0$ .

## 2. Calculation results

Based on the above-mentioned calculation formulas, we can calculate the effect on positioning accuracy by various factors. Let us assume that the two satellites are  $60^\circ$  apart over the equator, and the distance (between the satellite and the earth's center)  $r_0=42,164.19\text{km}$ . Consider the distance between the user and the datum station, on the one hand, and the earth's center, on the other is the average earth radius  $R=6371\text{km}$ . In the

following, we describe the effect of various errors.

### 2.1. Effect of surveying error

First, we analyze and calculate the effect of a simple surveying error. In other words, this is the positioning accuracy, assuming that the satellite position if it is assumed that the satellite position is without any error, and that the user's altitude also has no error.

Note

$$\sigma_L = \sqrt{\sigma_{L1}^2 + \sigma_{L2}^2} \quad (19)$$

That is,  $\sigma_L$  generally represents the two-dimensional accuracy of user positioning; this is the positioning accuracy within a plane. Its relationship between the covariance  $\sigma_{\Delta\phi}$  of the surveying error can be expressed as

$$\sigma_L = C_L \sigma_{\Delta\phi} \quad (20)$$

In the equation, the error transfer coefficient  $C_L$  is related to the relative geometric positions between the user and the two satellites. In the following, Table 1 lists the value with the variational value  $C_L$  of user's positions. In the table,  $\phi$  is the user's geometric latitude, and  $\lambda$  is the longitudinal difference between the user and the midpoint in the distance between the two satellites. Since it is symmetrical in the eastern and western sides, Table 1 only presents the east side, that is, the situation when  $\lambda > 0$ .

TABLE 1. Values of  $C_L$  Showing the Effect on Surveying Error

$\varphi$	$\lambda$	0	5	10	15	20	25	30	35	40
60		2.8	2.8	2.8	2.8	2.8	2.7	2.7	2.7	2.6
50		2.3	2.3	2.3	2.3	2.3	2.3	2.3	2.2	2.2
40		2.0	2.0	2.0	2.1	2.1	2.1	2.1	2.1	2.0
30		2.1	2.1	2.1	2.1	2.1	2.2	2.2	2.3	2.3
20		2.5	2.5	2.5	2.6	2.6	2.7	2.8	2.9	3.0
10		4.3	4.3	4.4	4.5	4.6	4.8	5.0	5.3	5.6
8		5.3	5.3	5.4	5.5	5.7	5.9	6.2	6.5	6.9
6		6.9	7.0	7.1	7.3	7.5	7.8	8.2	8.6	9.1
4		10.3	10.3	10.5	10.8	11.2	11.7	12.2	12.9	13.6
2		20.5	20.6	20.9	21.5	22.2	23.2	24.4	25.7	27.1

Fig. 2 is the isopleth diagram of  $C_L$ .

From the above-mentioned table and the isopleth diagram, we can clearly see that the positioning accuracy is relatively poor in the low-latitude zone. Error can be quite large in the near-equatorial zone. However, in the region north of  $20^{\circ}$  N. Lat., the value of  $C_L$  tends to stabilize between 2 and 3. Therefore, if the error is 3m when measuring the round-trip distance, then the error of a single distance is 1.5m. The distance difference is measured as  $1.5 \times (2)^{1/2}$  is approximately 2.5m. Due to this error, the induced positioning error is 5 to 7.5m.

## 2.2. Effect on positioning due to user's altitude error

As pointed out in the foregoing analysis, the two-satellite positioning system is incapable of determining the user's altitude. Only if the user first provides his altitude is it possible, on this basis, to determine the user's position longitude and latitude. From the positioning principle, this altitude data should be obtained independently, not relying on longitude and latitude of the user's position because these longitudes and latitudes are unknown. At present, two conventional methods of obtaining the altitude information, digitized terrain map or barometric altimeter, are relied on. In the former case, user's longitude and latitude are apparently relied on. In the latter case, the altitude thus measured is relative to the altitude over the geoidal surface. However, the data of the geoidal surface relative to the relief on the reference ellipsoidal surface are also relied on, longitude and latitude. In such problems, generally iteration is used. First, crude altitude data are given, then longitude and latitude are calculated. Then, based on longitude and latitude, the more accurate altitude is obtained, thus calculating the longitude and latitude. These iterative calculations are conducted until satisfying a certain accuracy. However, the effectiveness and reliability of any iteration has the prerequisite of being a one-value solution.

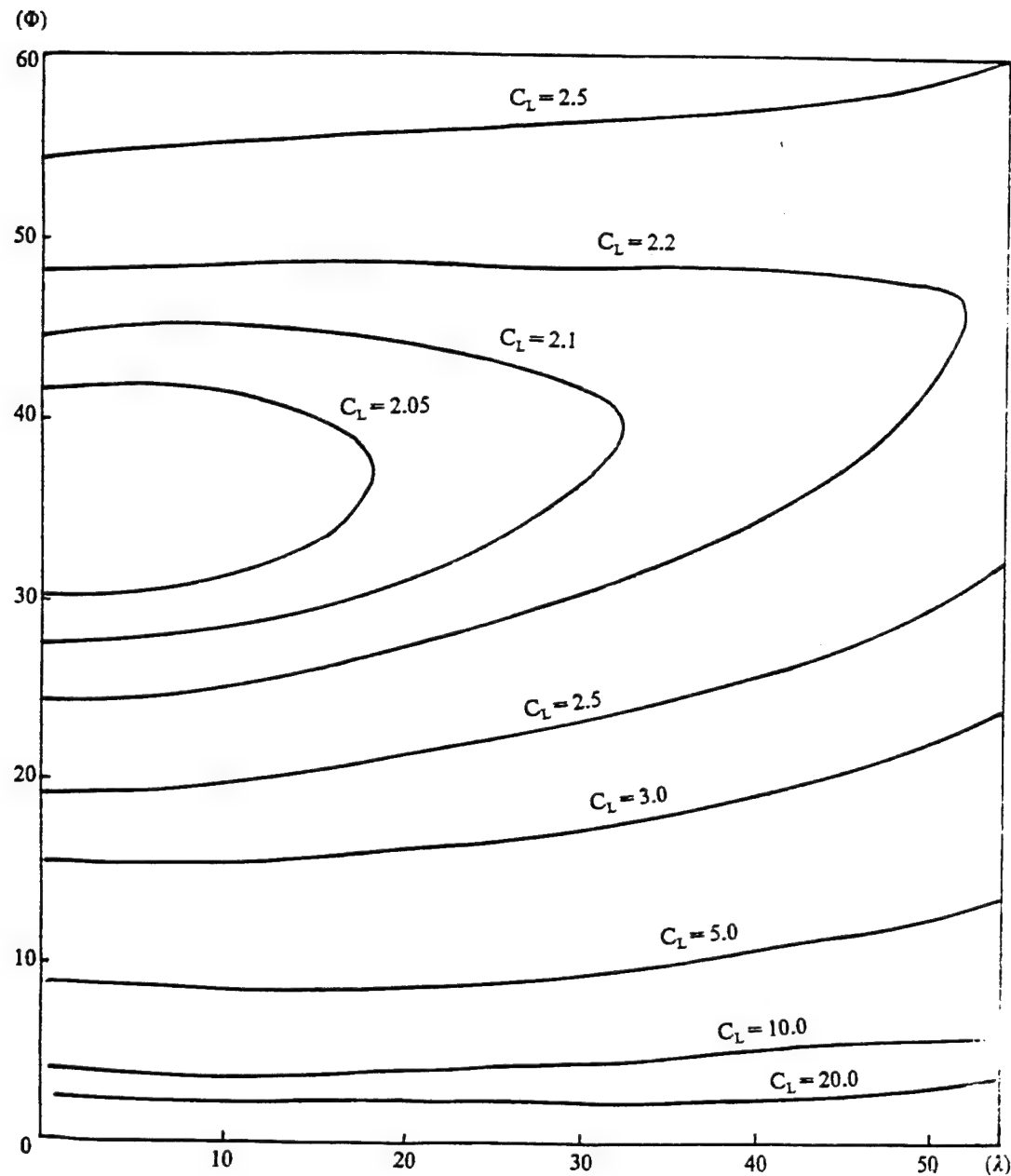


Fig. 2. Isopleths of  $C_L$  as affecting surveying error

If there are multiple values of the solution, the situation may arise that the iteration is not convergent, or that it converges to a different solution. If a user is on a flat zone,

this multiple-value solution will not appear. If there is much terrain relief, multiple-value solutions will appear. In practical applications, the digitized terrain map presents the approximate (after smoothing out) terrain. Alternatively, when the digitized terrain map is flat, multiple-value solutions can be avoided in positioning. Since the actual terrain has a greater difference from the terrain provided by the digitized map, altitude error may become relatively great, thus, more strongly affect the determination of user's longitude and latitude. The effect on the determination of longitude and latitude due to altitude error indicated is

$$\sigma_L = C_R \sigma_R \quad (21)$$

The error transfer coefficient  $C_R$  similarly also relies on the relative geometric relationship between the user and the two satellites. Table 2 lists the value of  $C_R$ . Fig. 3 shows the corresponding isopleths.

From the above-mentioned figure and table, the transfer factor of altitude error is not great. In the region above  $20^{\circ}$  N. Lat., the value can be taken as 2.0. However the altitude error is relatively large, thus the induced positioning error is also correspondingly large. If the altitude data error of a user is 30m, then the induced error of user's position may be as high as 60m.

TABLE 2.  $C_L$  Values Affecting Altitude Errors

$\varphi$	$\lambda$	0	5	10	15	20	25	30	35	40
60		0.38	0.38	0.38	0.39	0.41	0.42	0.44	0.46	0.48
50		0.61	0.61	0.62	0.62	0.63	0.64	0.66	0.67	0.69
40		0.92	0.92	0.93	0.93	0.94	0.95	0.96	0.98	0.99
30		1.4	1.4	1.4	1.4	1.4	1.4	1.4	1.5	1.5
20		2.2	2.2	2.2	2.3	2.3	2.3	2.3	2.3	2.4
10		4.7	4.7	4.7	4.7	4.7	4.8	4.8	4.8	4.9
8		5.9	5.9	5.9	5.9	6.0	6.0	6.0	6.1	6.2
6		7.8	7.9	7.9	7.9	7.9	8.0	8.1	8.1	8.2
4		11.8	11.8	11.8	11.9	12.0	12.0	12.1	12.3	12.4
2		23.6	23.7	23.7	23.8	23.9	24.1	24.3	24.5	24.8

### 2.3. Effect of satellite positioning error

As mentioned above, the effect on positioning due to satellite positioning error can apply the positioning method of the difference between two distances at the nearby datum station to greatly reduce the effect, but not to entirely eliminate it. Besides, generally the effect of error on three directions of satellite position is not the same. Here we assume that the mean square value of errors of the satellite in its distance from the

earth's center as well as longitude and latitude are the same, and are represented by  $\sigma_s$ , then the effect on user's position error can be indicated as  $\sigma_l = C_s \sigma_s$ . Here, the error transfer factor,  $C_s$  relies not only on the relative geometric relationship between the user and the two satellites, but is also related to the position of the datum station. We can see, from several examples calculated, that  $C_s$  is related mainly to the distance between the datum station and user. Moreover, in the range of not very great distances, this error and the distance form a linear relationship. In Table 3, the numerical results given in Table 3 and the isopleths in Fig. 4 apply the assumption that the datum station is at a location  $2^\circ$  east and north of the user, corresponding to 315km from the user. For a user in the west ( $\lambda < 0$ ), the datum station  $2^\circ$  west and north of the user should be applied to obtain the same results.

From Table 3 and Fig. 4, we can see that the transfer relationship of the positioning error due to satellite positioning error does exceed 0.15 in the regions above  $20^\circ$ N. Lat., therefore if there is an error of 100m in satellite positioning error in altitude, longitude, and latitude, the positioning error thus induced is less than 15m.

### 3. Prediction of overall error in positioning

In the foregoing, the discussion involved the numerical relationship dealing with the effect of positioning accuracy due to various error sources. The overall positioning is determined

by the magnitude of these error sources. From the current

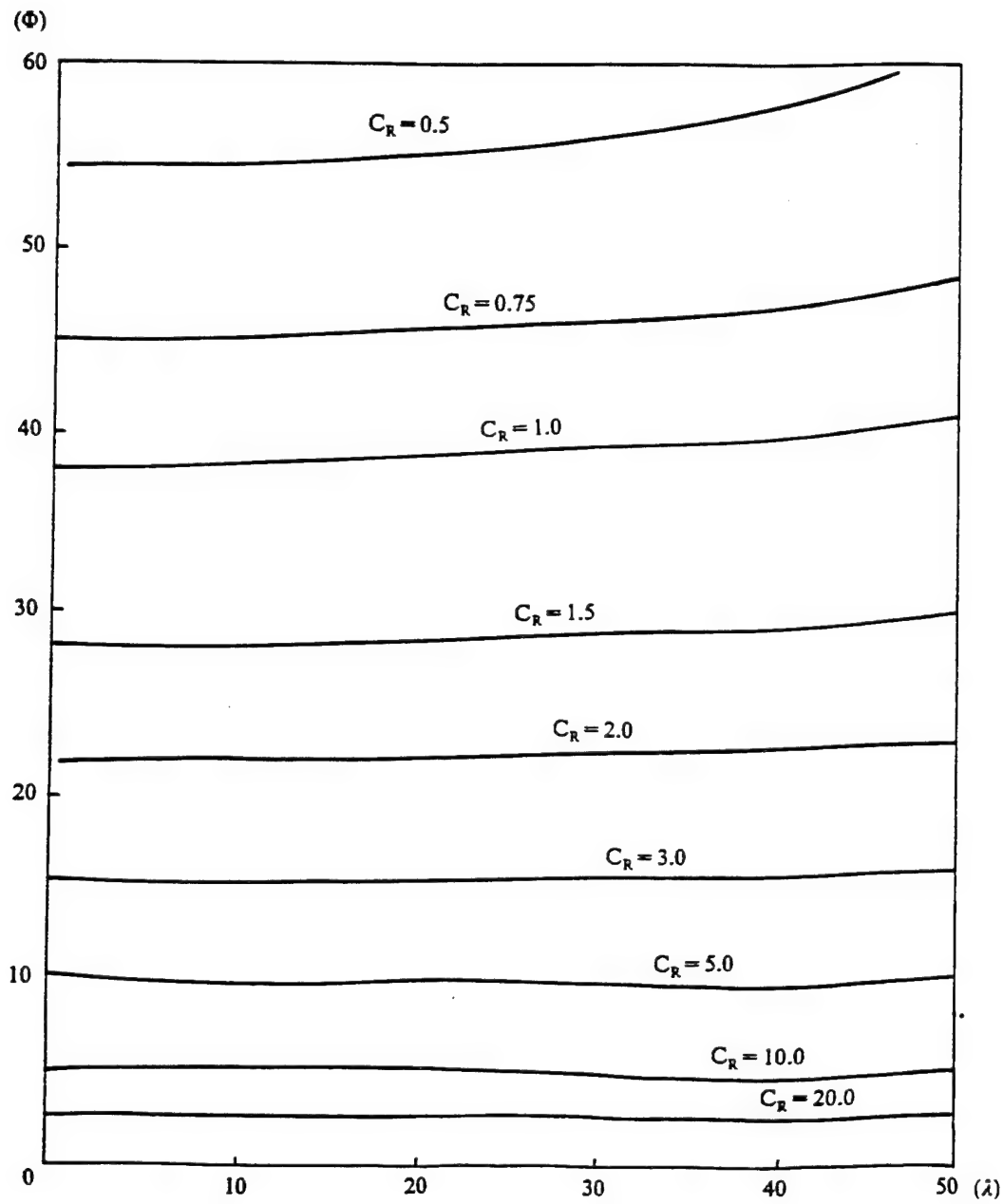


Fig. 3. Isopleths of  $C_R$  as affecting altitude

situation, it is possible to have an error of 3m in the round-trip distance of measurement due to noise in user's receiver and transmitter. If the altitude is 30m and the satellite positioning errors are within 100m in three aspects of altitude, longitude, and latitude, then the overall accuracy of positioning in the areas above 20°N. Lat can be better than

$$\sqrt{7.5^2 + 60^2 + 15^2} \approx 62 \text{ (m)}$$

If the altitude error is 40m, and the satellite positioning error is 400m for the three aspects, then the overall accuracy is

$$\sqrt{7.5^2 + 80^2 + 60^2} \approx 100 \text{ (m)}.$$

[text incomplete]

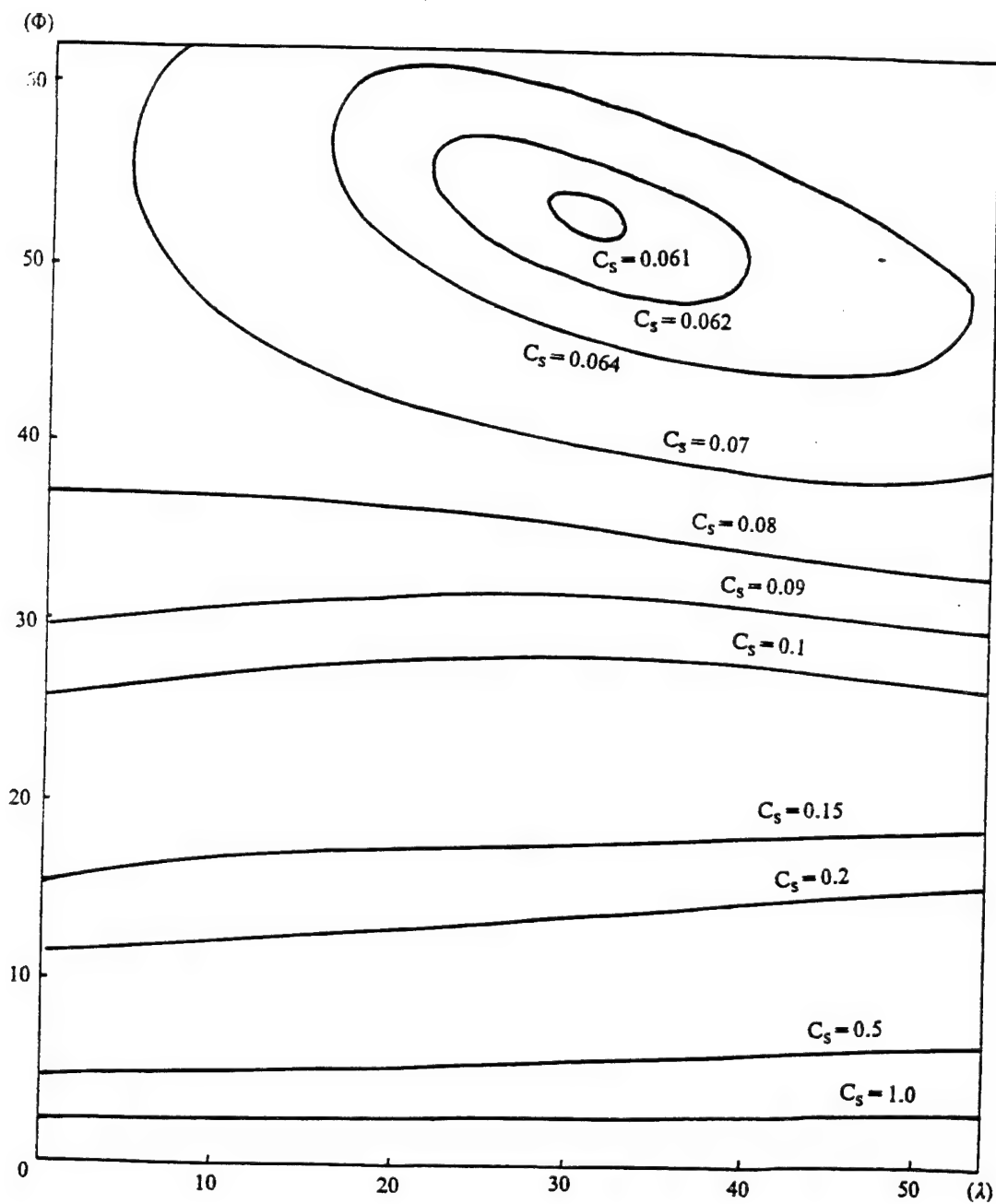


Fig. 4. Isopleths of  $C_s$  as affecting satellite positioning error

TABLE 3. Values of  $C_s$  as Affecting Satellite Positioning Error

$\varphi \backslash \lambda$	0	5	10	15	20	25	30	35	40
60	0.07	0.07	0.07	0.06	0.06	0.06	0.06	0.07	0.07
50	0.07	0.07	0.07	0.07	0.06	0.06	0.06	0.06	0.06
40	0.08	0.08	0.08	0.07	0.07	0.07	0.07	0.07	0.07
30	0.09	0.09	0.09	0.09	0.09	0.09	0.09	0.09	0.09
20	0.12	0.12	0.13	0.13	0.13	0.13	0.14	0.14	0.14
10	0.22	0.22	0.23	0.25	0.26	0.27	0.28	0.29	0.29
8	0.27	0.28	0.29	0.31	0.32	0.33	0.35	0.36	0.37
6	0.35	0.36	0.38	0.41	0.43	0.45	0.47	0.49	0.50
4	0.53	0.55	0.57	0.60	0.64	0.67	0.71	0.73	0.75
2	1.1	1.1	1.1	1.2	1.3	1.3	1.4	1.5	1.5

## LOW-COST NAVIGATION SATELLITES

translated by Ding Yi and Su Xi  
and edited by Li Ye

### I. INTRODUCTION

The subject of this research report is to explore the feasibility of adopting a low-cost design to accomplish satellite navigation tasks. The study includes an analysis of a small engineering economic satellite utility compartment operating in a large elliptical earth orbit. Since a satellite-based navigation system requires many satellites, the use of low-cost satellites in the system can save considerable costs and upgrade the feasibility of the entire system.

To keep total satellite costs at a minimum and to maintain acceptable reliability, one of the key factors is to have the design of the utility compartment and the payload system conform to the fundamental principles as follows:

To maintain tasks and an environment of the various subsystems to be thoroughly investigated, and to have components and techniques capable of fulfilling the tasks, an appropriate

and feasibility safety redundancy is maintained. If not required by functions or environment, one should not look for the output quota and quality because doing so will generally add to costs.

The primary utility compartment should be standardized; the design and hardware should be verified.

To adopt as far as possible flexible design in providing functional redundancy, a second set of equipment should not be adopted.

Clear-cut definitions and simple interfaces between subsystems should be used. Even if there is entirely identical hardware units, a subsystem should operate entirely independently.

Based on verified high quality enterprises should rely on batch production of elements and components to design subsystems. If batch-produced elements and components are relied on, any shortcomings can be solved. One should adopt, if possible, highly reliable or selected batch-produced components up to the military technical norm.

## II. GENERAL DESCRIPTION OF RESEARCH REPORT

As in the space navigation systems such as GPS-NAVSTAR and GLONASS, and system concepts such as the GRANAS and NAVSAT, the arrival-time principle is used to determine precise user locations. This is so even for high-speed moving bodies such as aircraft.

To determine three-dimensional positions, signals from four

satellites should be simultaneously received in order to calculate the X, Y, and Z coordinates and the time delay. In the NAVSTAR states, it is required to deploy 18 operating satellites in high circular orbits (20,000km) in order to provide a continuously globally covered operating system. Since this system includes quite a number of satellites, the cost of each satellite should be lowered to greatly reduce total system costs. This feasibility research determines whether or not to build a satellite-based navigation satellites with cost effectiveness.

This research is based on previous research results of the European Space Agency, such as comparative research on GRANAS/NAVSAT and ITALSPAZIO. These are verified effective satellites. This research aims at determining whether or not low-cost satellites can be compatible with the above-mentioned space navigation systems.

### III. RESEARCH TASKS

#### 1. First Task

A study of trade-off plan was conducted dealing with the design concept of a replacement system for the satellite and launch system. After accomplishing the study of the specific flight mission requirements, including the orbital situation, study of the trade-off plan was conducted with regard to the following criteria to solve the problems of stabilities, spin axis, three axes, and gravity gradient.

System performance was evaluated on the predetermined flight

lifetime in the required range of maintaining payload.

This includes the mechanical complexity compatible with the launcher.

This is evaluated on the related numbers of mechanical components or electrical devices with complexity. This evaluation is indicated with the sequence possibly required of a successful flight.

This is related to the cost, primary expenditures, and repetitive expenses, in addition to contractor experience and/or other experience related to possible subcontractors.

## 2. Second Task

A study of system design was made based on the selected satellite concepts realized down to the subsystem level, with satellite integrated design with the following system performance indicators:

Satellite block diagrams, including all main structural members. Verification is made of the satellite structure, as well as reaction control and attitude control, as well as the compatibility of electrical and payload subsystems, indicating the launch state.

Outline design and analysis of the heating control subsystems in various main flight stages were conducted. It is assumed that the power for a payload is 70% of the DC power input.

Outline design and analysis were conducted of the electrical

subsystem, including estimation of solar cell array performance in various flight stages, as well as a typical operational profile diagram of storage batteries.

This is the budgetary analysis of quality.

Given the required flight lifetime, profile design and analysis are made on the subsystems for reaction control.

Design and analysis were made on the attitude control subsystem, including the predicted orientation errors of the satellite.

The preliminary design was conducted on the remote measurement and remote sensing subsystems required for satellite control and maneuver.

This is the assembly drawing of the satellite at the working stage.

### 3. Third Task

The system design was conducted at the advanced launch concept down to the subsystem level. First, according to the launch state mentioned in the first task, diagrams are used to describe the flight sequence, including the following stages:

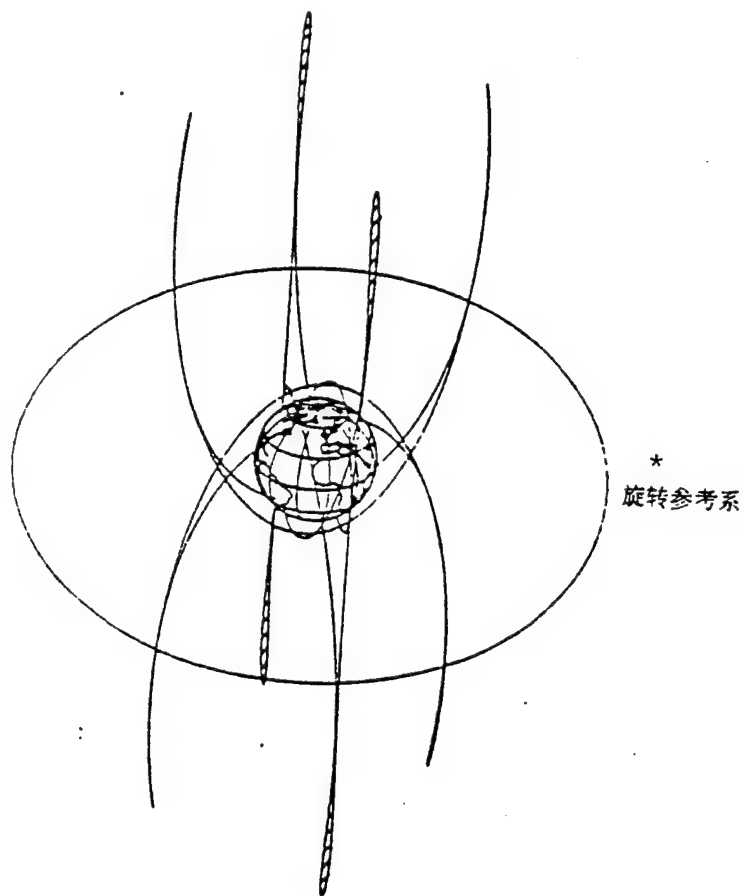
launch; orbital entry; orbital maneuver and control; as well as in-orbit redundancy and re-use.

## IV. RESEARCH REPORT ON THE FIRST TASK

### 1. Orbit of navigation satellite

In the normal state, the navigation satellite (NAVSAT) at

least provides four navigation targets with wider separation to a user at an earth location when the satellite is in the

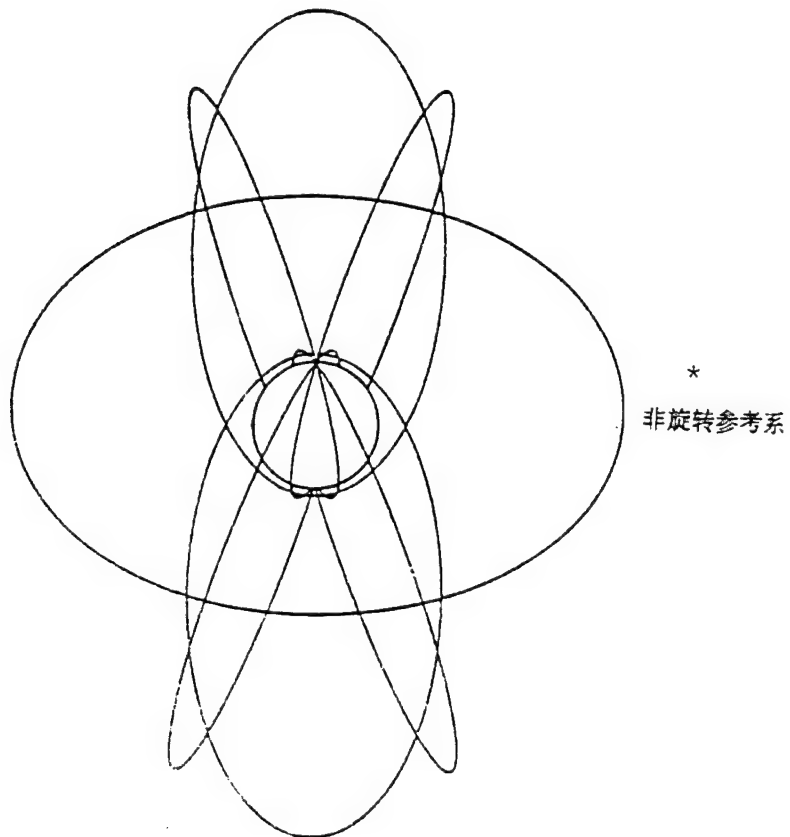


KEY: \* - spin reference system

geosynchronous orbit and a large elliptical orbit. For this purpose, each one of eight loops (shaded portion) is continuously filled with a satellite. In addition, more than three payload components are distributed to the geosynchronous satellites, such as the European Maritime Communication Satellite (MARECS).

The purpose of this research is to design low-cost

elliptically orbiting satellites.



KEY: \* - non-spin reference system

To maintain loops that are continuously filled, each of six elliptical orbits of orbital planes is filled with two satellites. In other words, the total number of satellites simultaneously in orbit is 12. The orbital parameters are as follows:

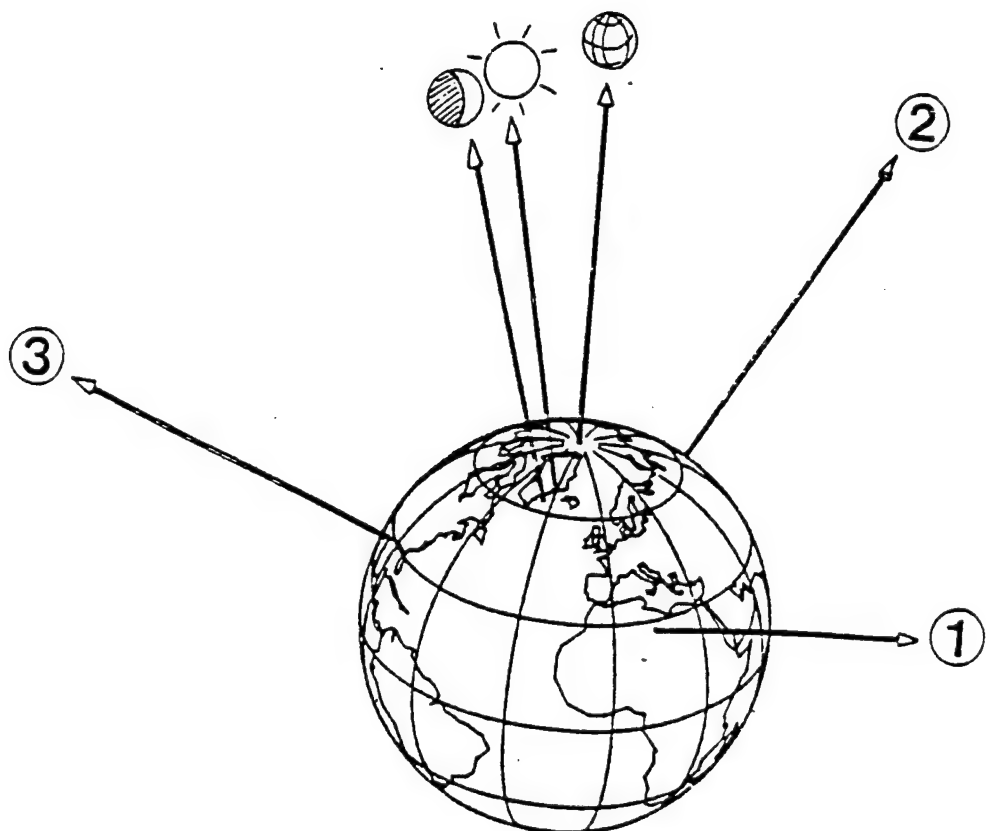
semimajor axis (a):	26,556km
angle of dip (i):	$63.45^\circ$
eccentricity (e):	0.713
argument at perigee ( $\omega$ )	$\pm 90^\circ$

right ascension of ascending node ( $\Omega$ )  $45^\circ/165^\circ/285^\circ$

The orbital period is 12h; the apogee altitude is 39,105km, and the perigee altitude is 1.250km.

## 2. Orbital perturbation

Orbital orientation can be indicated with its vector of angular momentum; this is the vector perpendicular to the orbit.



If only the long-term perturbation ( $t > 1$  year) is considered, the solar orbit and the lunar orbit are also realized as momentum vectors. In other words, this is a mass loop of even distribution. The following interaction of the angular momentum vector is induced due to the gravity gradient:

satellite orbit ①, ②, ③ ( $\Omega = 45^\circ / 165^\circ / 285^\circ$     $i = 63.45^\circ$ )

oblateness of earth  ( $i = 0^\circ$ )

solar orbit  ( $\Omega = 0^\circ$     $i = 23.45^\circ$ )

lunar orbit  within a 17-y cycle it revolves around the solar orbit with a vector  $5.15^\circ$  angular value.

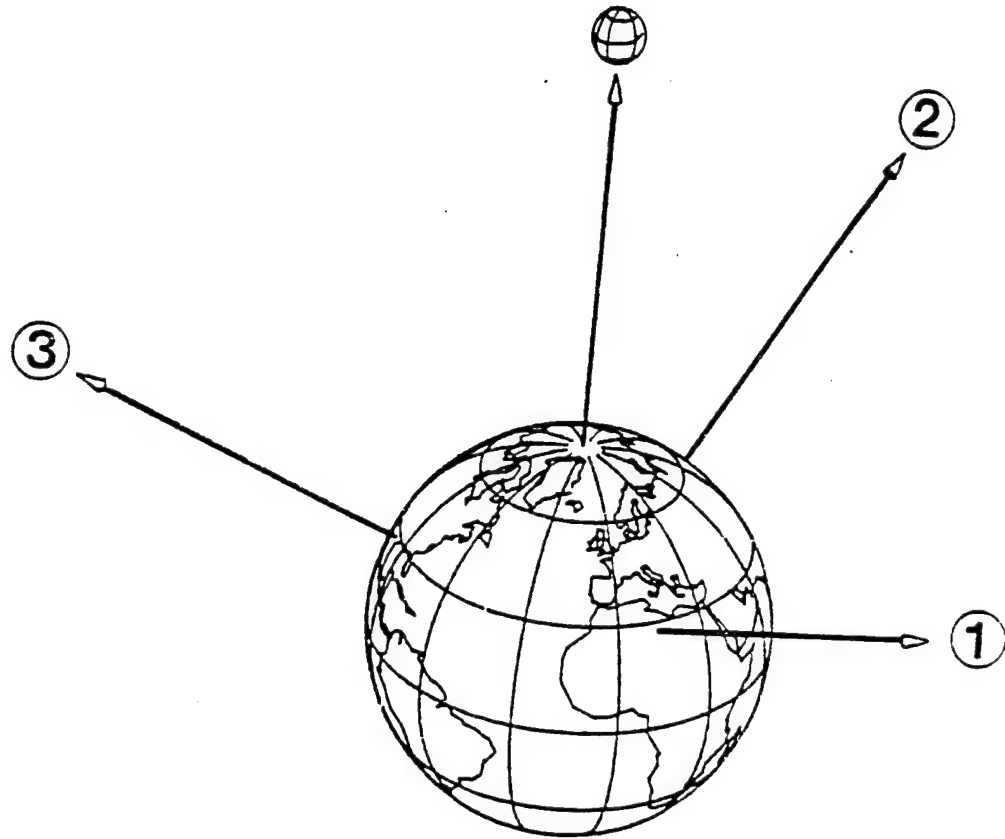
### 3. Earth's Oblateness

Due to earth's oblateness, the argument at perigee rotates with constant speed.

$$\dot{\omega} = \frac{4.9821}{(1-e^2)^2} \left( \frac{Re}{a} \right)^{3.5} \cdot (5\cos^2 i - 1) \text{ deg/day}$$

If the angle of dip is selected such that no content in the parenthesis appears, the selected value of  $63.45^\circ$  can satisfy this condition. As a result, there is regression at the points of intersection in the satellite orbit.

$$\dot{\Omega} = - \frac{9.9641}{(1-e^2)^2} \left( \frac{Re}{a} \right)^{3.5} \cos i \text{ deg/day}$$



This is approximately  $45^\circ/y$ , causing no problem, because it does not affect the range of the navigation target. The variation due to the dip angle of  $\pm 10$  is as follows:

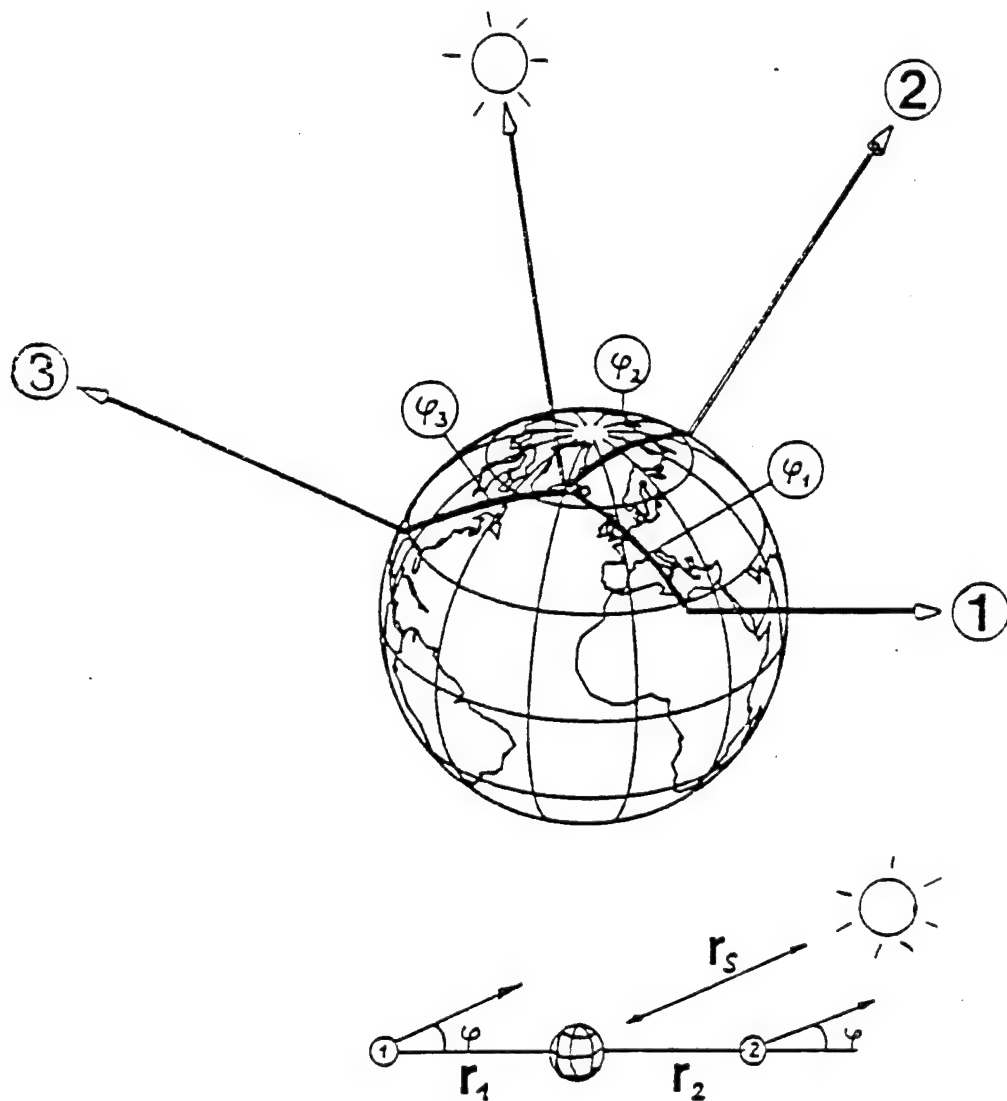
$$\Delta\dot{\omega} = \mp 3.51 \text{ deg/year} \quad \Delta\dot{\Omega} = \mp 1.57^\circ \text{ deg/year}$$

#### 4. Solar Attraction

Because of the sun, the gravity gradient and satellite acceleration between position 1 and position 2 are

$$\begin{aligned}\Delta A &= \frac{\mu_s}{(r_s - r_2 \cos\varphi)^2} - \frac{\mu_s}{(r_s + r_2 \cos\varphi)^2} \\ &= \frac{z(r_1 + r_2) \cdot \mu_s \cdot \cos\varphi}{r_s^3} \quad r_s \geq r_1, r_2\end{aligned}$$

$\Delta A$  can be divided into component  $\Delta A \cos\varphi$  within the orbital plane, and another component  $\Delta A \sin\varphi$  outside the orbital plane,



thus causing precession of the orbital vector. To compensate for

the  $\Delta A$  effect, the fuel consumption is proportional to  $\Delta A$  and it is linearly related to the orbital diameter,  $\sin\phi$  and  $\cos\phi$ .

Compared to the geosynchronous orbit, the orbital diameter is smaller (26,556km versus 42,164km), but angle  $\phi$  is relatively disadvantageous:

$$\begin{array}{ll} \varphi_1 = 48.56^\circ & \sin\varphi_1 \cos\varphi_1 = 0.496 \\ \varphi_2 = 86.20^\circ & \sin\varphi_2 \cos\varphi_2 = 0.066 \\ \varphi_3 = 59.85^\circ & \sin\varphi_3 \cos\varphi_3 = 0.436 \end{array}$$

When comparing  $\phi=23.45^\circ$  and  $\sin\phi \cos\phi=0.365$ , in the geosynchronous orbit the worse case is  $\phi=45^\circ$  and  $\sin\phi \cos\phi=0.5$ .

## 5. General Description

oblateness of earth: absence of perturbation

solar-lunar attraction; same as in the geosynchronous orbit

air drag: not applicable

propellant to maintain position: 50m/s (year)

Similar consideration should be applied to the interaction between satellite and lunar orbits. Therefore, the propellant for maintaining the position is not much different from the quantity of the propellant used in the geosynchronous orbit, if the following position-maintenance schemes are adopted:

- (1) conduct maneuver outside the plane only once a year
- (2) correction of  $\Omega$  and  $i$  should be combined into one maneuver at appropriate points in the orbit, and
- (3)  $\omega$  should not directly control the maneuver within the

plane, but should apply the control by appropriately conducting the offset adjustment through  $i$  indirectly.

## 6. Task Requirements

Payload mass: 60kg

payload power: 150W

antenna diameter: 1.98m (hexagonal-shaped)

orientation accuracy:  $\pm 1^\circ$

Lifetime: 3y (the average time between malfunctions).

The payload mass includes the transponder mass (40kg) and the platform mass (20kg) of the phase-controlled array antenna. To provide 150W of power to the payload, the solar cell should provide 200W of power. This corresponds to the design of an average area of  $2\text{m}^2$  facing the sun.

The satellite operating cycle terminates at the low-intersection point of the loop, which is 10,635km in altitude. The highest point of the loop is 39,117km. Between the highest point  $16.1^\circ$  and the point of intersection  $44.0^\circ$ , the diameter of the earth's shadow changes correspondingly.

In the substitute scheme, a replacement satellite is launched every three months. This means that, on the average, a satellite is replaced every three years. If a satellite develops malfunctions ahead of schedule, another satellite should extend its replacement time. Therefore, the satellite lifetime is not regularly limited to longer than 3y, such as exhaustion of fuel or radiation damage.

## 7. Design Scheme

Structure, reaction control subsystem, as well as attitude and orbital control subsystem employ available elements and components.

In the new design of on-board satellite electronic equipment, there is no redundancy with compact design.

A typical example of the available product, mechanical components, is as follows: central force-acting cylinder of the satellite structure, fuel tank, booster, valves, momentum wheel, attitude sensor, as well as shaft and electrical energy transmission components.

Typical examples of the newly developed items are as follows: TTC [tracking, telemetry, and command] channels, data processing, attitude control electronic equipment, and power supply electronic equipment. Consideration is given to adopting more advanced elements and components, such as highly integrated circuits, as well as elements and components of the CMOS technique and the application of the MIL Standard. The service orientation remote measurement and remote control items will be reduced in number as much as possible, this is simultaneously for simplifying earth station operation.

Since the average satellite lifetime is 3y, and the cost due to mass and equipment is very important, therefore no redundant parts exist. By this method, the number of switches, the number of TTC channels, and the functions of ground operators are reduced, thus enhancing reliability.

The aim is avoiding as far as possible structures that are mechanically complex.

## 8. Selection of Elements and Components

Central force-acting cylinder: German postal satellites-Kopernikus

fuel tank: German postal satellite-Kopernikus

proportional technique: hydrazine

area of solar cell array: 10m<sup>2</sup>

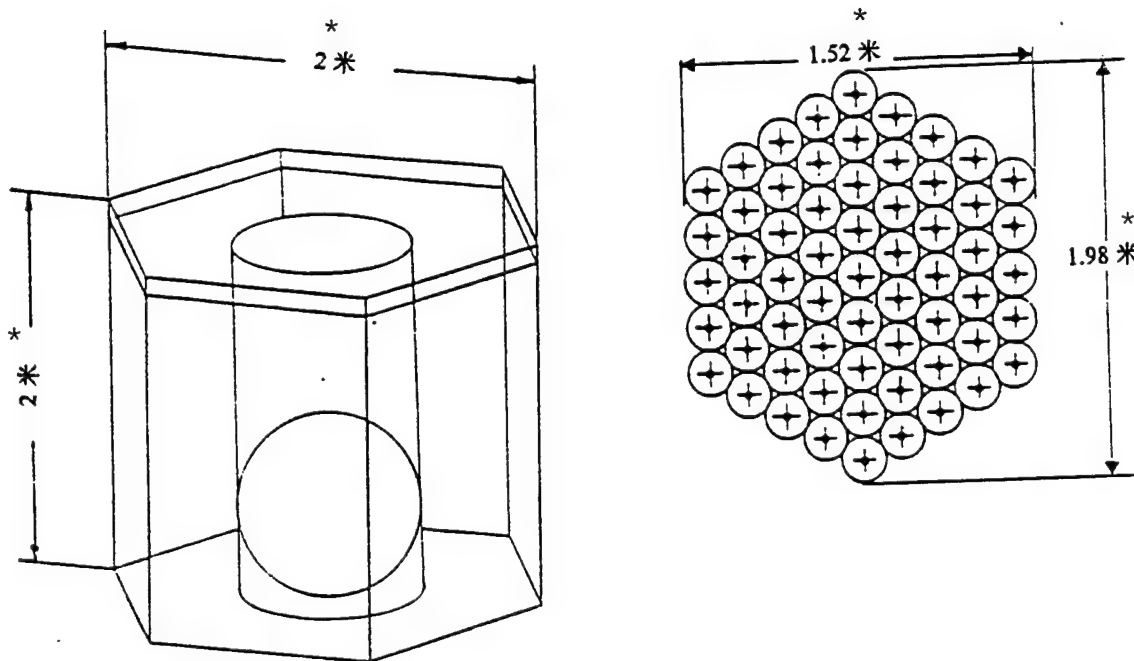
The central force-acting cylinder can be bought from many suppliers, since this is designed for DELTA/PAM-D satellites. The typical dimensions are 37inches as diameter (for standard interface) and approximately 1.8m in length (restricted by the length of the shuttle/PAM-D). All these limitations are acceptable. The force-acting cylinder of the German postal satellite-Kopernikus, was selected as the basic component because it has very attractive carbon fiber technique and is light in mass (20kg).

The fuel tank of the German postal satellite-Kopernikus was selected as one of the basic components because it can match with the central force-acting cylinder. The combination of force-acting cylinder and fuel tank are commercially available. This surface tension fuel tank can store as much as 350L of propellant. The capacity can be further extended by inserting a cylinder segment.

By comparing with the dual-element propellant, although the

specific thrust of hydrazine is smaller, yet it is still proposed to be adopted because of its lower complexity and low cost. Thus, one of two fuel tanks of the German postal satellite can be left out, to be replaced with the equipment platform of the payload and service compartment.

#### 9. Fundamental Structure



KEY: \* - meters

The central force-acting cylinder is a loaded structural member of the satellite. A single-element hydrazine tank and all the satellite equipment and payload equipment are contained in the cylinder, which is mated with the carrier through a 37-inch adapter. On the other terminal, there is installed a platform

for the phase-controlled array antenna. The central force-acting cylinder is surrounded by rigid solar cell structure of light hexagonal honeycomb structure.

This hexagonal shape is mainly required by the antenna's structural shape, and must also mate with the standard cowl dimensions of 2.16m in diameter of DELTA class satellites. The typical dimensions of such satellites is 2m long and 2m wide. In other words, 4m<sup>2</sup> of the solar cell array can face the sun. Such dimensions are suitable because on the average 3m<sup>2</sup> are required and the antenna surface cannot cover the solar cells.

#### 10. Fundamental Mass Distribution

Payload:	60
central force-acting cylinder	20
fuel tanks	20
reaction control subsystem	5
solar cell array	10
storage battery	10
attitude and orbital control subsystem	10
tracking remote measurement and command	5
excess amount	10
<hr/>	
dry mass of satellite	150kg

This mass distribution is very strict, but it seems to be feasible. The payload mass is specified, and the masses of the

central force-acting cylinder, fuel tank, and the reaction control subsystem are measured values; therefore, 105kg of mass has been confirmed.

A main design work is concentrated in the satellite-borne electronic equipment. For students and radio amateurs, lighter mass than the commercial design is preferred. The design targets of the attitude and orbital control subsystems, tracking, remote measurement, and command, as well as power supply are 35kg. Another 10kg is added as a suitable allowance.

#### 11. Distribution of Fundamental Cost Items

Central force-acting cylinder	0.5
Fuel tank	0.5
Reaction control subsystem	0.5
solar cell array	0.5
storage battery	0.3
attitude and orbital control subsystem	0.7
tracking, remote measurement, and command	0.5
allowance	1.5
<hr/>	
utility compartments	5.0
payload	3.0
<hr/>	
satellite	8.0 million ECU

[European currency units]

The figures for costs and expenses of the central force-

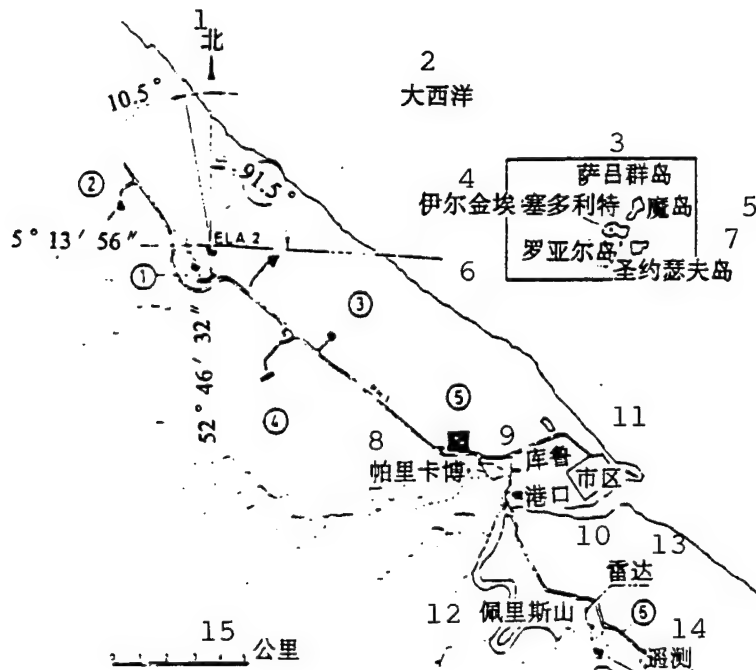
acting cylinder, fuel tank, and reaction control subsystem were verified. For the solar cell array, this approximately costs 50,000 ECU per square meter. The other cost items are based on, as far as possible, the estimation of the available usable equipment. With rational averaging of the single item costs, allowance for the 1.5 million-ECU costs can be used to pay for the unforeseen development risks. In series production, the total cost of a 90kg utility compartment is approximately 5million ECU. With allowance, this comes to 5600 ECU per kg. Excluding the allowance, this comes to 3900 ECU per kg. The estimated cost of the payload is based on 50,000 ECU per kg.

The hydrazine cost is 200 ECU per kg. For 350kg hydrazine, this comes to 70,000 ECU.

## 12. Ariane Carrier Rocket

The Ariane-4 rocket was launched toward the northwest direction from Kourou, then the orbital dip angle of  $63.45^{\circ}$  can be attained as expected. This three-stage carrier rocket should not have gliding flight. Thus, at the position when the third-stage fuel is burned up, a circular orbit of any altitude, or perigee of elliptical orbit can be obtained.

Since the rotation at the perigee argument within the orbital plane consumes too much fuel and time, the circular orbit with semimajor axis of 7628km is selected. Since four satellites can orbit within the same orbital plane (but only two satellites operate in the same orbit), the additional advantage of this



KEY: 1 - north 2 - Atlantic Ocean 3 - Iles du Salut  
 4 - Yi'erjinai Seduolite [transliteration] 5 - Devil's  
 Island 6 - Luoya'er [transliteration] Island 7 - Saint  
 Joseph Island 8 - Palikabo [transliteration] 9 - Kourou  
 10 - Port 11 - urban area 12 - Peilisi [transliteration]  
 Mountain 13 - radar 14 - remote sensing 15 - kilometers

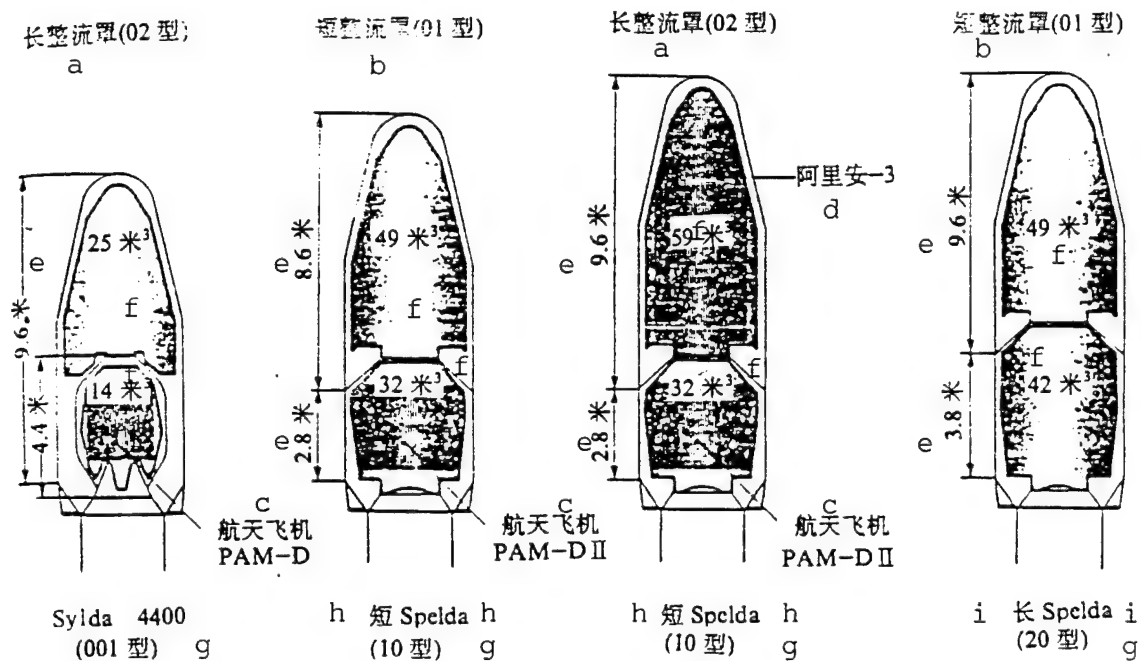
selection is that four satellites can be sent together into orbit. To raise the apogee to 39,105km, the velocity increment ( $\Delta V$ ) of 2500m/s should be provided. Including  $3 \times 50$ m/s for maintaining its position, the total  $\Delta V$  is required to be 2650m/s. This is equal to the required mass of the fuel.

$$m_{\text{燃料}} = (e^{\Delta V / V_s} - 1)m_{\text{干重}} \quad V_s = 2250 \text{米/秒}$$

$$1 = 2.25m_{\text{干重}} \quad 2$$

KEY: 1 - fuel 2 - dry mass 3 - m/s

The present fuel tank (350L in capacity) is sufficient to contain the required fuel of 337.5L; the fill ratio is 96%. In addition, the fuel tank size can be increased by adding a cylinder segment at a cost of an increased inspection fee.



KEY: a - long fairing (model 02) b - short fairing (model 01) c - Space Shuttle d - Ariane-3 e - meters f - m³ g - model h - short i - long

There are two independent compartments for the long Spelda structural shape of Ariane-4. Each compartment has sufficient length and diameter for launching two satellites. Since the current SYLDA is too long, a special similar structure of SYLDA should be provided by the user for loading the satellite.

The total launch mass of the four satellites is as follows:

Four satellites at 500kg (wet mass each)	2000
One long SPELDA	400
Two SYLDA with 200kg each	400
<hr/>	
	2800kg

On this basis, the Ariane AR44P carrier rocket will be selected; the cost is approximately 80million ECU. In other words, each satellite costs 20million ECU.

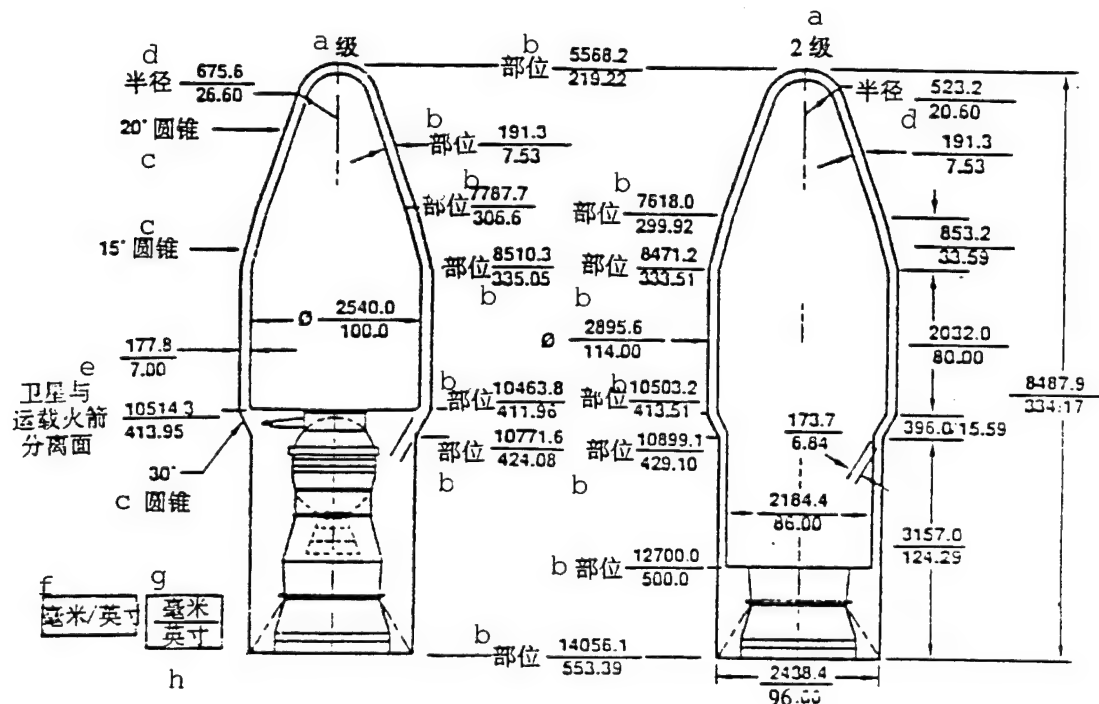
### 13. DELTA 6925 Carrier Rockets



KEY: a - West Target Range b - Launch pad 1  
 c - orbital dip angle  $80^{\circ}$  to  $145^{\circ}$  (designated)  
 d - East Target Range e - Launch pad 2  
 f - orbital dip angle  $28.5^{\circ}$  to  $51^{\circ}$

DELTA carrier rockets are launched from Vandenberg (West Target Range) or Canaveral (East Target Range). With the West Target Range launch, the minimum dip angle is  $75^{\circ}$ ; with a launch

from the East Target Range, the maximum dip angle is  $51^\circ$ . So to reach the required dip angle of  $63.45^\circ$ , a dip angle variation maneuver should be conducted. Since the thrust of the upgraded DELTA model is quite high, this carrier has no problem in handling this task.



KEY: a - stage b - site c - circular cone  
 d - radius e - separation plane between satellite and carrier rocket f - value in millimeters/value in inches g - millimeters h - inches

A DELTA 6925 carrier rocket can directly send 962kg into a Molniya type satellite orbit. Therefore, the mass distribution for a dual satellite launch is as follows:

Two satellites (dry mass)	300kg
one SYLDA	200kg
2x231kg of fuel	462kg
<hr/>	
962kg	

There is more fuel required to maintain the position.

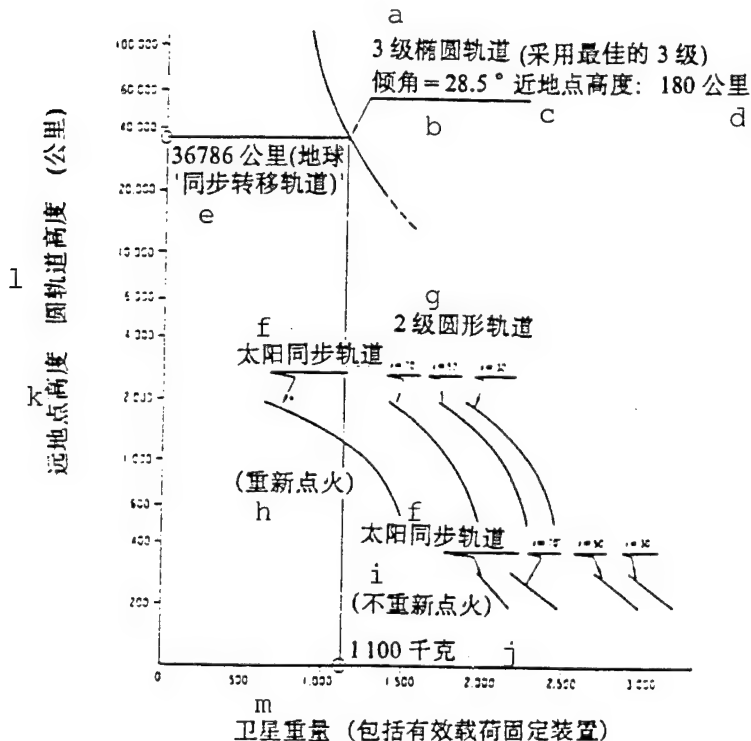
The cowl dimensions in the DELTA 6925 carrier rocket allow for the launching of dual satellites. Although there is some limitation in the effective length of the 2m diameter cylindrical segments, before third-stage ignition the stage can have rotation of 60rpm via a rotating platform. Therefore, the dual satellite configuration will rotate about an unstable axis that a large amount of fuel is carried in the semi-empty fuel tank. It is feasible to separate the dual satellite configuration with smooth rotating state.

The cost of one DELTA 6925 carrier rocket launch is approximately 40million ECU. In other words, the launch cost for each satellite is 20million ECU.

#### 14. H-1 Carrier Rocket

The H-1 is a Japanese carrier rocket. Although its thrust is smaller than that of a DELTA 6925 carrier rocket, still it can provide sufficient launch capability. Launched from the Seed Island Launch Center of Japan, a satellite can be sent directly into a parking orbit with the required dip angle of 63.45°.

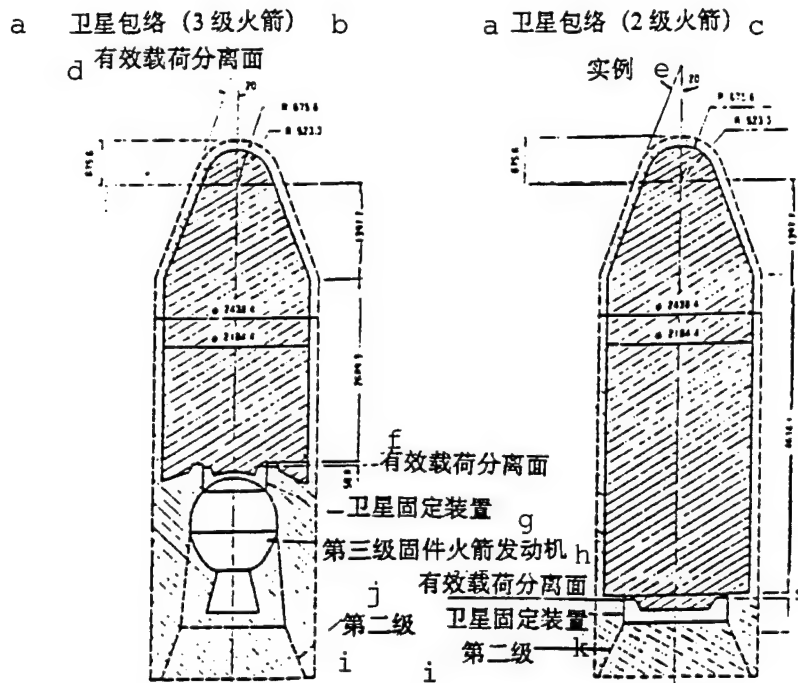
This two-stage carrier rocket can send 1800kg into a circular orbit of 1250km in radius. Therefore, the rocket can produce the same situation as that of Ariane-4.



KEY: a - third-stage elliptical orbit (adopting the optimal third stage b - dip angle c - altitude of perigee d - 180km e - 36,786km (geosynchronous orbit) f - solar synchronous orbit g - second stage elliptical orbit h - re-ignition i - absence of re-ignition j - kilograms k - altitude at apogee l - altitude of circular orbit (km) m - satellite weight (including payload)

A three-stage carrier rocket is unable to provide sufficient length for a dual satellite launch. The cowl dimensions of the two-stage H-1 carrier rocket are sufficient for dual-satellite launches, although the diameter is quite hindered, and limits the SYLDA design.

The cost can be estimated as 40,000 ECU. In other words, this is 20million ECU per satellite.



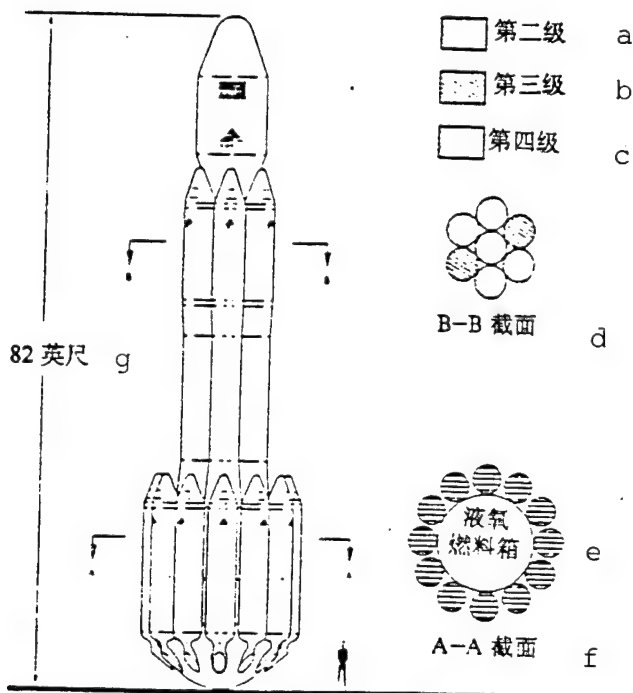
KEY: a - satellite casing b - (third-stage rocket)  
 c - (second-stage rocket) d - payload separation  
 plane e - example f - payload separation plane  
 g - satellite mount h - third-stage solid-fuel  
 rocket engine i - second-stage j - payload  
 separation plane k - satellite mount

## 15. American Rocket

The American Rocket Corporation provides a mixed-proportion carrier rocket with a re-ignition stage. The rocket uses the same launch site as that of the DELTA carrier rocket, and is restricted by the same dip angle. Although the capability of the American carrier rocket is smaller, but it still can meet the requirements, but only if the satellites are kept slender and small.

An American Rocket (AMROC) can send a 400kg satellite into

elliptical orbit, with the altitude at perigee of 1250km, and the altitude at apogee of 25,000km, and the dip angle  $75^\circ$ . To raise

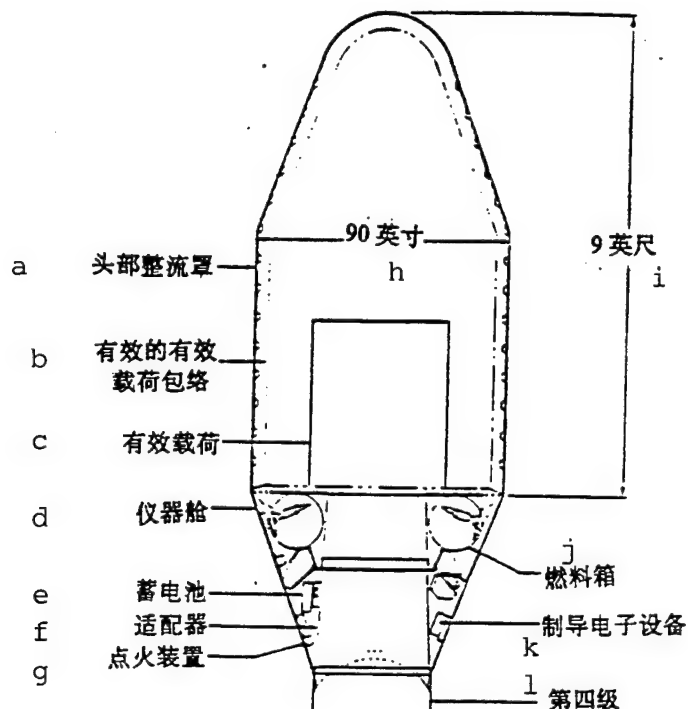


KEY: a - second stage b - third stage  
c - fourth stage d - cross-section B-B  
e - liquid oxygen and fuel tanks  
f - cross-section A-A g - 82feet

the apogee altitude to 39,105km, a velocity increment of 1350m/s is required. For maneuvering in changing the dip angle at the apogee, another velocity of 300m/s should be added. Including the velocity increment of 400m/s for station keeping, the total velocity increment is 200m/s. This requires the loading of 215kg fuel with a fill ratio of 61%. This fill ratio allows a purging operation.

Generally, the cowl dimensions are adapted to single

satellite launches. The diameter for the standardized adapter in this carrier rocket is 37inches.



KEY: a - nose fairing b - effective payload casing  
c - payload d instrumentation compartment  
e - storage batteries f - adapter g - ignition  
equipment h - 90inches i - 9feet j - fuel  
k - guidance electronics l - fourth stage

The major attractive feature of this carrier rocket is price. The cost of each launch is 8million ECU. This carrier rocket has not been certified. A parabolic test flight is scheduled to be launched from the Vandenberg Launch Center by the end of 1987. A circular test flight is scheduled to be launched

by the end of 1988. Consecutively, two experiments will be conducted in early 1989. This can become a practical type of carrier rocket only in the second half of 1989.

## 16. General Description

The American rocket is the most economical carrier.

It is compatible with the following carrier rockets:

Ariane-4 (launches 4 satellites)

DELTA 6925 (launches 2 satellites)

H1 carrier rocket (launches 2 satellites)

The American rocket is thus far the lowest-cost scheme.

Each launch of a satellite costs 8million ECU, not 20million ECU.

The American rocket is the only selective scheme for matching launch costs (8million ECU) and satellite costs (8million ECU).

The American rocket avoids the restrictions of a dual satellite launch, that is the mass and costs for one SYLDA. In addition, flexibility of replacing a single satellite is upgraded because it is impossible for simultaneous malfunctioning of two satellites in the same orbit.

Although it is proposed to use the American rocket as the basis, but competitiveness in selecting other launch schemes is still maintained.

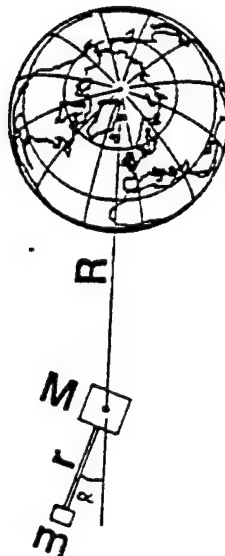
The potential development problem with the American rocket, and the potential problem of research progress.

## 17. Stability of Gravity Gradient

### (1) General description

A long slender object in a circular earth orbit has a natural tendency toward stability along the direction of the gravity gradient field. Between the satellite mass  $M$  and the pendulous mass  $m$ , the force through a rod is:

$$F = m\mu \frac{3r \cos \alpha}{R^3} \quad \mu = 398\ 600 \quad \text{km}^3/\text{s}^2$$



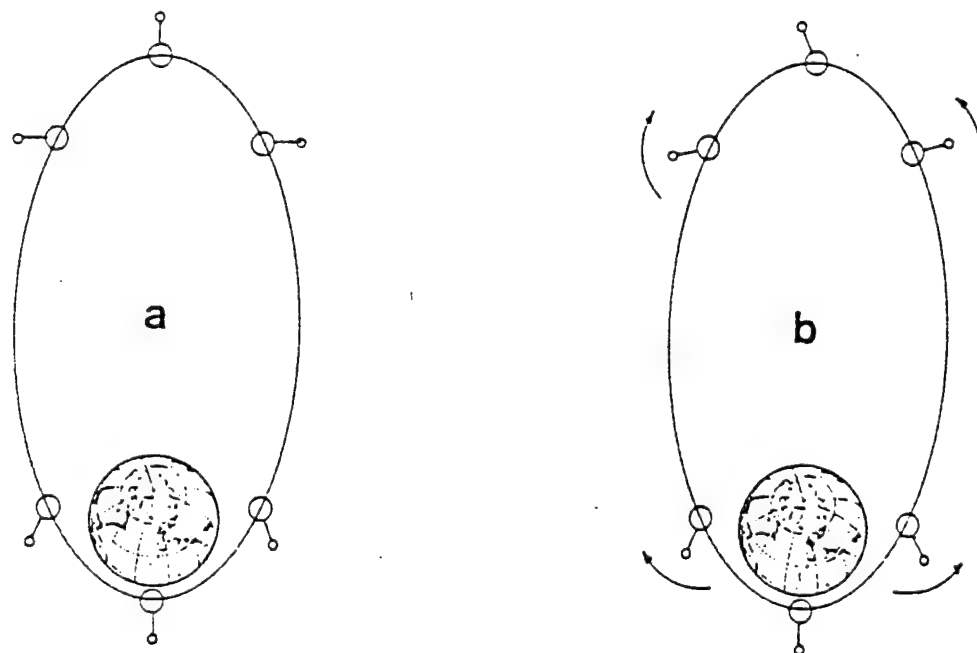
And the stability torque is:

$$T = m\mu \frac{3r^2}{R^3} \sin \alpha \cos \alpha$$

For a low earth orbit (such as TUBSAT), this principle is very attractive because  $R$  is very small. In the situation of  $m=10\text{km}$  and  $r=10\text{m}$ , the force  $F$  becomes  $0.4 \cdot 10^{-3} \cos \alpha$  [newton-meter], and torque becomes  $4 \cdot 10^{-3} \sin \alpha \cos \alpha$  [newton-meter]. For

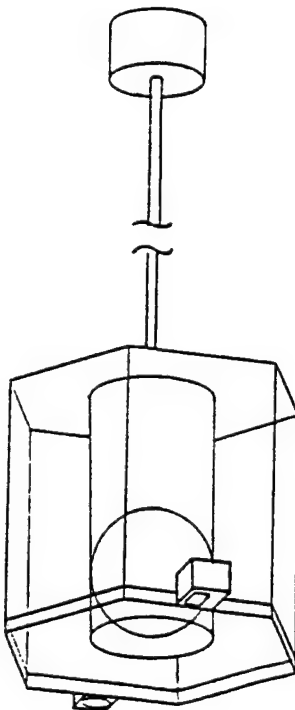
small values of  $\alpha$  a pendulum is formed in the gravity field of  $0.4 \cdot 10^{-5} g$  by the satellite; however, the oscillatory period of this pendulum and the orbital period are of the same numerical magnitude, not determined by the mass  $m$  or length  $r$  of the pendulum. It is very difficult to damp this low-frequency oscillation by adopting the method of passive damping attachment. Therefore, if the accuracy target of  $\pm 10$  is specified, sometimes even some active damping circuit (such as a magnetic torque apparatus) is required in low earth orbit.

In the high circular orbits, such as the geosynchronous orbit, with decrease in  $R^3$ , that is, with a reduction in the stability torque for the same satellite structural shape, it is reduced to  $1.6 \cdot 10^{-5} \sin\alpha\cos\alpha$  [newton-meter]. Besides, the oscillatory period is reduced to the orbital period of the geosynchronous orbit.



(2) Elliptical orbit

The stability state of a circular orbit is that the satellite rod is continuously aligned along the gravity gradient field. The gravity gradient field is obtained by continuously rotating the satellite with orbital velocity. In other words, the satellite maintains a constant angular momentum. In



elliptical orbits, it is contradictory between the requirements of continuously aiming at the gravity gradient field and the principle of maintaining angular momentum. The stability state is effective only at a certain point with respect to the elliptical orbit; this point is the perigee. If the satellite rotates at an appropriate velocity and if we can neglect the

gravity gradient force (a), then the satellite will point towards the required direction at apogee. At this time, the attitude error will be as large as  $67^{\circ}$ .

If we consider the gravity gradient (b), the satellite will accelerate along the clockwise direction between perigee and apogee, and reduce its velocity in another half-orbit, thus changing its attitude at the apogee. In any situation, the specified  $1^{\circ}$  orientation accuracy cannot be realized by using this stabilization method.

#### (3) Structural shape of satellite

To adapt to the rod installation of the mass (that can be ejected) in the force-bearing cylinder, the fuel tank should be moved upward, that is, to be at the location of the second tank in the German postal satellite. Environmental stresses of the central force-acting cylinder will be increased; however, this force-acting cylinder is designed for two fuel tanks, therefore, this is acceptable.

#### (4) System performance

The predetermined lifetime is not affected when this control mode is selected. However, the requirements of satisfying payload cannot be met because the orientation accuracy greatly exceeds the technical specifications.

#### (5) Mechanical complexity

Overall mechanical complexity of the satellite and its compatibility with the carrier rocket are not affected. Increased complexity is limited to the rod itself and the deployment mode thus selected. It is proposed to adopt the mode which has passed space flight certification. If the rod is too soft, and the resonance frequency of the mass of the rod is too low, the corresponding control algorithm should be adopted in order to avoid interaction with the booster control system in the period while the maneuvering flight is being supported for the position. Collision with the streamline flow is considered as a potential problem because the stabilizing mass operates at a distance from the satellite.

#### (6) Electrical complexity

There are two major sources of greater electrical complexity.

- Rod deployment and locking mechanism:
- before the rod is released, the control system will adjust the attitude in a beneficial direction, and adjust its rotational speed. This system requires an attitude sensor and an execution mechanism, among other devices, such as reaction flywheel and the related control electronic circuits.

Structural shape: gravity-gradient rod

central fuel tank (pointing upward)

Performance: exceeding the technical specifications

Complexity: rod deployment

earth sensor

Cost: based on the basic values.

### (7) Relative costs

The primary attraction of the concept of gravity-gradient stabilization is its simplicity, low cost, and low power consumption. However, in this large elliptical orbit, to orient the satellite before rod deployment, and to stabilize the satellite during the position-maintaining mobile flight period and afterwards, it is required to install a complete routine attitude control system. Thus, the rod costs add only slightly to the relative costs.

(8) Contractors' experience

Contractors intend to conduct a gravity-gradient stabilization experience on the TUBSAT satellite, by using a rigid deployed mass or a tie-rope mass. A system composed of a magnetic torque device and a satellite sensor gyroscope will be used for initial orientation before deployment.

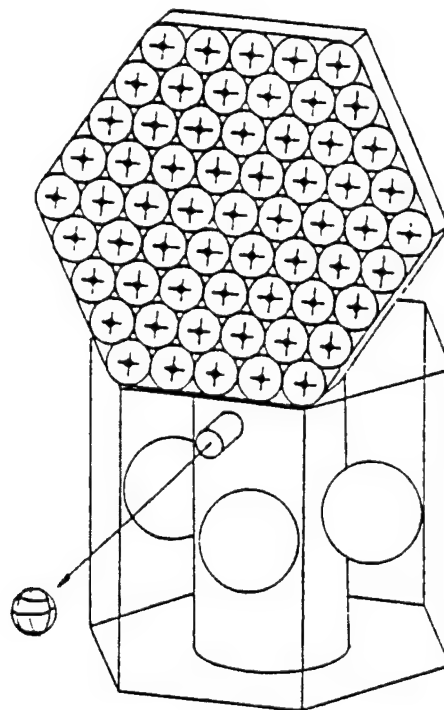
#### (9) Preliminary conclusion and final conclusions

The attitude control adopting gravity-gradient stabilization is a quite attractive poor-man's stabilization concept used by students and radio amateurs. In particular, in low earth circular orbits without mobile flight for orbital control, this system is all-passive from the outset, without any power

consumption, but the orientation accuracy is very limited.

Since it is necessary to conduct frequent station-keeping maneuvers, and because of orbital eccentricity, an attached control apparatus should be available even if the apparatus does not operate continuously. Therefore the overall complexity corresponds to a conventional system. Its major shortcoming is that it cannot satisfy the requirements of orientational accuracy.

#### 18. Dual-spin Stabilization



##### (1) General description

Dual-spin stabilization is a standard technique applied by

geostationary communication satellites. The satellite utility compartment rotates at a rate of 60rpm; however, the utility compartment rotates in a direction that reverses through the shaft and power transmission components.

The main advantages are as follows:

Since the angular momentum is high, there is the inherent passive stabilization around two shafts.

The propellant orientation is applied with centrifugal force.

There is the thermal gravity balance (baking type).

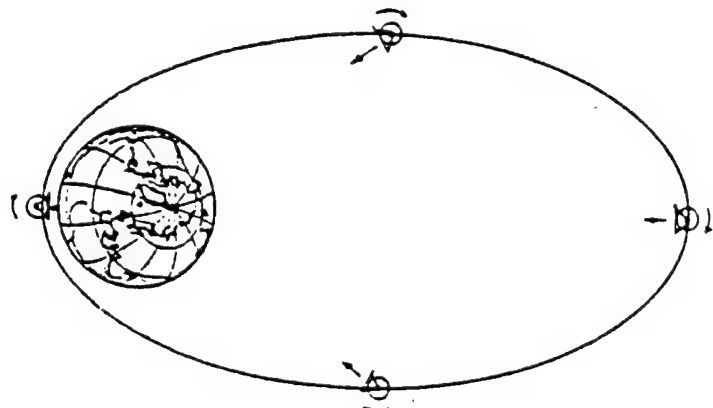
The first point can be used in the present research. The second point requires some design changes in multiple-tank shape. The third point is not applicable because there are too many variations along the solar-acting direction with the flight lifetime of the satellite.

## (2) Structural shape of satellite

To avoid unpredictable fuel wobbling, fuels should be packed into three fuel tanks around the central force-acting cylinder installed equidistantly. This requires a strengthened central force-acting cylinder in order to withstand the stress during the launching environment period. Since surface-tension apparatus is not to be installed in the fuel tank, a fuel tank within the available diameters can be applied. The major advantage is reduction of the complexity of the reaction control system. A total of three hydrazine boosters is enough to accomplish all

maneuvers for attitude control and station-keeping.

Since the angular momentum vector should be kept perpendicular to the orbital plane, the effective loading platform should rotate in the reverse direction in order to maintain earth orientation. Thus, the available shaft and power transmission components can be used. In addition, the phase control array antenna platform should be deployed. This is the main reason for adding more complexity to the payload.



### (3) System performance

The expected flight lifetime is not related to this control principle. There is no constraint on the performance of the entire system, especially orientation accuracy.

### (4) Mechanical complexity

To be free of the effect by means of this control principle

to the carrier compatibility, due to fuel tank layout, a shaft and power transmission components separate the payload compartment and the utility compartment. Together with the antenna deployment mechanism, such mechanical structure is very complex. During the launch period, interlocking should be present between payload compartment and utility compartment.

#### (5) Electrical complexity

With regard to the attitude control subsystem, electrical complexity is relatively low. However, due to the deployment of the antenna platform, there is an alternative inertia product. During power interruptions, the ovoid shape shows a tendency of rotational stabilization. Since the requirement for orientation accuracy is very low, a single acute-angled wave beam earth sensor is sufficient for attitude determination. Because of the adoption of a shaft and power transmission components for converting power and signals through a slip ring, electrical complexity is increased. It is further required of the deployment antenna platform and delocking payload compartment, adding further to the complexity of the electrical equipment.

Structural complexity: distributed fuel tank

simple attitude and orbital  
control subsystem

performance: as per technical specifications

complexity: shaft and power transmission

components  
antenna deployment  
costs: according to basic values

(6) Relative costs

Much of the costs can be saved in attitude control (acute-angle wave beam relative to scanning-type horizon sensor with the addition of a simpler control logic) and orbital control (three boosters are used instead of the typical eight boosters). The low cost of a single fuel tank (excluding surface tension measurement device) is better than multiple fuel tanks and more complex installations. By using a shaft, power transmission components and an antenna deployment mechanism, this leads to further additional costs. So, generally speaking, the costs of this approach are similar to the case when the selection is made of standby operational parts.

(7) Contractors' experience

Contractors are familiar with dual-spin satellite structural forms of the spin-stabilization of orbital transfer and communication satellites (especially the HS series communication satellites of the Hughes Aircraft Manufacturing Company).

(8) Preliminary conclusions and final conclusions

With respect to attitude and orbital control, dual-spin stabilization is very attractive, especially due to the very low

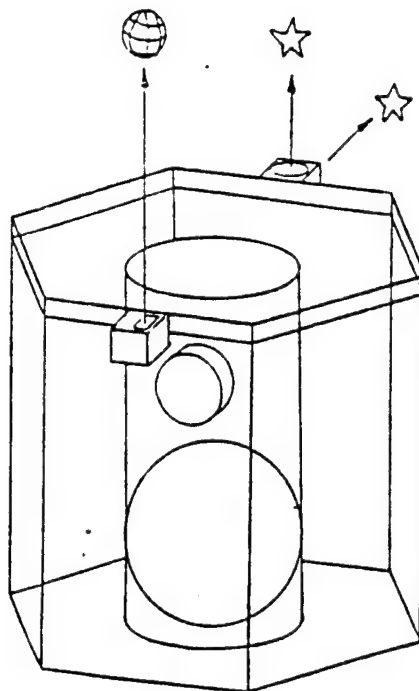
requirements on power sources and orientational accuracy. However, there are no advantages in thermal control. Since there is a great variation in direction of sunlight, we cannot apply the thermal baking mode. A major restriction is that the momentum ratio is required to be larger than 1.45. Since the satellite shape is subject to the central force-acting cylinder, the natural shape is quite long and slender. Due to this reason, and to avoid fuel wobbling that cannot be controlled, the concept of a single central fuel tank should be abandoned.

Deployment of the phase control array antenna platform may bring forth many problems in payload design. This is not the main topic in the research, but an explanation is in order. For the two other selection schemes on file, these schemes can also avoid the use of an induction shaft and power transmission components.

## 19. Three-axis Stabilization

### (1) General description

The most suitable control concept is momentum wheel stabilization, especially because the value of the perturbation torque (due to rigidity and compact satellite design) is so small that only a small amount of angle momentum vector is required for compensation. Usually the roll channel of the infrared earth sensor can be used to determine the direction of the angular momentum vector which should be perpendicular to the orbital platform with an accuracy of  $\pm 10^\circ$ . For example, when using the



Galileo infrared earth sensor used on the Orbital Test Vector (OTV) it is very difficult to continuously determine the roll angle because of changes in the earth image. However, in a satisfied separated orbital position, the result of at least two noncontinuous determinations is sufficient to determine the satellite roll angle and yaw angle.

The pitch control circuit should continuously use the pitch channel of the infrared earth sensor and the reaction torque of the flywheel. In powered flight during station-keeping, it is required to have the information source of the roll and yaw angles; the information can be provided with two integrated-rate gyroscopes. It is proposed to use the optical gyroscope,

developed for the TUBSAT.

(2) Structural shape of satellite

The fundamental shape of a satellite can be maintained, however when adding a momentum wheel, it is best installed in the inner wall of the central force-acting cylinder without requiring components for deployment or rotating structures.

(3) System performance

It is expected that the flight lifetime is not related to this control principle, and is not restricted to the performance of the entire system.

Structural shape: momentum wheel

central fuel tank (lower side)

Performance: as per specifications of technical norms

Complexity: earth sensor

Costs: based on fundamental values.

(4) Mechanical complexity

It is very simple for the mechanical status, especially the moving components and the installation of ignition components.

(5) Electrical complexity

Electrical complexity is determined by the momentum wheel, infrared earth sensor, and gyroscope, including the related electronic circuitry. Some minor improvements may be required in

the infrared earth sensor in order to adopt to orbital eccentricity.

(6) Related costs

The additional costs for the momentum wheel, infrared earth sensor, and gyroscope correspond to the cost of the reaction flywheel, or to the cost of the shaft and power transmission components, antenna deployment mechanism, and acute wave constrained earth sensor in the previous scheme. Development costs are very low because available hardware can be used.

(7) Contractors' experience

Contractors are familiar with this control mode of the OTS and other similar satellites. The TUBSAT is a three-axis stabilized satellite with the adoption of standard momentum wheel, solar sensor, and an optical gyroscope.

(8) Preliminary Conclusions and Final Conclusions

The three-axis stabilization control mode is more complex than dual-spin stabilization. Especially since there are great variations in the earth image, it is more advantageous and simpler in other respects.

20. Overall Conclusions

Gravity-gradient stabilization of the gravity gradient is not considered.

Three-axis stabilization is fundamental.

Dual-spin stabilization is an effective substitute scheme.

Gravity-gradient stabilization is not considered because its inherent simplicity cannot be sufficiently utilized, mainly because the orientation accuracy exceeds one numerical magnitude of a target at  $\pm 1^\circ$ .

Comparison between dual-spin and three-axis stabilization is similar to the comparison of the concept of a geostationary satellite. In other words, system performance and relative costs are very close in both cases. However, with regard to this structural shape, the three-axis system is somewhat superior.

Deployment of the solar cell array can be avoided:

in this case, the dual-spin system is somewhat lower in grade.

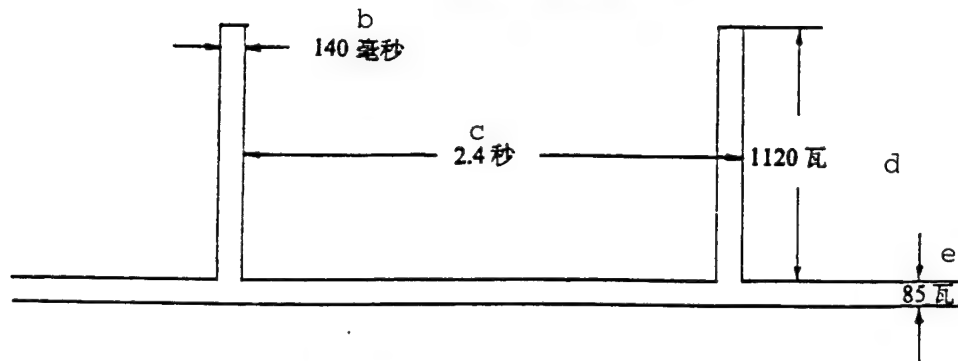
Since the solar direction is almost omnidirectional, the thermal control advantage of the baking type disappears. Therefore, although further study is made on the three-axis stabilization scheme, but the spin-stabilization scheme is not abandoned.

## V. RESEARCH REPORT ON SECOND TASK

### 1. Power Source

Payload power requires a constant load  $L_c$  of 85W, and short-pulse loading lasting 140ms. Short-pulse loading is 280W in radiofrequency power. For a 25% efficiency, the power supply should be 1120W. The pulse repetition rate of time-division

a 有效载荷功率剖视图



KEY: a - payload power profile diagram  
b - milliseconds c - seconds d - 1120W  
e - 55W

multiple access is 2.4s, so the average additional load  $L_a$  is:

$$L_a = \frac{0.14}{2.4} \cdot 1120 = 65 \text{ W}$$

The total required power of an average payload is:

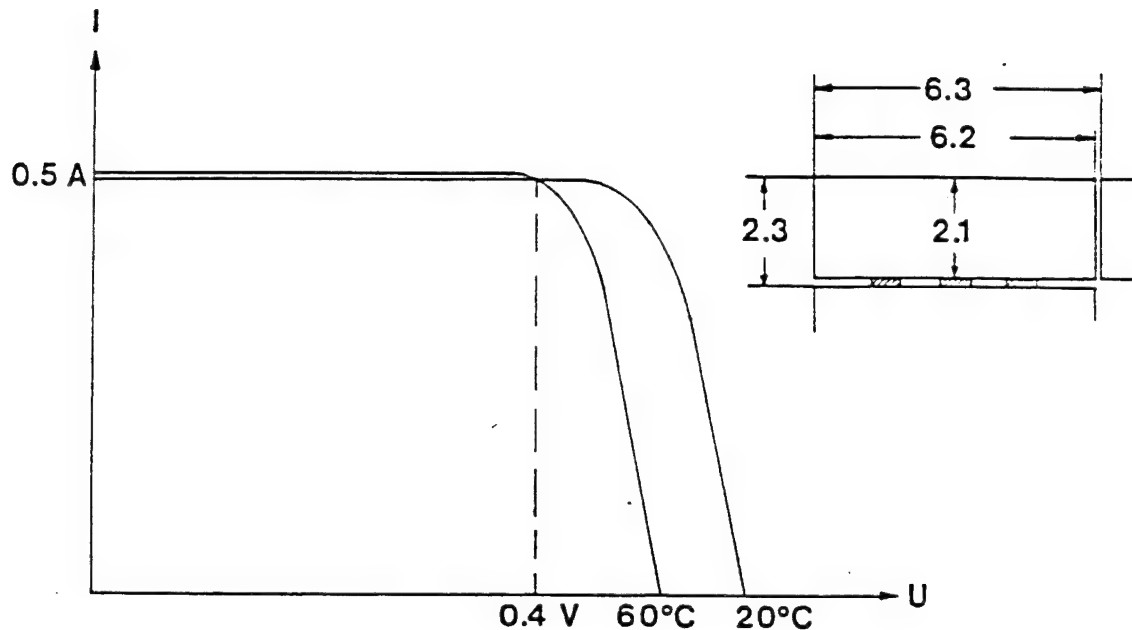
$$L = L_a + L_c = 150 \text{ W}$$

The average power consumption for the satellite utility wheel is 25W, which is mainly made of 10W for the attitude and orbital control subsystem, 10W for heater power in the thermal control subsystem. The remaining 5W is used for the on-board computer (less than 1W) and as reserve. The operating cycle for charging the storage battery is estimated to be 10%; so 25W can be used for charging the storage battery.

Used on the International Communication Satellite VI and the TUBSAT, the Spectrolab K-7000 solar cell provides the primary power. The dimensions of a block of solar cells (including the distance between two adjacent cell sheets in the array) are

6.3x2.3cm. The rated voltage at the operating point is 0.4V and the rated current is greater than 0.5A.

Solar Cell



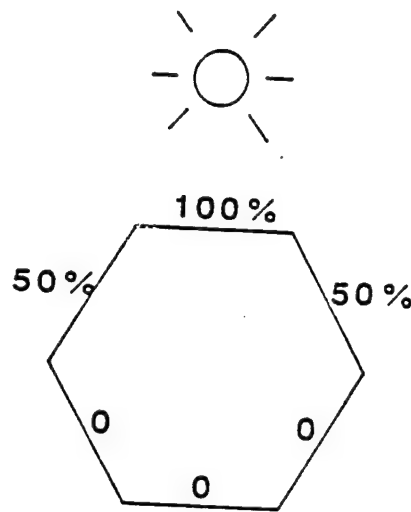
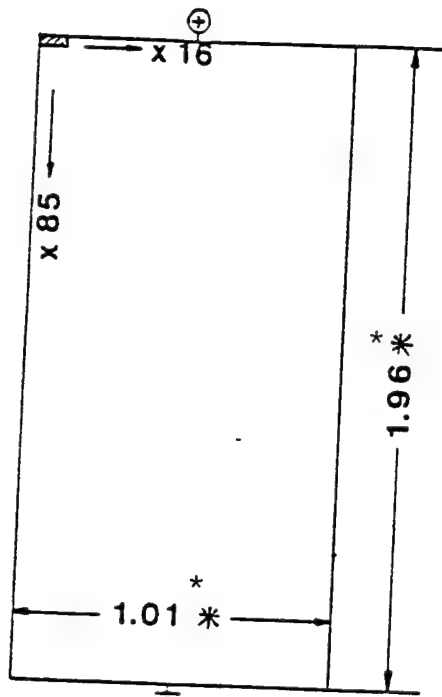
85 cell sheets can be connected into one band, providing the following rated voltage:  $U=85 \times 0.4=34V$ .

Such voltage is sufficient to maintain the rated voltage of 28V for the storage battery. Each module of boards can provide as many as six bands of such cells for parallel connection. When the solar cells receive enough sunlight, an overall current of 8A can be generated. A module of fully-illuminated boards provides the following maximum power for a 28-V trunk line:  $P=8A \times 28V=224W$ .

In this situation, two modules of adjacent solar cell boards

are in a semi-illuminated state, thus the overall maximum solar power is:  $P_{\text{max}} = 2 \times 224 \text{W} = 448 \text{W}$ .

### Solar Cell Array



KEY: \* - meters

If the direction of sunlight and the satellite equatorial surface form the angle  $\alpha$ , the total power  $P_{\text{eff}}$  is reduced to:

$$P_{\text{eff}} = P_{\text{max}} \cdot \cos \alpha.$$

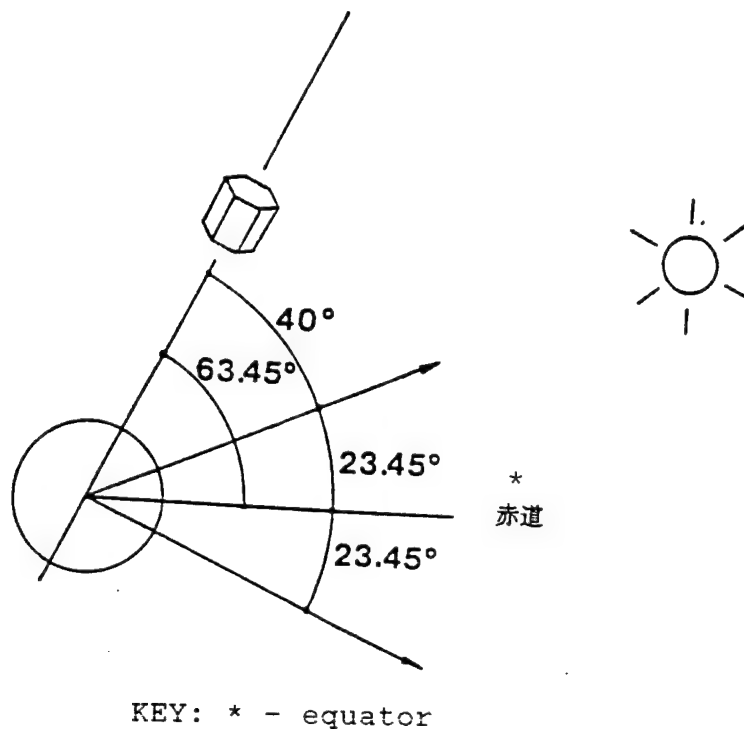
To differentiate the storage battery requirements, we discuss the two extreme situations of solar illumination:

(a) when the vector of the sunlight direction vector is outside the orbital surface and (b) when the vector of sunlight direction is parallel to the orbital plane.

In the situation (a), the sunlight vector dip angle,

relative to the orbital plane, varies between  $40^\circ$  (summer solstice) and  $86.9^\circ$  (winter solstice). Even in the worse condition (summer solstice while the satellite is at apogee), the output power of the solar cell array is:  $P=448 \cdot \cos 40^\circ = 343W$ .

Sunlight Illumination [outside orbital plane]



KEY: \* - equator

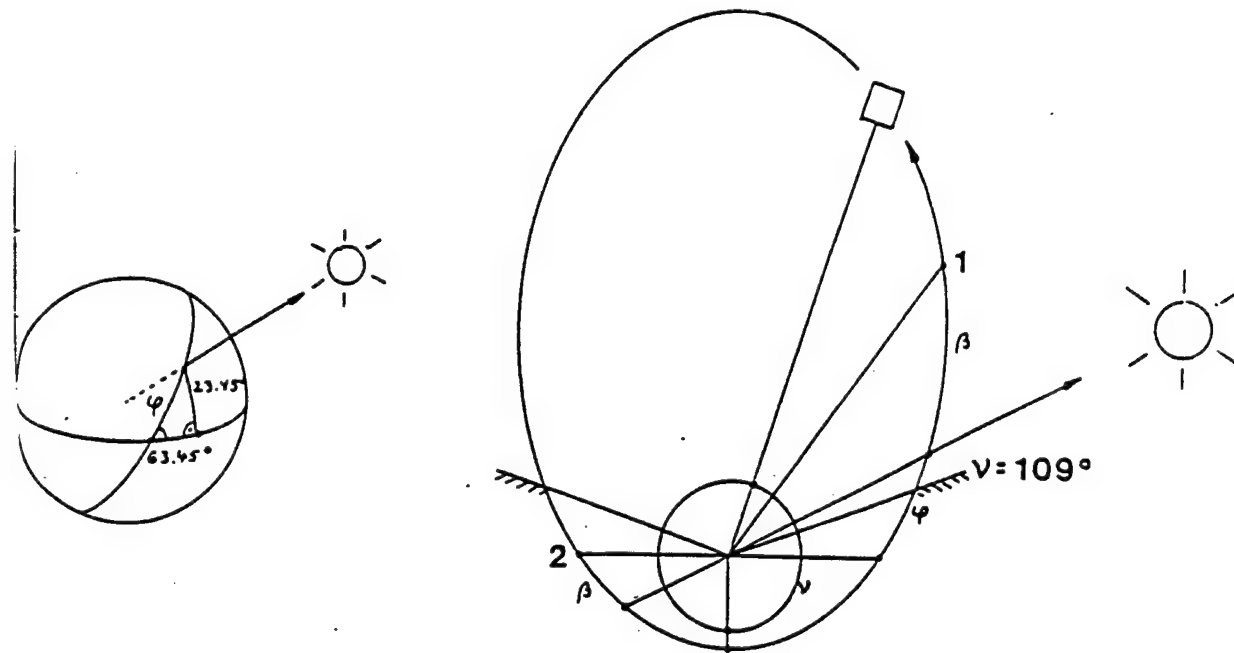
This value greatly exceeds the trunkline load of 200W. During this period of the year, the satellite does not require power from its storage battery.

When the sunlight direction vector is just coincident with the orbital plane, the included angle between the satellite yaw and the sunlight direction vector can vary between  $0^\circ$  and  $360^\circ$ . So a storage battery is required for auxiliary power.  $\phi$  can be calculated as a portion of the spherical triangle:

$$\sin \phi = \frac{\sin 23.45^\circ}{\sin 63.45^\circ} \quad \phi = 26.41^\circ$$

$\beta$  is the minimum angle between the satellite yaw axis and the sunlight direction providing 200W of solar power. In other words, the power for the load is required at:

$$\sin \beta = \frac{200W}{448W} \quad \beta = 26.51^\circ$$



$T$  is the period calculated for the last time passing through the perigee:

$$T = \sqrt{\frac{a^3}{\mu}} \cdot \left(\frac{\pi}{90} \cdot \arctan\left(\sqrt{\frac{1-\varepsilon}{1+\varepsilon}} \tan \frac{\nu}{Z}\right) - \frac{\varepsilon \sqrt{1-\varepsilon^2} \sin \nu}{(1+\varepsilon) \cos \nu}\right)$$

Since  $\nu = 90^\circ + \beta \pm \phi$ , the derived results are:

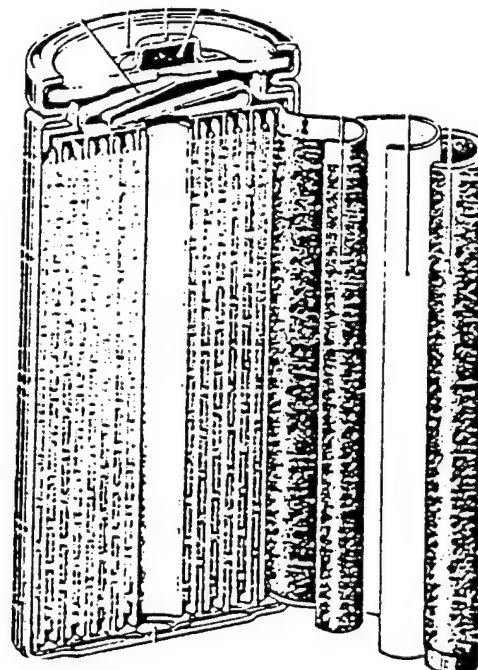
$$T_1 = 1.35h \quad T_2 = 0.25h.$$

When the satellite is higher than 10,635km, it is only

required to operate for the payload. In other words, when radius  $R$  is at least 17,013km, the corresponding orbital angle  $\nu$  is:

$$\nu = \text{arc cos} \left( \frac{a(1 - \varepsilon^2) - r}{\varepsilon \cdot r} \right) = 109.04^\circ$$
$$T_0 = 0.40 \text{ h}$$

Storage Battery



During the orbital period when it is required to operate for the payload but there is insufficient sunlight (due to under-illumination, in the earth's shadow), the overall time period  $T_W$  is in the worse situation:

$$T_W = T_1 + T_2 - 2T_0 = 0.8 \text{ h.}$$

With respect to the power supplied by the storage battery, in the worse situation when the load at  $200V \cdot 0.8h = 160Wh$ , cadmium-nickel storage battery is selected because of its well-known flight record. At least the storage capacity  $C$  should be

provided:

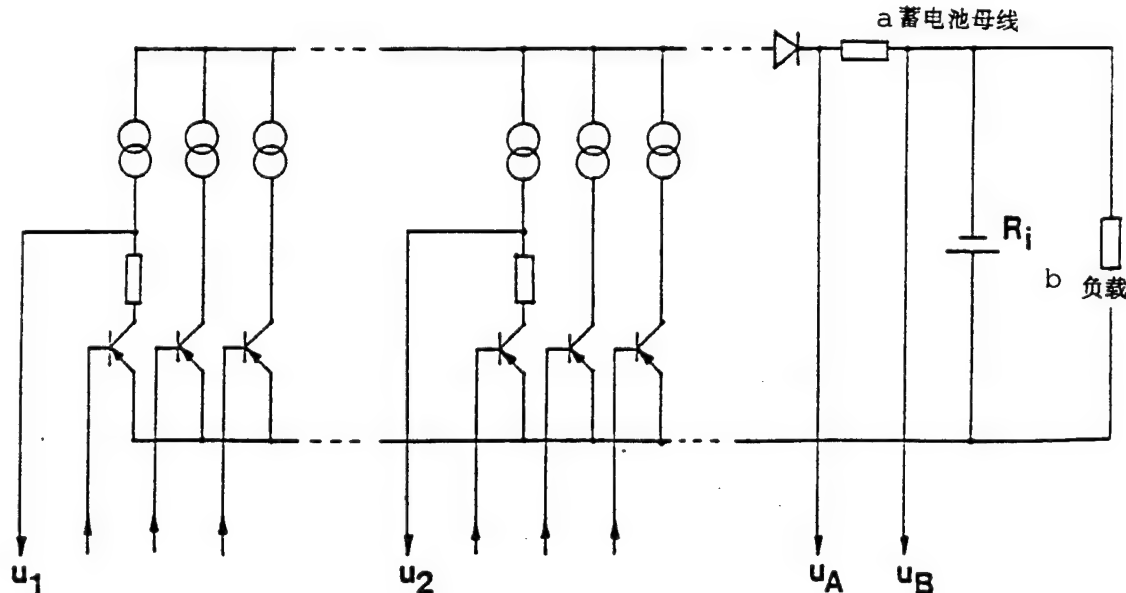
$$C = (\text{load}) / [(\text{bus voltage}) \times (\text{discharge extent})] = \\ = (160\text{Wh}) / [28\text{h} \times 0.6] = 9.5\text{Ah}$$

The 10Ah capacity storage battery was selected from the shaft production line. The total number N of the series storage battery is:

$$N = (\text{bus voltage}) / (\text{voltage of unit cell}) = (28\text{V}) / (112\text{V}) \\ = 24 \text{ [sic]}$$

The total mass of 24 unit cells is  $24 \times 0.49 = 11.76\text{kg}$ . The total mass of the cell combination is 20kg. There are two sets of cells with 10kg per set in order to install and balance in the satellite.

Control Scheme



KEY: a - battery bus b - load

The 6x16 solar cell band and the storage battery is connected in parallel to the main bus. Each single band is controlled by a switch transistor, in turn controlled by the on-board computer. To select the appropriate series condition of the solar cells, the computer input data are:

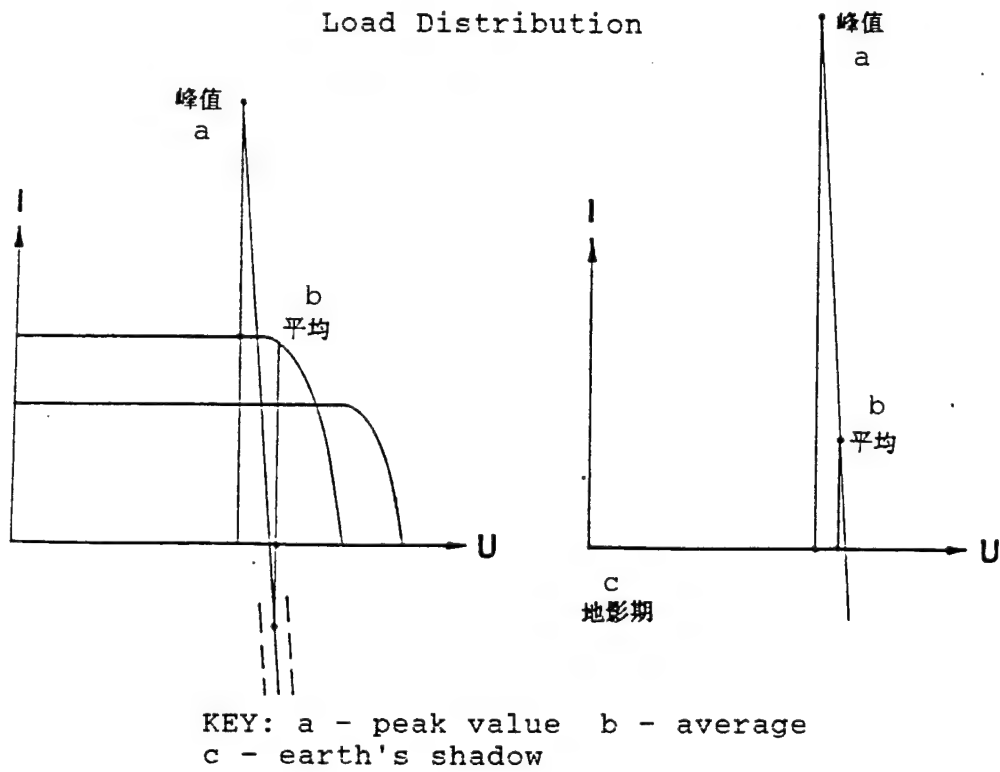
- sunlight illuminating each solar cell band:  $U_1$  to  $U_2$
- charging status of storage battery:  $U_A$ , temperature of storage battery
- current in bus to storage battery:  $U_A - U_B$
- estimated power consumption for the load.

The series connection of the solar cells is selected as follows: once the solar cell array is in the sunlight, generally the trickle charge current to the storage battery should be maintained.

The main portion in the bus control scheme is to maintain low total resistance in the bus of the storage battery in order to minimize the bus voltage ripple due to time-division multiple-access. The internal resistance of a single cell is 40milliohms. With 24 single cells in series, the total resistance is  $R_i=0.1\text{ohm}$ . The maximum load current is 40A. Therefore, even given such low bus resistance, 4V of ripple will also be generated.

Although a single band of solar cells may possibly exhibit their different properties (mainly because of variations in single cells, solar illumination, and temperature), however the bus voltage is determined by the nearly-vertical inclination

indicating low internal resistance in the storage battery. The bus voltage of the standard storage battery is determined by its charge/discharge status. The typical long-term variation range is 4V.

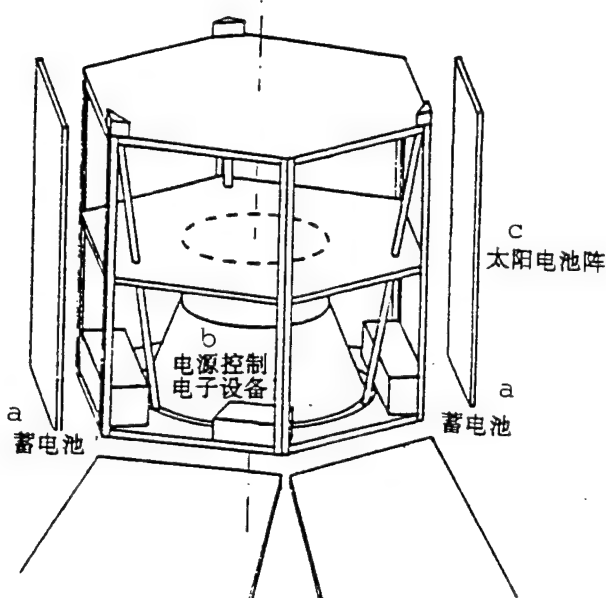


The series conditions of solar cells are determined by the on-board computer. The total current slightly exceeds the current for the average load, so that the excess current can be used for trickle charging of the storage battery. The peak load is mainly provided by the storage battery for buffering some solar cell bands. During periods in the earth's shadow, power supply comes mainly from the storage battery.

Generally, the power supply bus is not controlled by voltage because the voltage fluctuates due to the charging status of the battery. Therefore, if necessary the voltage should be

controlled by the various power users. The advantage of this control scheme is its simplicity, favorable to low-voltage conditions in bus use in time-division multiple access, and this control scheme can be used for operation in sunlight and in the earth's shadow.

Layout Diagram



KEY: a - storage battery b - power control electronics c - solar cell array

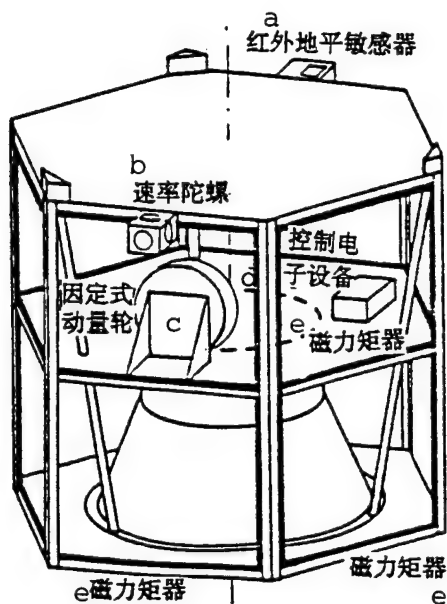
The upper portion of the lower equipment platform (outside the lower skirt of the fuel tank supporting members) is used to install the power supply system, especially for installing two battery sets. The lower surface of the lower equipment platform can be reserved for beneficial thermal control, such as adherence of a second surface mirror.

Since the switch transistor of the solar cell band is also installed in a position near the lower equipment platform, this

position can also serve for installation of power control electronic equipment (PCE).

## 2. Attitude and Orbital Control Subsystem (AOCS)

Layout Diagram

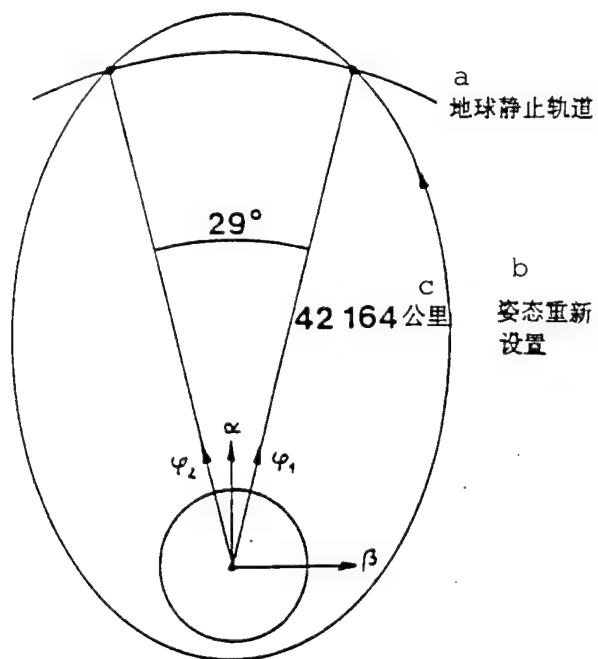


KEY: a - infrared horizon sensor b - rate gyroscope c - fixed type momentum wheel d - control electronics e - magnetic torque device

The attitude and orbital control subsystem is composed of the following equipment: one fixed momentum wheel, one infrared horizon sensor, three rate gyroscopes, and one control electronic unit.

Any standard products used for the OTS satellite can be adopted for the fixed-type momentum wheel and the infrared horizon instrument. The magnetic torque device is an aluminum coil around the satellite, arranged so that the dipole axes are

perpendicular to each other. For the rate gyroscope, we can use the products of the current scheme (such as Olympus satellite), or to apply the satellite-direction discriminator which was developed for this purpose. The control electronic units include the AOCS computer, booster, and magnetic torque drivers.



KEY: a - geostationary orbit b - attitude  
reset c - kilometers

Specifications of the fixed-type momentum wheel should satisfy the requirements for only adjusting once the momentum vector in each orbit. The momentum vector attitude is reset around the apogee (advantageous field of view for infrared horizon sensor), and adjusted to the beneficial magnetic field around the perigee. By reaction torque to control the momentum wheel, the closing of a pitch-rate gyroscope is acted upon in the

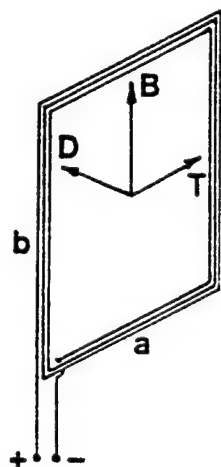
pitch circuit.

The infrared horizon sensor is designed with a certain size of earth's shadow. The sensor is usually employed in a geostationary orbit. To avoid redesign costs, off-the-shelf stock items can be purchased from Official Galileo, Soderm, MBB, or American suppliers. The sensor is used in two positions:  $14.5^{\circ}$  prior to and following apogee. At this time, the radius of the NAVSAT satellite orbit is equal to the radius of the geostationary orbit.

To reset the inertial direction of the momentum vector for roll readings  $\phi_1$  and  $\phi_2$ ,  $\alpha$  and  $\beta$  are used to indicate the following:

With the velocity integration mode, pitch readings can be used for the rate gyroscope for marking the pitch control circuit. Due to the earth's oblateness, the gyroscope targets should be continuously calculated by the AOCS computer.

#### Momentum Loading



The loading momentum is the redirection-setting of the momentum vector. This action is accomplished by the magnetic torque device. With the dimensions of axbxn coils, the coils provide the polar moment D of the magnetic dipole:  $D=a'b'n'i$ .

i represents the current passing through the coil. The vector of the magnetic torque is the vector product of the earth and the magnetic induction intensity B:  $T=DxB$ .

B varies between  $2.75 \cdot 10^{-5} \text{ Vs/m}^2$ , on the earth's surface, and  $10^{-7} \text{ Vs/m}^2$ , in the geostationary orbit. Near perigee, the value of B is  $10^{-5} \text{ Vs/m}^2$ . By substituting  $a'b=2 \text{ m}^2$ ,  $h=100$  and  $i=1 \text{ A}$ , T becomes:

The power input  $\omega$  is  $H=25 \text{ Nms}$ :

$$\omega = \frac{T}{H} = 0.8 \cdot 10^{-4} \text{ rad/s} = 0.275^\circ / \text{min}$$

The proposed cross-section of aluminum wire is  $1 \text{ mm}^2$ . Then the coil resistance is:  $R = \frac{1}{K} \cdot \frac{1}{q} = \frac{1}{33} \cdot \frac{600}{1} = 18 \Omega$

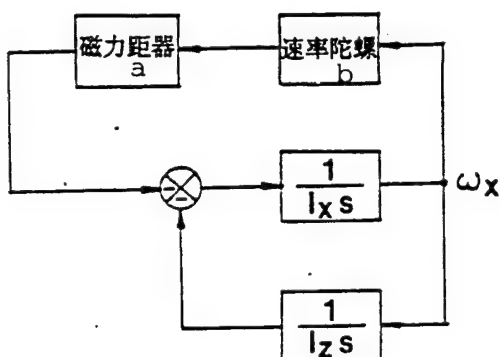
The mass of the coil is:  $m=1 \cdot q \cdot \rho = 600 \cdot 1 \cdot 2.7 = 1620 \text{ g}$

To measure roll (or yaw), the rate gyroscope and the corresponding magnetic torque device can be used to sense and damp the fluctuations of the satellite around the roll axis. This maneuver is accomplished near the perigee.

In all normal operating modes, the booster remains closed. Only during the position-capturing/station-keeping does its self-locking valve open. Moreover, three rate gyroscopes operating in the velocity-integration mode are used to control the corresponding opening or closing of the booster. The momentum

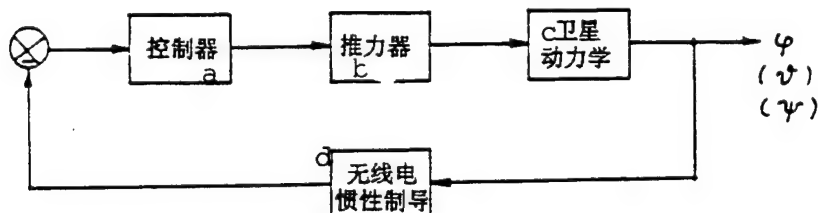
wheel is off-loaded with a switch to the intermediate-voltage power level. This corresponds to a flywheel with a counter-voltage for maintaining the rated speed.

#### Flutter Damping



KEY: a - magnetic torque device b - rate gyroscope

#### Position-capture/Station keeping



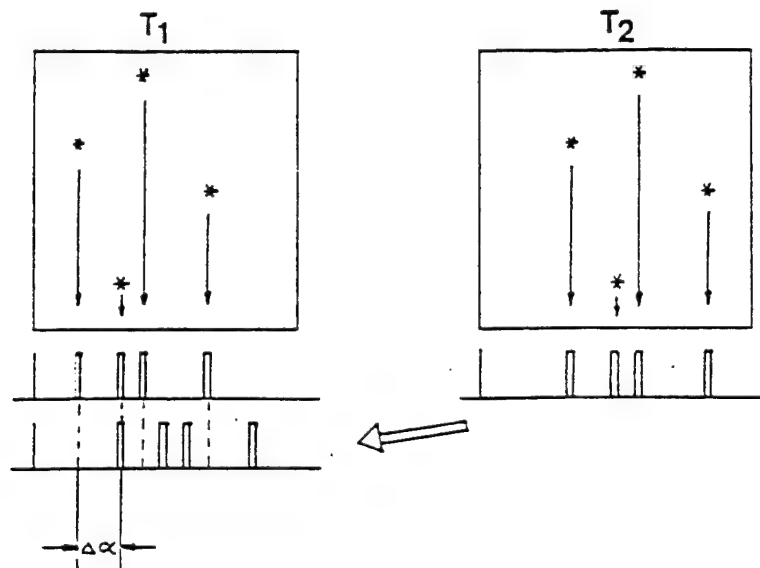
KEY: a - controller b - booster c - satellite dynamics d - radio inertial guidance

It is proposed to use the satellite-direction discrimination sensor to replace the rate gyroscope.

Such sensors were developed at Berlin Technical University; its certification in outer space will be conducted in the TUBSAT satellite scheme. Its operating principle is as follows:

- a standard CCD camera photographs the satellite position image in its  $T_1$  visual field. This measurement is repeated on

$T_2$ . If at least one satellite shows up in a data train, its position is at logic 1 on the train locator, otherwise at data 0 as marked. The second train search device applies the reference locator as its datum motion until the optimization is attained. If the sensor applies the velocity-integration mode, in order to reach the result that the stepping number of a direction is proportional to the angle  $\alpha$ ,  $T_1$  is the origin of events, such as station-keeping or the maneuver-onset time.

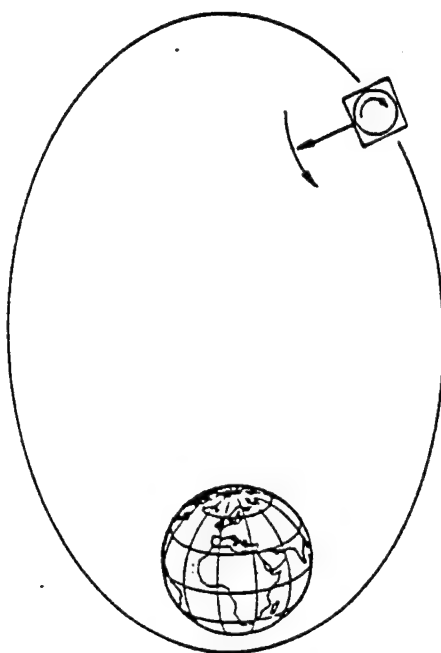


When applying the velocity-integration mode with short interval readings, the new readings are compared with the previous readings. The most optimal reading divided by the value of the time interval between two adjacent readings is proportional to the angular velocity of the satellite rotating about its single axis.

Compared with conventional gyroscopes, such sensors have the

following advantages: drifting without radio inertial guidance, low power consumption, freedom from wear, and low cost.

#### Emergency Safety

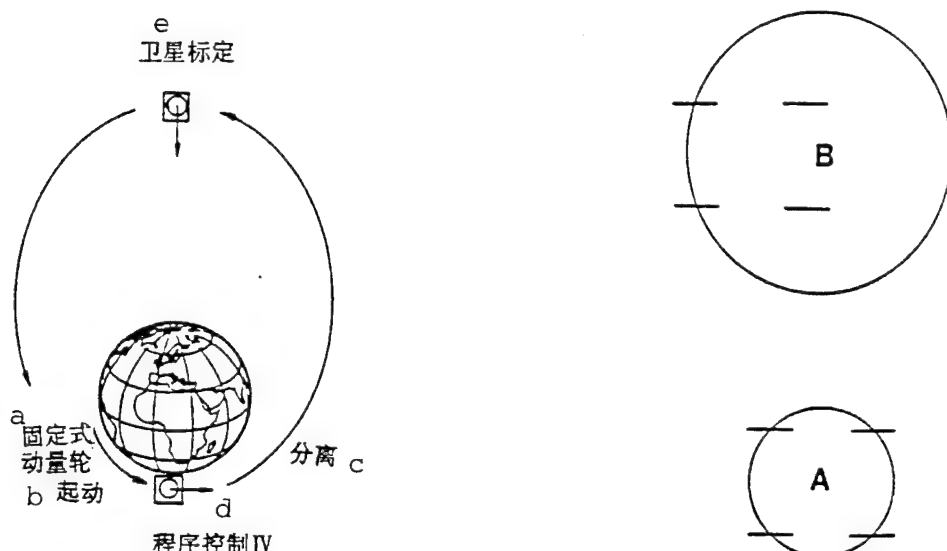


Since a booster is not used during the normal operation mode and also very small magnitude of torque is generated by the magnetic torque device, the only correlated source is variation of the pitch control circuit. If unforeseen events occur, it is important to restrict the malfunction within the pitch control circuit. Even when the self-locking valve remains closed, to avoid spin of the oblate body, the satellite computer will switch the flight wheel to the main bus voltage. In other words, the satellite is converted to its safety mode.

If any abnormal trace occurs during the positioning

maintenance period, the on-board computer will immediately shut off the self-locking valve in order to prevent booster leakage in the system. Such leakage may damage the momentum vector.

#### Earth Capturing Sequence



KEY: a - fixed type momentum wheel    b - starting  
c - separation    d - program control IV  
e - satellite marking

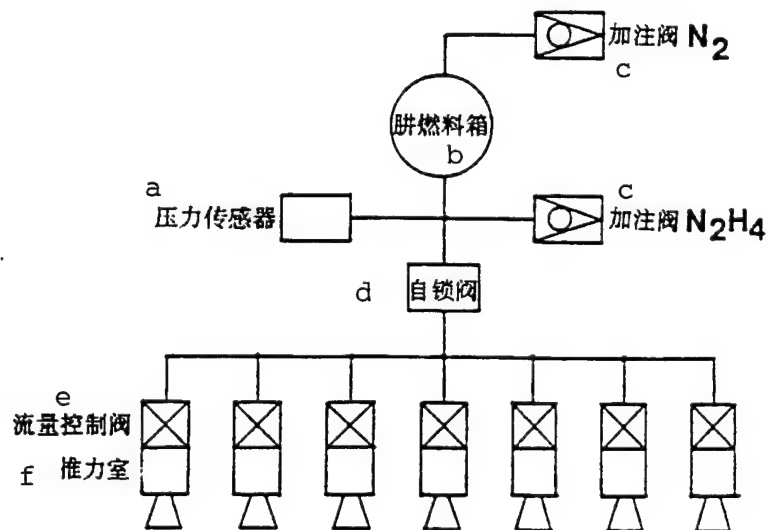
Before the fourth and final operation of the carrier second stage takes place, at some appropriate time the momentum wheels of both satellites rotate at high speeds at the rated velocity. In program control IV, the direction of the momentum vector is perpendicular to the orbit without further adjustment. The initial conditions of the pitch angle are determined by the inertial guidance system of the carrier up to separation; these conditions are inspected by the pitch gyroscope of the satellite.

At apogee, the earth's image is quite small (B). Although it is not as small as the geostationary orbital distance (A),

however, the pitch angle can be marked in relative accuracy. Therefore, the pitch angle should be measured by the radiation thermometer (thermocouple) either in the left sets or right sets of the infrared horizon sensor. In addition, proper adjustments to the enlarged dimensions of the earth should be made. To obtain the high accuracy of orbital insertion for the final proportion of the satellite proportion system, it is very important to have low gyroscopic drift for the high quality marking at perigee of the last orbit, and between the perigee and apogee.

### 3. Reaction Control Subsystem

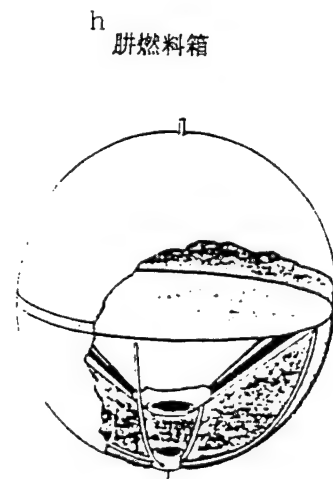
Block Diagram of Reaction Control Subsystem



KEY: a - pressure sensor b - hydrazine fuel tank  
 c - intake valve d - self-locking valve e - flow control valve f - thrust chamber

The reaction control subsystem (RCS) is composed of the following main equipment components: one hydrazine fuel tank, two fuel intake valves for N<sub>2</sub> and N<sub>2</sub>O<sub>4</sub>, one pressure sensor, one self-locking valve, seven flow control valves, and seven thrust chambers.

类型 a	容积(分米 <sup>3</sup> ) b	尺寸(毫米) c	质量(千克) d
OST01 / 0	235	赤道内直径: 748 内高度: f 786	16
OST02 / 0	350	赤道内直径: 912 内高度: f 786	20
OST03 / 0	416	赤道内直径: 1070 内高度: f 769	30
OST05 / 0*	38	球形箱内直径: 420	4
OST04 / 0	428	赤道内直径: 875 内高度: f 875	29
OST06 / 0	516	赤道内直径: 875 内高度: f 1150	23
OST07 / 0	267	赤道内直径: 600 内高度: f 1150	16



KEY: a - model b - capacity (decimeter<sup>3</sup>)  
 c - dimension (millimeters) d - mass (kg)  
 e - internal [satellite] equatorial diameter  
 f - internal height g - internal diameter of  
 spherical fuel tank h - hydrazine fuel tank

A hydrazine fuel tank may be purchased from many suppliers. In the MBB/ERNO production line, the model OST02 surface tension was selected because it has a large enough capacity, at 350L, and

its mass is relatively moderate, at 20kg. This fuel tank is suitable to the German postal satellite/Kopernikus scheme.

This fuel tank is composed of two compartments. The upper portion serves for fuel discharge from the exit terminal of the tank in the acceleration stage. In other words, fuel is discharged in the normal application situation at the maneuvering period when entering the orbit at apogee. In this operation, the upper portion of the fuel will be exhausted during the station-capture period. Then the boosters in three planes accelerate the satellite to continuously feed the fuel to the exit.

As the satellite arrives at the geostationary orbit, only 79kg of propellant is required for 10y of station-keeping. This fuel remains in the lower portion of the compartment, and the fuel is collected by the separation panel that simultaneously controls the center-of-gravity position and excessive fuel sloshing, and the surface tension of the inner lining.

The film separation type tank is an effective substitute scheme. However, with regard to long-term application, small particles will be produced in the film separation material. These particles may possibly block the flow control valve or filter. Since the hydrazine fuel has a spontaneous dissolution reaction, gas will always be generated. As there is no gas bubble collector in the film separation tank, the gas produced enters the pipeline system and may interfere with booster action, as indicated in operating experiences with the OTS satellite.

The CHT20 is a hydrazine fuel booster made in a production

line of the MBB/ERNO Corporation. A substitute scheme can apply the SEP.20-Newton booster. The SEP.20-Newton indicates a medium-thrust level booster. The applicable range is between 0.5 and 2500Newtons. This booster is a relatively good trade-off with respect to large thrust requirements during the position-capture period, and low thrust requirements during the station-keeping period. These boosters can be also used for attitude control.

#### Components of Thrust Chamber



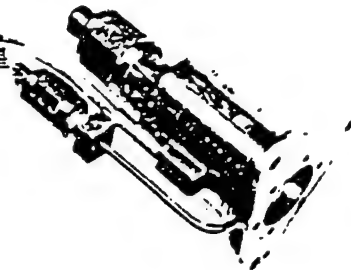
Such boosters have been used in many schemes, including the International Communication Satellite III, AEROS, GEOS, and EURECA. The specific thrust is higher than 2.25km/s, and the thrust mass is 200g.

Type 102.1 flow control valves are made on the MBB/ERNO Corporation production line. Such valves are suitable to the thrust chamber CHT20. This is a double-seat valve, capable of providing interior replacement when one seat leaks. According to

the type 102.1 flow control valve, successful flight records in OTS and MARECS satellites, such valves operate in the ECS, TELECOM-1, and the ISPM satellites; the valve mass is reduced to 100g.

#### Flow Control Valve

- a 轻型流量控制阀 102.1 适用于 20 牛顿真空推力
- b 推力器的流率, 1979 年鉴定合格
- c 用于欧洲通信卫星、电信-1、ISPM 和所有后继星
- d 质量: 100 克



KEY: a - type 102.1 light flow control valve is suitable to vacuum thrust of 20Newtons b - flow rate in thrust device, passed certification in 1979 c - used in European Communication Satellite (Telecommunication-I, ISPM, and all succeeding satellites) d - mass (100g)

LV104.1 is a single-seat self-locking valve made on the MBB/ERNO Corporation production line. Substitutes for this valve can be bought in the United States. During power failure, such valves still remain in their switched position. The valve includes an indicator for the switching position. Such valves are compatible with hydrazine fuel and have been certified on the METEOSAT, EURECA, and HIPPARCOS satellites. The valve mass is 180g.

The intake/exhaust valve for nitrogen and hydrazine may be purchased from many suppliers in Europe and the United States. The intake/exhaust valve 105.1/106.1 is an example of products by the MBB/ERNO Corporation. Its mass is 55g.

The pressure sensor cannot be bought directly from the MBB/ERNO Corporation, but may be available from several suppliers in the United States. Its mass is approximately 100g.

#### Self-locking Valve

a 用无源正向开关位置关  
闭阀门相应位置显示器

b 与肼燃料相容

c 于 1987 年鉴定

d 质量: 180 克

e 流量: 40 克 / 秒

f 1型:单组元推进剂肼

g

应用: Meteosat 卫星 h

Eureca 卫星 h

Hipparcos 卫星 h

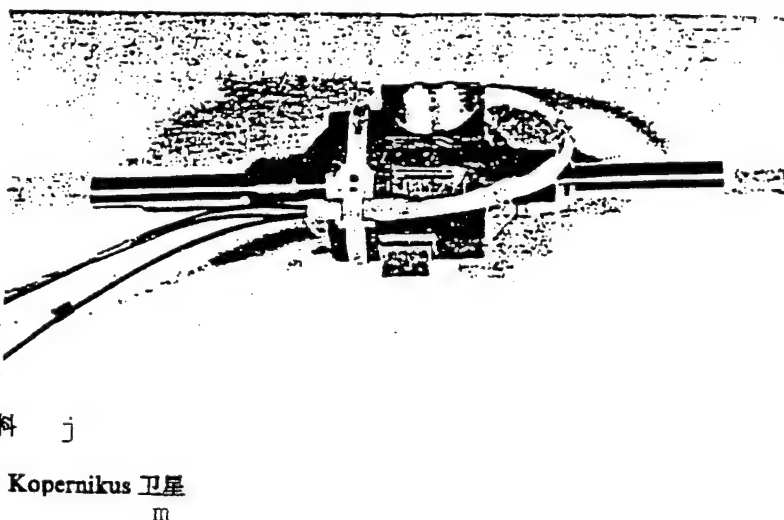
i

2型: 双组元推进剂燃料 j

k 应用: 西德邮政卫星 Kopernikus 卫星

l

m



KEY: a - by use of powerless positive-direction switching position to close the valve, corresponding to the position indicator  
b - compatible with hydrazine fuel c - certified in 1987 d - mass: 180g e - flow: 40g/s  
f - model 1: monopropellant hydrazine  
g - applications: h - satellite i - model 2  
j - bipropellant fuel k - applications l - West German postal satellite m - Satellite Kopernikus

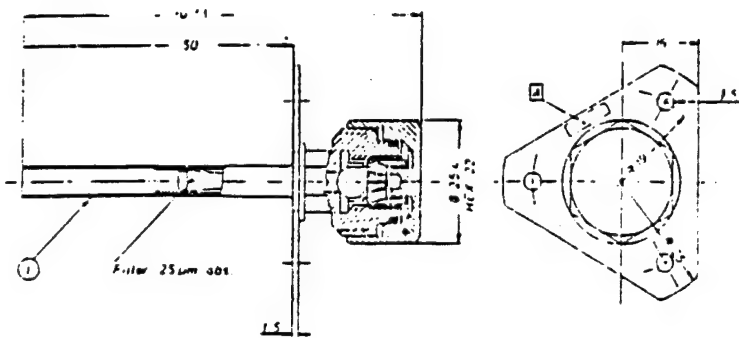
The reaction control system should be installed, if possible, inside the fuel tank support. The intake valve can be installed or removed from a platform at the bottom of the satellite. The hydrazine fuel tank is used for maneuvering within the orbital plane. The intake valve, the self-locking

valve, and three flow control valves/thrust chamber are installed within the fuel tank support frame.

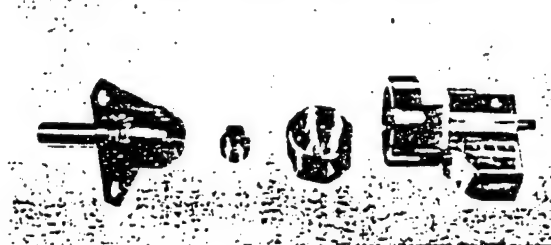
a 飞行质量: 55 克

b 应用:

OTS, ECS, MCS  
Telecom 1  
Skynet 4  
ISPM/Ulysses  
Giotto  
Eureca  
Hipparcos  
Meteosat  
Mato 4



c 加注和排泄阀



KEY: a - flight mass:55g b - applications  
c - intake and exhaust valve

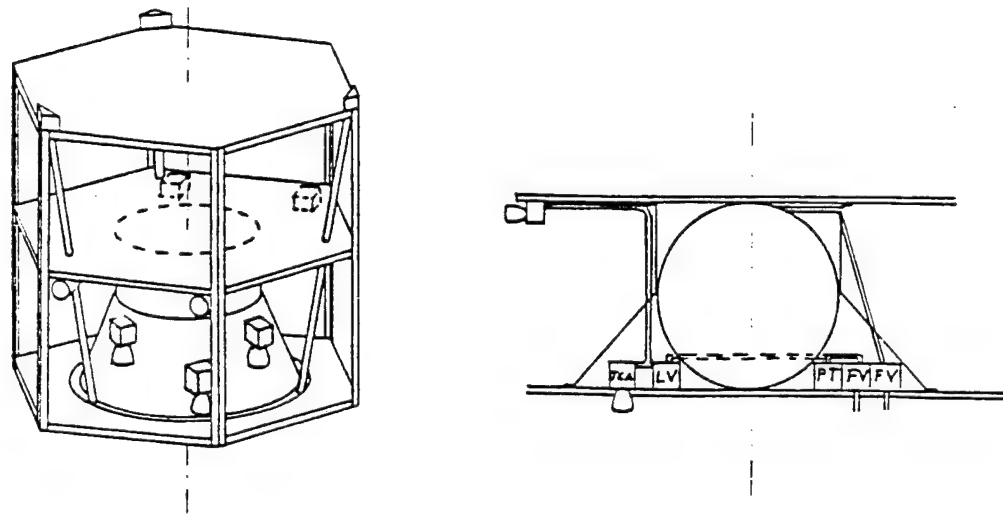
Used for maneuvering outside the orbital plane, four flow control valves/thrust chamber are installed beneath the central platform. It is proposed that before final assembly, the fuel tank support frame, the intermediate platform, and the entire reaction control system are assembled first as a structural member.

#### 4. On-Board Data Handling (OBDH) System

In the TUBSAT satellite, its tracking, remote sensing, and

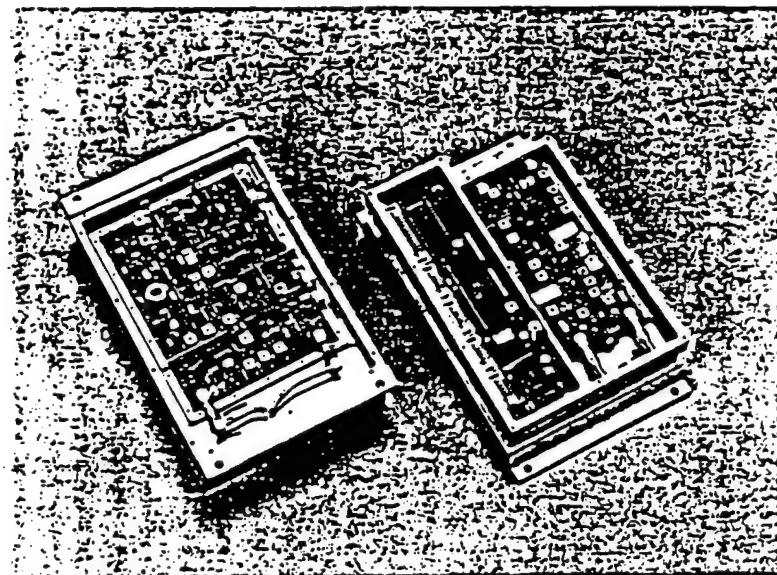
command subsystems includes the on-board data handling system in a chamber at the left side of the upper bottom plate. On the bottom plate, a transceiver transmits and receives the data at a frequency of 29MHz; a converter in the right-side chamber of the upper bottom plate converts the signals into the 138MHz (remote sensing) and 149MHz (remote control) frequency bands. This frequency band is the same as the frequency band used in the ECS satellite. The total mass is 1.8kg and the modulation mode is AFSK/FM.

#### Layout



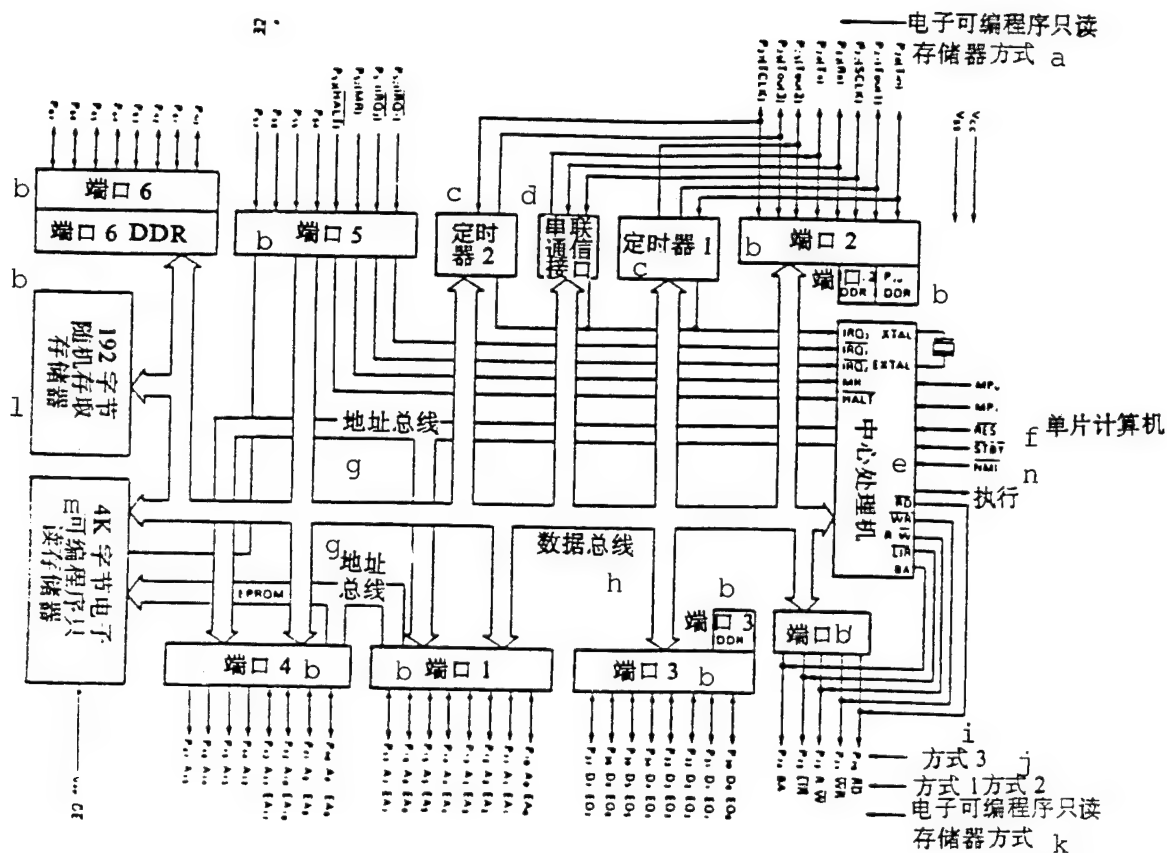
As discussed in the design evaluation conference, the portion of the transceiver and converter are considered as payload, especially due to different modulation modes (PSK), and transmission frequencies (S- and C-bands). The OBDH system is considered as the utility system in the satellite. The interface includes a bidirectional data flow of 5/0 volt power level. The

baud rate is to be determined (the highest is 64kbits/s).



The main component in the middle is the single-chip processor. The component at the upper right-hand corner is the RAM, and the component in the upper left-hand corner is the A/D converter. A timer circuit is placed in the lower right-hand corner. Through a 25-chip parallel interface and a 49-chip serial interface, the OBDH connects with the satellite.

The Hitachi single-chip processor (HD 63701 XO) is a CMOS 8-bit processor with a 16-bit trunk line. In the highest operating rate (200Hz), the maximum power consumption is 100mW. This system consists of a central processor, a 192-byte RAM, a 4k-byte ROM for compiled programs, two timers, one serial communication interface (SCI), and a 53-pin parallel input/output socket. The central processor provides four operating modes,

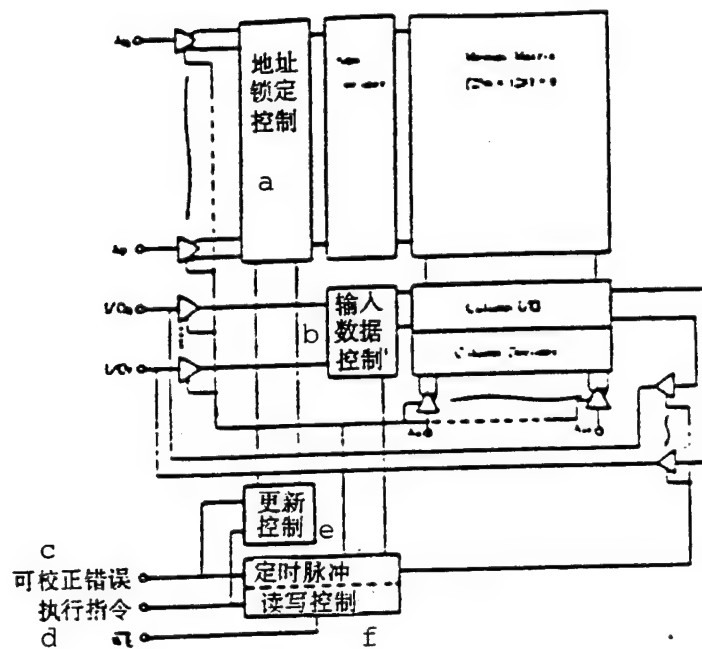


KEY: a - electronic programmable program read-only memory  
 mode b - interface c - timer d - serial communication  
 interface e - central processor f - single-chip  
 computer g - address trunk line h - data trunk line  
 i - mode 3 j - mode 1, mode 2 k - electronic  
 programmable program read-only memory mode l - 192-byte  
 random access memory m - 4K-byte electronic programmable  
 read-only memory n - execution

REMARKS:

Effective Address (EA)      Correctable Error (CE)  
 Digital Data Receiver (DDR)      Execution Order (EO)  
 Electronic Programmable Read-only Memory (EPROM)  
 Halt (HALT)      Interrupt Request (IRQ)  
 Odd/even Inspection (OE)      Message Processor (MP)  
 Memory Register (MR)      Nonshielding Interrupt (NMI)  
 Readout (RD)      Clear, Set 0 (RES)      Rewrite (RW)  
 Standby (STBY)      Write (WR)

## Random-Access Memory



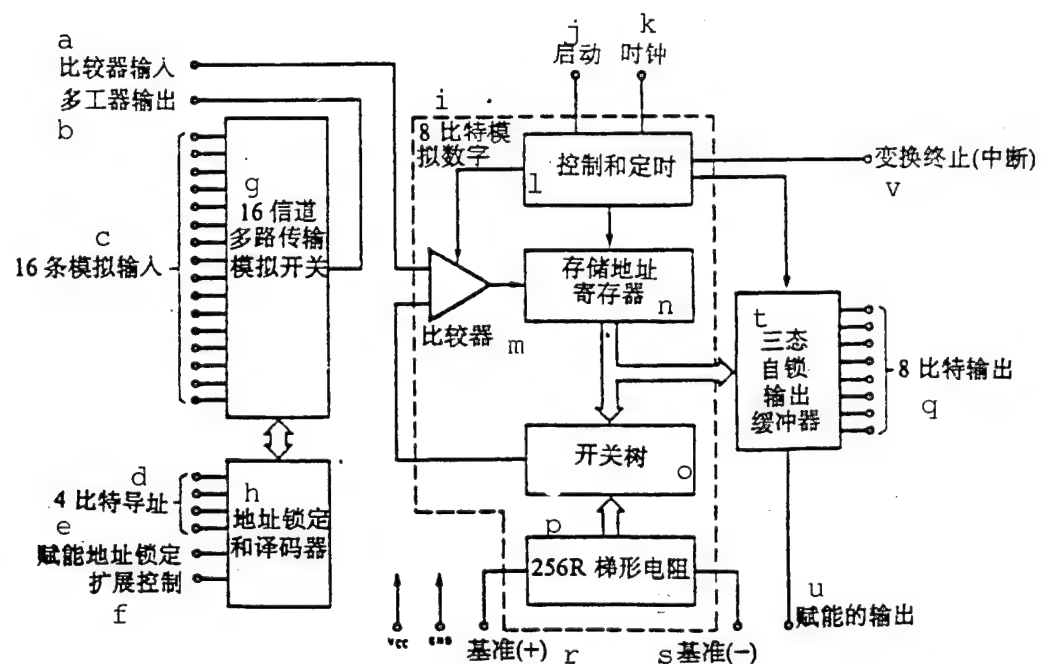
KEY: a - address locking control b - input data control  
c - correctable error d - execution command e - renewed control  
f - timing pulse rewrite control

including a single-chip mode (the largest number of terminals can be used) and an expansion mode (internal data and address trunk lines).

The SCI can conduct data exchange between (a) the payload reception and transmission mentioned above, and (b) other intelligent installations on board the satellite. Although all control functions in the satellite can be easily processed by chips of the single-board computer, yet the control function can be used more easily for software compilation and testing of

distributed functions, such as testing of the function of the

### Analog-Digital Converter



KEY: a - comparator input b - multiplexer output c - 16-line analog input d - 4-bit addressing e - energized address locking f - expansion control g - 16-channel multicircuit transmission analog switch h - address locking and decoder i - 8-bit analog digit j - start k - clock l - control and timing m - comparator n - stored address register o - switching tree p - 127R trapezoidal resistance q - 8-bit output r - datum (+) s - datum (-) t - 3-state self-locking output buffer u - energized output v - end of conversion (interrupt)

power control, thermal control, and attitude computers in the same kind of microcomputers. Through a OBDH computer, these data are collected. The mass of each chip is only several grams, and the size is  $10\text{cm}^2$ , power consumption is 100mW. Together with costs, these parameters can be neglected.

The Hitachi high-speed pseudo-static RAM HM 65256 AD provides a memory capacity of 32K bytes. In the extended-memory mode, 2 RAM can be connected directly through the 16-bit data trunkline of the microcomputer. Computer terminal 6 can be used for chip selection. When necessary, multiplexers can be connected to RAM of 8x64K bytes.

The analog/digital converter ADC 0816 is made available by the National Semiconductor Corporation. The converter can input 16 analog channels and 8-bit three-status locking output, up to the data trunk line of the microcomputer with expanded-operation mode. The 4-bit address trunk line requires 16 analog channels for addressing. The remaining 12-bit address trunk line can be used to select as many as  $12 \times 16 = 192$  analog channels without multichannel communication.

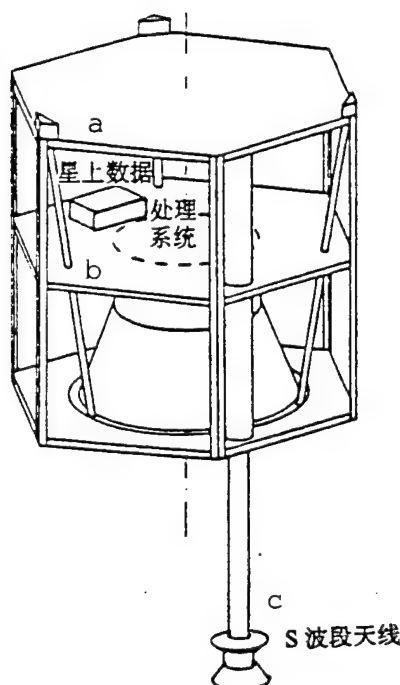
Even when the OBDH is expanded to maximum capacity, larger than that required to satisfy the NAVSAT, the mass is kept at less than 1000kg, and the average power consumption is less than 1W. The power source voltage is 5V.

Since the CMOS component and large-scale integration circuits are used, the only remaining important point to be taken care of is possible damage from radiation. In the ESA Pathfinder Scheme, the orbital test situation was observed for the TUBSAT system. The orbit (Ariane test orbit) is similar to the orbit of the navigation satellite. Possibly, some shielding effect may result in most sensing elements.

The on-board data handling system (OBDH) can be installed on

the middle platform. The S-band remote sensing and remote control antenna for orbital capture, and emergency and safety

Layout



KEY: a - on-board data    b - processing system  
c - S-band antenna

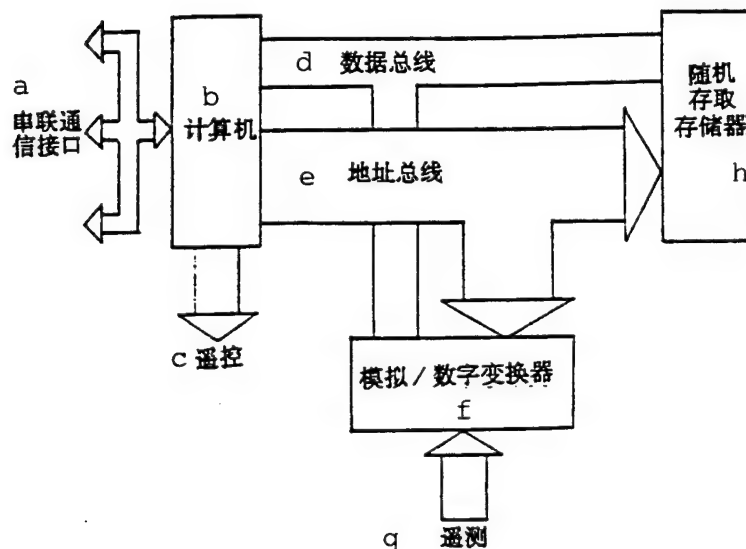
modes can be placed in a 2-m long cylindrical container within the satellite structure during launch. The antenna can be deployed after launch.

## 5. Thermal Control

The thermal control model of the satellite is composed of three platforms. Each platform is composed of a uniformly heat-dissipating device (payload power source, attitude and orbital

control subsystem, as well as a remote sensing and remote control power source, and power control and consumption), a central force-acting cylinder for containing the reaction control

Functional Block Diagram



KEY: a - serial communication interface b - computer  
c - remote control d - data trunk line e - address  
trunk line f - analog/digital converter g - remote  
sensing h - random-access memory

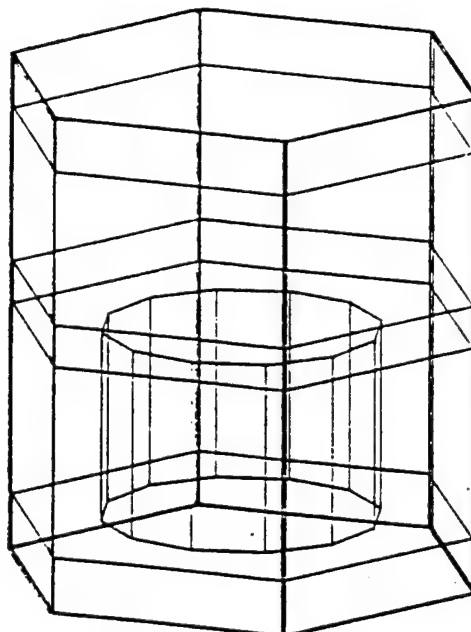
subsystem, and six solar cell panels.

The lower platform, middle platform, and central force-acting cylinder are mutually thermocoupled by an internal black paint coating; in addition, there is good thermal conductivity. This module is separated from the outside environment with 20 layers of superinsulated materials. During worse-case analysis

(low thermal inertia), it is assumed that the fuel tank is almost empty (loading with 5kg propellant).

Black paint coats the internal side of the solar cell panels in order to increase radiation coupling. During the first test,

#### Thermal Control Model

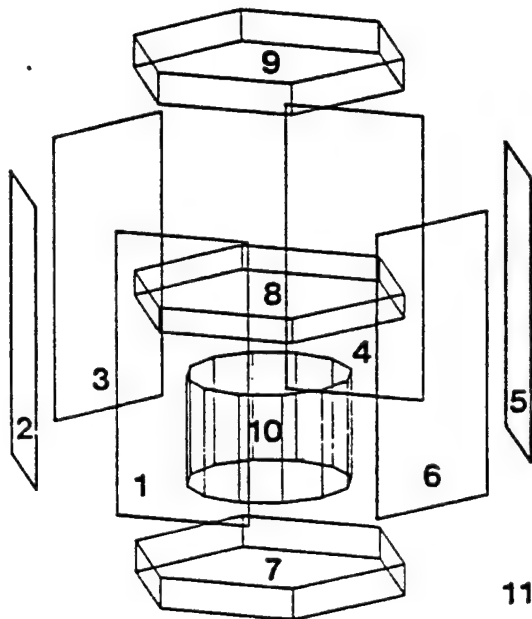


the upper platform was designed for radiation directly into outer space, but the temperature level was too low. Therefore the upper platform is wrapped with 20 layers of superinsulating materials to replace the radiator solar cells by transmission coupling.

The thermal analysis is based on an 11-nodal point model, in a set of 11 differential equations:

$\sigma = 5.67 \cdot 10^{-8} \text{ W}/(\text{m}^2 \text{k})$  is the Stefan-Boltzmann constant. The following values are selected as the heat capacity  $W_i$  ( $\text{kW}_s/\text{k}$ ) at each nodal point, and the thermocouple between nodal points due to the coefficient of thermal conductivity  $K_{ij}$  ( $\text{W}/\text{K}$ ), and the radiation coefficient  $R_{ij}$  ( $\text{m}^2$ ).

#### Determination of Nodal Points



To simulate the exterior heat flow  $Q_i$  ( $\text{W}$ ), an analysis is conducted of two extreme situations: (1) the coincidence of sunlight direction and orbital plane and (2) sunlight almost perpendicular to the orbital plane ( $86.9^\circ$  during the winter solstice). Simulations are conducted on continuous variation of orbit  $Q_i$  approximate to 12 equal interval orbital angles, as follows:

$$W_i \left( \frac{dt}{dt} \right)_i = \sum k_{ij} (T_j - T_i) + \sigma \sum R_{ij} (T_j^4 - T_i^4) + Q_i$$

### Nodal Points

		1	2	3	4	5	6	7	8	9	10	11
1		4.5	0.09	0.03	0.03	0.03	0.09	0	0	0	0	1.65
2		5	4.5	0.09	0.03	0.03	0.03	0	0	0	0	1.65
3		0	5	4.5	0.09	0.03	0.03	0	0	0	0	1.65
4		0	0	5	4.5	0.09	0.03	0	0	0	0	1.65
5		0	0	0	5	4.5	0.09	0	0	0	0	1.65
6		5	0	0	0	5	4.5	0	0	0	0	1.65
7		0.1	0.1	0.1	0.1	0.1	0.1	32	0	0	0	0.01
8		0.1	0.1	0.1	0.1	0.1	0	0	25	0	0	0
9		0.4	0.4	0.4	0.4	0.4	0	0	0	63	0	0.01
10		0	0	0	0	0	50	50	0	0	36	0
11		0	0	0	0	0	0	0	0	0	0	$\infty$

$k_{ij} = k_j$

$R_{ij} = R_j$

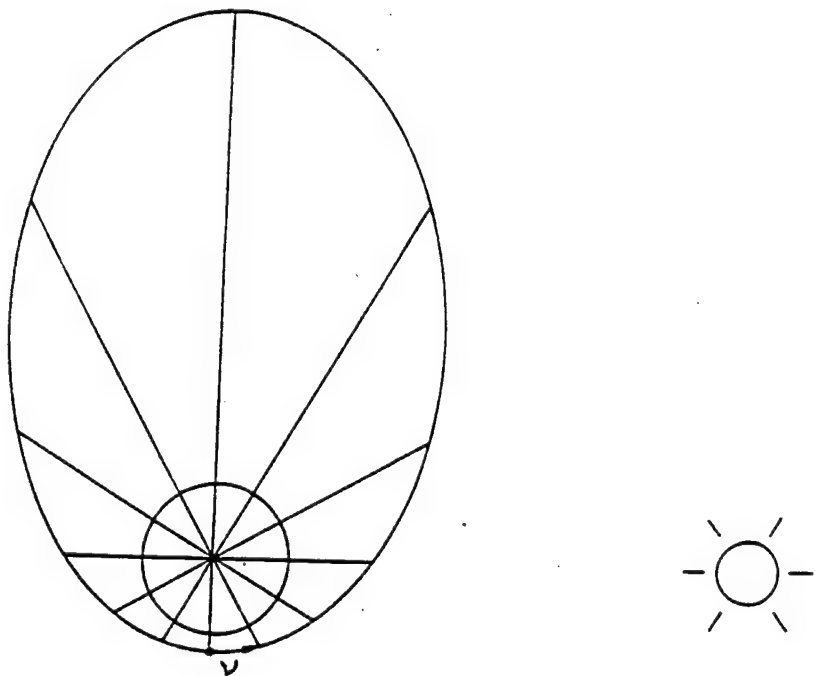
$W_i$

Simulation begins at the temperature  $T_i(k)$ , which is carefully selected. Continuous simulation is conducted until two adjacent orbits display similar results. This situation is obtained after eight orbits. As shown in the example of nine nodal points, there is the highest thermal inertia at this nodal point.

From the actual simulation results of obvious temperature variations in the solar cell array between -90 and +35°C, the

temperature variation is not the key because the voltage of the power source bus is controlled by the storage battery, and not by the solar cell array. The relatively low average temperature is very advantageous to solar cell efficiency.

Heat Outflow



The simultaneous result of the second case indicates a linear stabilization situation, because the sunlight situation is maintained relatively unchanged with the absence of earth shadow, the stable temperatures of the solar cell array are as follows: at nodal point 1,  $52^{\circ}\text{C}$ , at full illumination; at nodal points 2 and 6,  $19^{\circ}\text{C}$ , at semi-illumination; at nodal points 3 and 5,  $-35^{\circ}\text{C}$ ; and at nodal point 4,  $-50^{\circ}\text{C}$ .

As for the other nodal points, the temperature variations

are relatively low for the equipment platform (nodal points 7 and 8) and the reaction control subsystem (nodal point 10). This is because of the relatively high thermal inertia of this module, good internal coupling, and separation from external environment.

Nodal Points

	1	2	3	4	5	6	7	8	9	10
$\nu = 0^\circ$	0	0	0	0	1359	1359	30	30	120	0
$30^\circ$	0	0	0	351	1177	1177	40	30	120	0
$60^\circ$	0	0	0	608	679	679	45	30	120	0
$90^\circ$	0	0	0	0	0	0	50	30	120	0
$120^\circ$	608	679	679	0	0	0	45	30	120	0
$150^\circ$	351	1177	1177	0	0	0	40	30	120	0
$180^\circ$	0	1359	1359	0	0	0	30	30	120	0
$210^\circ$	0	1177	1177	351	0	0	30	30	130	0
$240^\circ$	0	679	679	608	0	0	30	30	135	0
$270^\circ$	0	0	0	0	0	0	30	30	140	0
$300^\circ$	608	0	0	0	0	0	30	30	135	0
$330^\circ$ *	351	0	0	0	1177	1177	30	30	130	0

对于(2)的情况, 估计了下列常值功率输入:

1567	783	0	0	0	783	30	30	125	0
------	-----	---	---	---	-----	----	----	-----	---

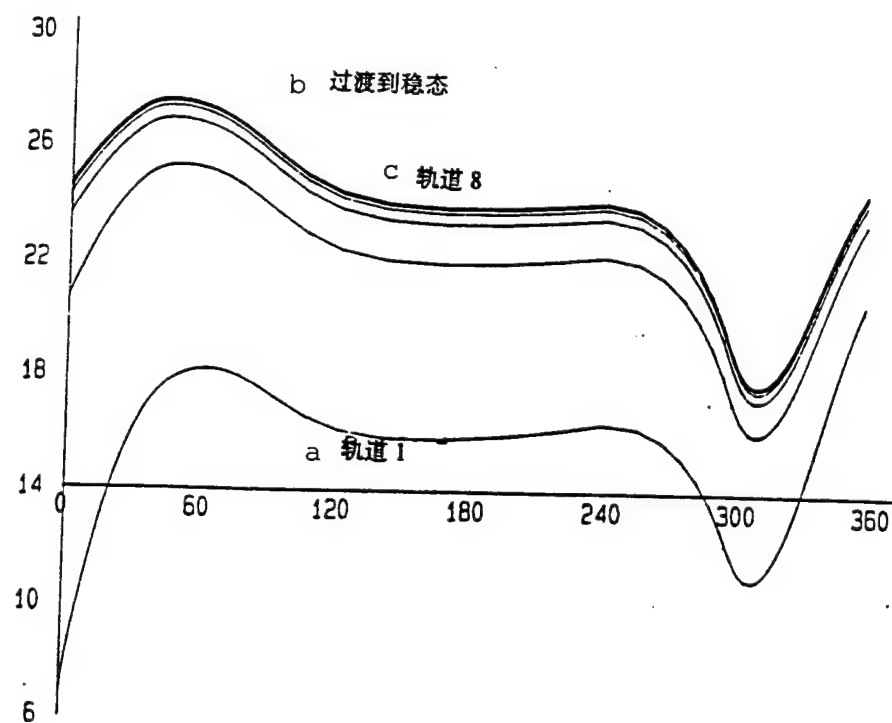
KEY: \* - For situation of (2), the following constant power inputs are estimated:

We must pay attention to the following: four thrusters and propellant line outside of the plane because the individual shapes are not sufficiently contained within the model of 11 nodal points. It is required to have some remote control command

and line heaters.

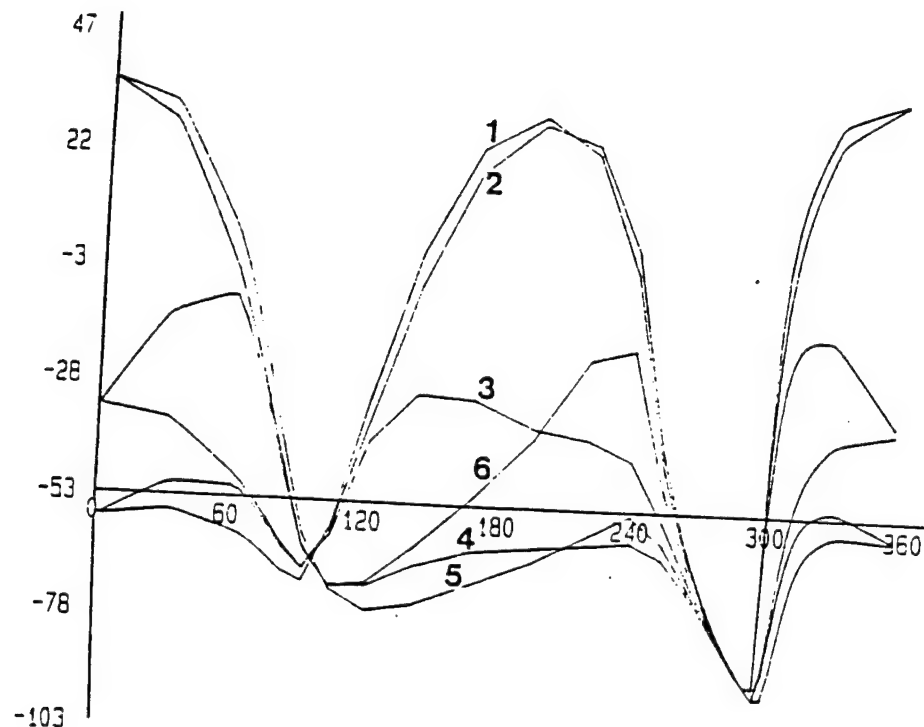
The simulation results in the second case again indicate the following linear temperatures: at nodal point 9,  $45^{\circ}\text{C}$  (payload); and at nodal points 7, 8, and 10,  $36^{\circ}\text{C}$ .

Generally, as indicated by the first experimental operation, the overall temperature range is in the vicinity of  $0^{\circ}\text{C}$ . This temperature is too low; therefore, it is required to upgrade the thermal insulation from the space environment. Especially on the



KEY: a - orbit 1 b - transition to stability c - orbit 8

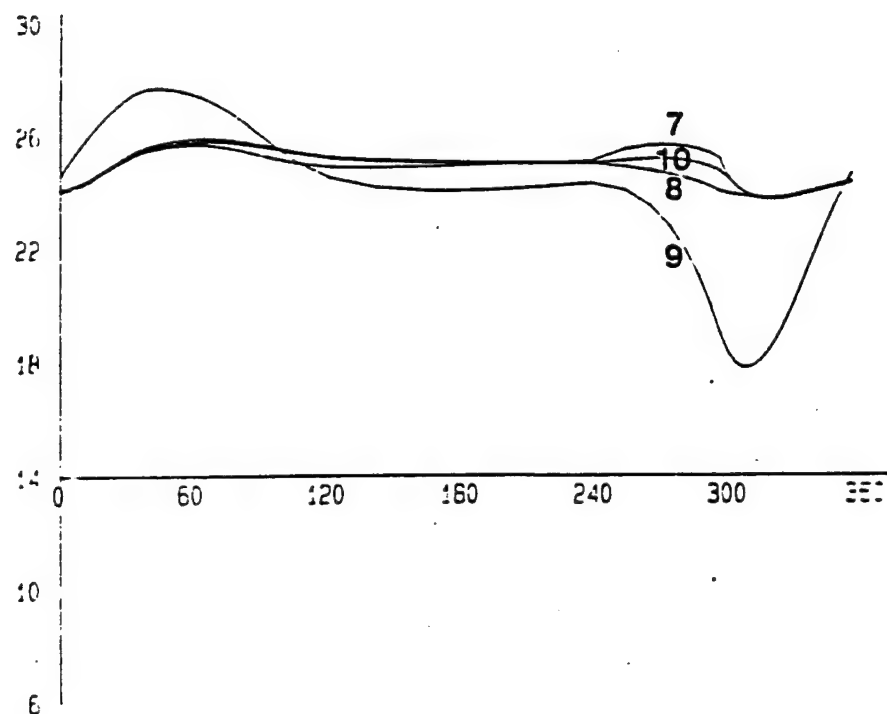
### Solar Cell Array



payload platform, the results show a slightly higher temperature, possibly slightly higher than the overall temperature range.

In the third experimental operations, any required temperature can be obtained by using the method of gradually and optimally reducing the local thermal insulation layers.

### Satellite Platform



### 6. Mass Distribution

Payload	60
Structure	55
Power supply	55
Reaction control subsystem	25
Attitude and orbital control subsystem	20
On-board data management subsystem	5
<hr/>	
Dry mass of satellite	220

Unforeseen eventualities	96
Propellant	184
Overall mass	500kg

The mass distribution of the subsystems is as follows:

3 equipment mounting boards	24	6 solar cell panels	30
1 fuel tank support skirt	10	2 sets of storage batteries	30
3 support rods	9	cable and electronic equipment	5
6 interfaces	12	structure	55kg
1 momentum wheel	7	1 hydrazine fuel tank	20
1 horizon sensor	2	7 boosters + valves	2
3 on-board sensors	5	1 self-locking valve	1
3 magnetic torque devices	5	1 intake valve	1
1 control electronic unit	3	1 pressure sensor	
attitude and orbital control subsystem	10m piping		2
	20kg	reaction control subsystem	25kg

## VI. Research Report on Third Item of Task

### 1. Task of Design Evaluation

- (1) Three-axis fundamental stabilization scheme
- (2) Mass distribution to be revised: dry mass of satellite, 200kg--too small for American rocket
- (3) With DELTA rocket as the basis for dual-satellite launch
- (4) Compatibility with other carriers

In a design evaluation meeting on July 7, 1987, three-axis

stabilization was selected as the fundamental scheme.

Proposed by the Design Evaluation Committee, the estimated mass of the power supply and substructures is increased. In addition, the total dry mass of the satellite is increased from 150 to 200kg. Therefore, the American rocket, as originally proposed as the fundamental carrier, is not adaptable to normal flight missions. However, the demonstration flight task of reducing payload mass is still an attractive scheme for selection.

As proposed by the Design Evaluation Committee, the commercial DELTA carrier rocket is used as the basis. If possible, compatibility should be ensured when selecting other carrier schemes.

## 2. Dual-satellite Launch

Strengthened satellite structure: dry mass of satellite -- 220kg.

The DELTA carrier rocket does not provide facilities for dual-satellite launch. To carry the second satellite, the satellite structure should be strengthened. It is estimated that the mass of the payload support rod and the interface for each satellite is 20kg. Thus, the dry mass of the satellite will be further increased to 220kg.

## 3. Fundamental Satellite Scheme

Dry mass	220
----------	-----

Propellant	280
	500kg

$\Delta V$  is 1.847km/s

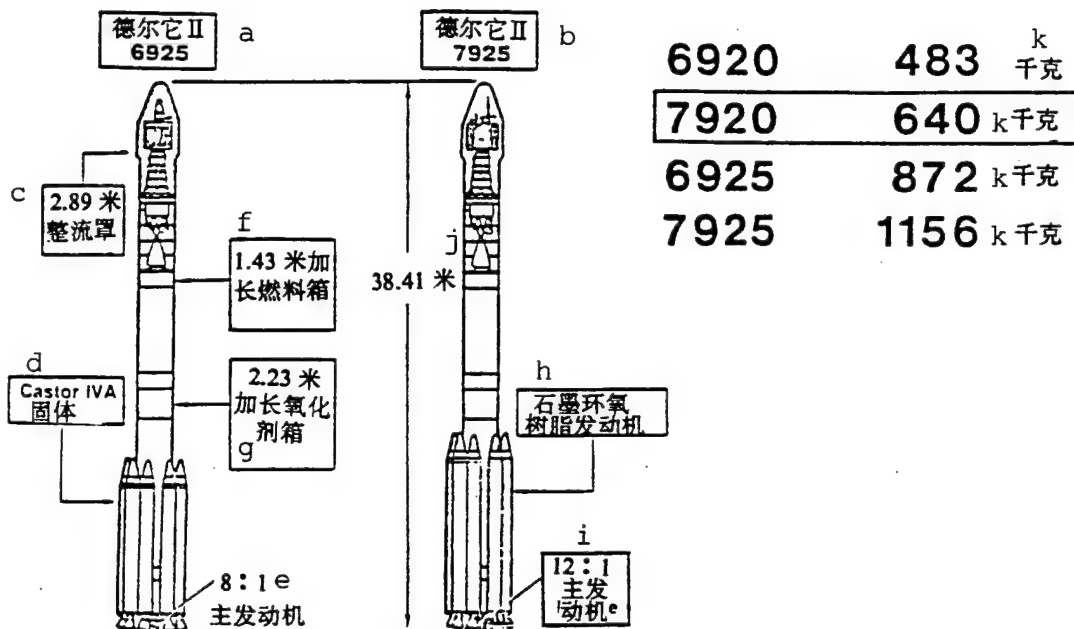
The total mass of each satellite is approximately 500kg, or the total launch mass is approximately 1000kg, which corresponds to the fuel tank capacity of the German postal satellite that is proposed to be used. When compared to the capacity of 280kg propellant and 350kg of fuel tank capacity, the filling rate is 80%. In other words, the blowdown ratio is 5:1.

When the DELTA carrier rocket is used in a launch, this propellant capacity would be too high. When it is required to increase the dry mass, the liquid can be considered as the compromise surplus quantity. As previously discussed, this propellant emergency mass is very useful when considering the other carrier rocket selection scheme, especially to use the Ariane carrier rocket in launches.

#### 4. Selective Scheme of DELTA Carrier Rocket

Produced on a commercial DELTA-II carrier rocket production line, there are distinctions between a large solid-fuel booster (7 is the first digit), and a small solid-fuel booster (6 is the first digit), as well as a three-stage (5 is the last digit), and a two-stage (0 is the last digit) types. McDonnell-Douglas Corporation intends to develop a standardized production line. Therefore, beginning in 1991, the 792 series carrier rocket will be sold at the same price as the 692 series carrier rocket. In

other words, smaller-thrust type carrier rockets are not encouraged.

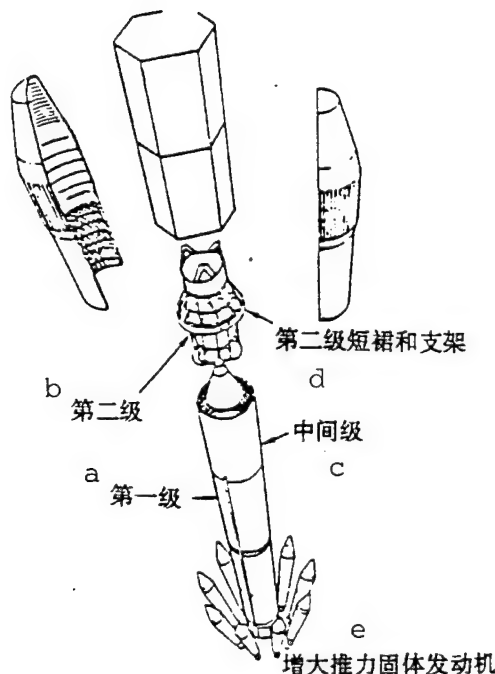


KEY: a - DELTA-II 6925 b - DELTA-II 7925 c - 2.89-m fairing  
 d - solid-fuel e - main engine f - 1.43-m stretched fuel tank  
 g - 2.23-m stretched oxidizer tank h - graphite-epoxy resin  
 engine i - main engine j - 3841m k - kilograms

When comparing the three-stage DELTA-II 7925 to the two-stage 7920 model, the first-named model is able to send a satellite with approximately twice the mass into the predetermined navigation satellite (NAVSAT) orbit. However, the reasons for selecting the two-stage DELTA-II 7920 are as follows:

(1) Launch capability is sufficient to satisfy dual-satellite launch requirements. With the geometric shape of the

fairing, it is forbidden to launch more than two satellites at a time.



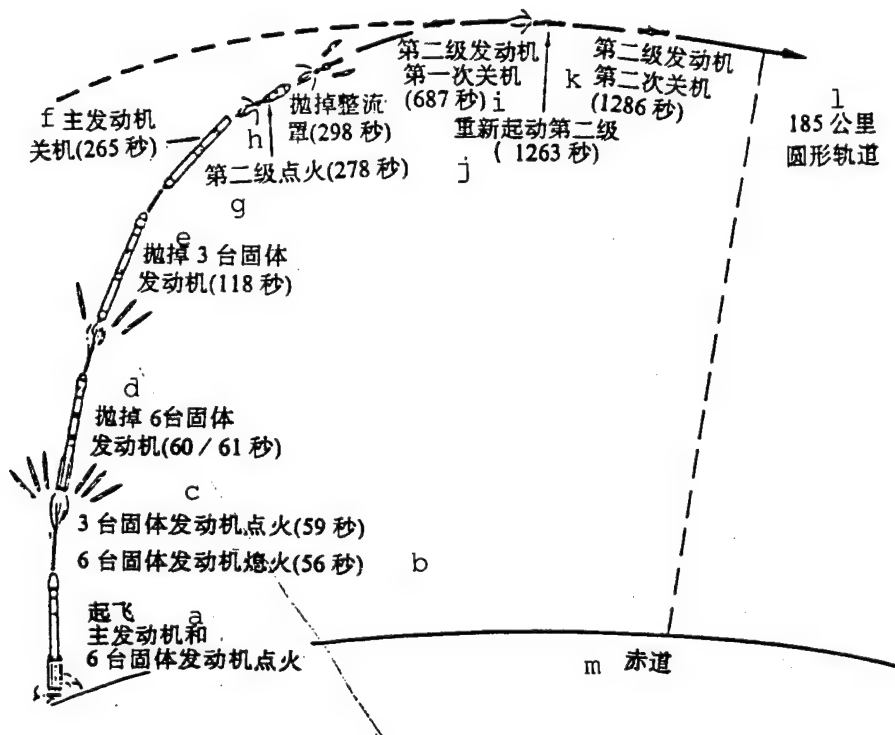
KEY: a - first stage b - second stage c - intermediate stage  
d - second-stage short skirt and frame e - increased-thrust  
solid-fuel engine

(2) The effective fairing casing of the three-stage carrier rocket is also restricted, because the third stage occupies the variable-effective cylindrical portions.

(3) Spin is required before operating the solid-fuel engine on a model 48 satellite. It is proposed to use a large propellant tank with partial filling consistent with the rotating

shaft, for the dual-satellite launch. Before operating the third stage, there are great risks of fuel sloshing and excitation perturbations.

(4) When the solid-fuel rocket engine and the spin platform are eliminated, 5 million U.S. dollars of cost can be saved.



KEY: a - at launch, ignition of main engine and six solid-fuel engines b - burnout for six solid-fuel engines (56s)  
 c - ignition for three solid-fuel engines (59s) d - jettisoning of six solid-fuel engines (60-61s)  
 e - jettisoning of three solid fuel engines (118s) f - cut-off of main engine (265s)  
 g - second-stage ignition (278s) h - jettisoning of fairing (298s)  
 i - first cutoff of second-stage engine (687s)  
 j - restart second stage (1263s) k - second cutoff of second-stage engine (1286s) l - 185km circular orbit m - equator

## 5. Improved Launch Scheme

A DELTA model 7920 carrier rocket can send a 1000kg satellite into a transfer orbit with perigee at 1250km, apogee at

18,162km, and a dip angle of  $63.45^{\circ}$ .

The satellite accomplished the final orbital insertion. The mass in stationary orbit is  $2 \times 395 = 790$ kg.

In the selected DELTA 7920 scheme, a satellite with a total mass of 640kg can be directly inserted into a predetermined NAVSAT orbit. In principle, this launch scheme can satisfy two satellites, each with 100kg propellant for control maneuver while in orbit.

However the quality of the initial orbital lifetime, the fuel tank loading can be increased to the most suitable capacity, that is, 280kg. The intermediate transfer orbit is reached with a carrier rocket; the final orbital insertion is accomplished with a satellite propulsion system.

A DELTA 7920 rocket can send a 1000-kg satellite into a circular orbit with an altitude of 185km and a dip angle of  $63.45^{\circ}$ . The second-stage rocket provides a velocity increment of 2264km/s. If required, the second stage can be started several times. The next ignition of the second-stage is at the northernmost (or southernmost) position of the orbit in order to attain a Hohmann transfer elliptical orbit of 185/1250km in altitude. This maneuver requires a velocity increment of 0.287km/s. The remaining 1.977km/s velocity increment of the second stage can be used to reach the second transfer orbit, which is the elliptical orbit of 1250/18,162km.

To reach the standard orbit, the satellite propulsion system should provide a velocity increment of 0.531km/s. It is assumed

that the specific thrust of a hydrazine system is 2.25km/s. This maneuver requires 210kg of hydrazine fuel. The initial mass of the two satellites for the service lifetime is 790kg, which is considerably higher than the 640kg required for direct orbital insertion.

#### 6. Unforeseen Mass

Mass in stationary orbit	395
minus propellant needed for station-keeping (10y)	79
minus dry mass of satellite	220
unforeseen mass	96kg

In this case of a launch scheme, even if the propellant for satellite station-keeping is for a 10-y lifetime, not the predetermined 3y, the relatively sufficient unforeseen mass of 96kg is also useful. This mass is usually maintained in the hydrazine fuel tank, as the residual quantity of liquid fuel for unforeseen control maneuvers if there are sufficient reasons for other kinds of use. The following sufficient reasons exist:

- (1) To increase the satellite operating life from 3 to 10y, redundant equipment is considered.
- (2) Adoption of another carrier rocket, especially the Ariane-4 and the H1 carrier rockets.
- (3) Due to adoption of simpler, but heavier-weight technology to cut costs, for example, in satellite structure and power supply, and
- (4) Increase of payload mass.

This unforeseen mass should not be used to add to design complexity.

## 7. Launch

The DELTA 9720 includes the first-stage liquid fuel rocket of nine bonded solid-fuel boosters, and the second-stage liquid fuel rocket connected to the components of the two satellites. Three-axis stabilization is used during satellite separation.

Although the solid-fuel rocket exhausts its fuel within a minute, it still provides greater velocity increment for the carrier rocket.

The first-stage rocket shuts off after a 4.4-min burn. Part of the energy of the second stage is used to send the carrier to a circular orbit of 185km. As mentioned previously, the energy of the velocity increment of 2.264km/s can still be reserved in the second stage, for orbital insertion of a 1000-kg payload.

After launch, the first equatorial intersection point is reached after about 20min. The orbital period is:

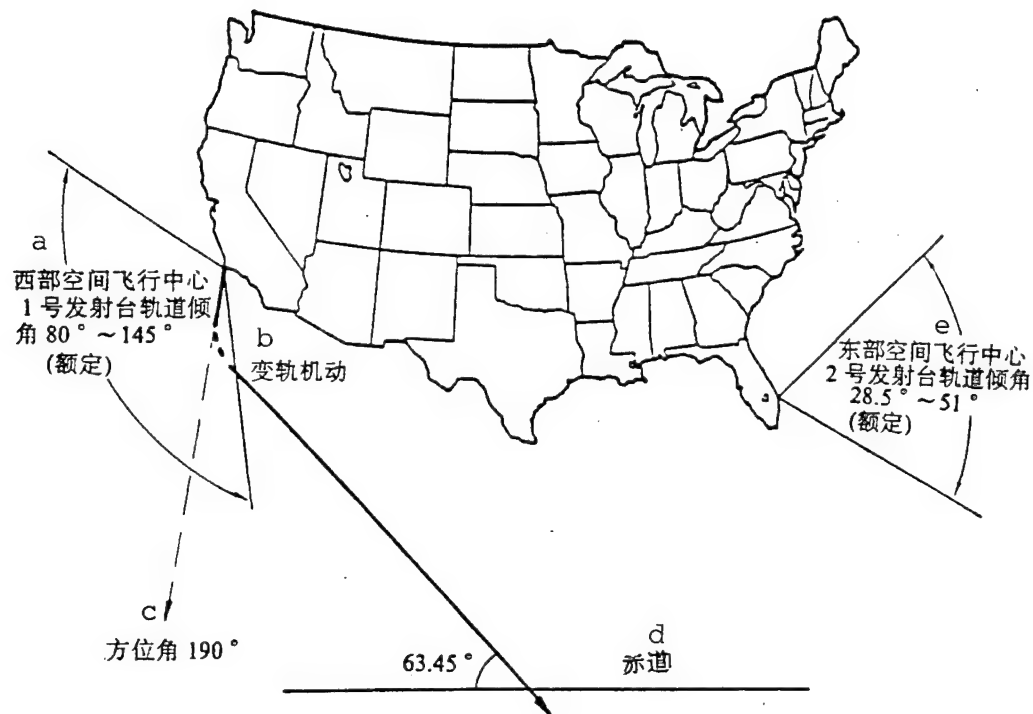
$$T = 2\pi \sqrt{\frac{a^3}{\mu}} = 2\pi \sqrt{\frac{(6378 + 185)^3}{398600}} = 88 \text{ min.}$$

Safety in the launch pad area is an important point for discussion of commercial launchers, since third-party insurance could be very expensive. To avoid the Los Angeles area, the launch orientation angle of 185° or 190° should be chosen. The flight direction of the NAVSAT satellite orbit will be changed within the first 2min after ignition of the solid-fuel engine in order to reach the rated orbital plane ( $i=63.45^\circ$ ) after fuel exhaustion of the solid-fuel engine.

## 8. Orbital Insertion

The first orbital insertion is accomplished at the southernmost point ( $W=-90^\circ$ ) or the northernmost point ( $W=+90^\circ$ ) of the orbit. This is determined by the predetermined coverage of

the rated orbit. The orbital insertion time can be  
 $20+0.25 \times 88 = 42$  min, or  $20+0.75 \times 88 = 86$  min after launch.



KEY: a - West Space Flight Center, Launch Pad No. 1: orbital dip angle between 80 and 145° (rated) b - orbital transfer maneuver c - orientation angle 190° d - equator e - East Space Flight Center, Launch Pad No. 2: orbital dip angle between 28.5 and 51° (rated)

a  
 $h_a = 1250$  公里



第二级发动机第三次关机 b

$W = -90^\circ$

b  
第二级发动机第三次关机



a  $h_a = 1250$  公里

$W = +90^\circ$

KEY: a -  $h_a = 1250$  km b - third cutoff of second-stage engine

The velocity of the carrier prior to orbital transfer maneuvering is:

$$V_1 = \sqrt{\frac{\mu}{r_1}} = \sqrt{\frac{398600}{6563}} = 7.793 \text{ km/s}$$

The semimajor axis of the Hohmann transfer orbit is:

$$a_2 = r_E + (h_s + h_a) / z = 6378 + (185 + 1250) / 2 = 7095.5 \text{ km}$$

The velocity after orbital transfer maneuvering of the carrier is

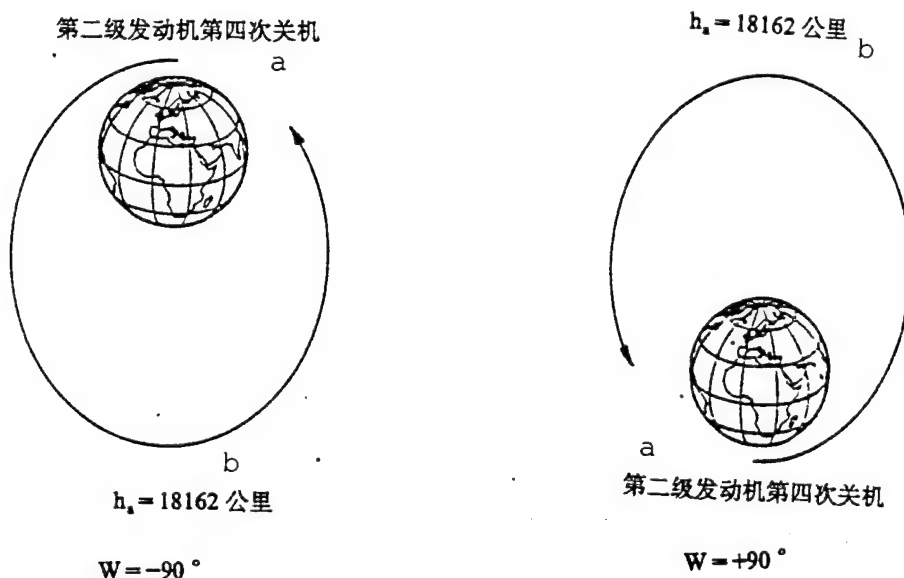
$$V_2 = \sqrt{\left(\frac{2}{r_1} - \frac{1}{a_2}\right)\mu} = 8.080 \text{ km/s.}$$

The velocity increment of orbital transfer maneuvering is:

$$V = V_1 - V_2 = 0.287 \text{ km/s.}$$

The velocity of the carrier at apogee is:

$$V_3 = \sqrt{\left(\frac{2}{r_E + h_A} - \frac{1}{a_2}\right)\mu} = 6.952 \text{ km/s.}$$



KEY: a - fourth cutoff of second-stage engine  
b -  $h_a = 18,162 \text{ km}$

The flight time from perigee to apogee is

$$T = \pi \sqrt{\frac{a_2^3}{\mu}} = 49.6 \text{ min.}$$

The maneuvering of the second orbital insertion is also accomplished by the carrier second-stage engine. At the first

apogee, the previous apogee becomes the new perigee of the Hohmann transfer orbit.

The residual velocity increment of this maneuver is:

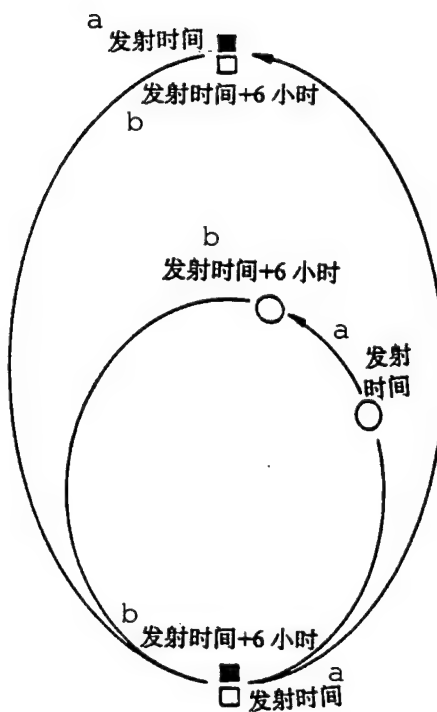
$$\Delta V_2 = 2.264 - 0.287 = 1.977 \text{ km/s.}$$

Therefore, the velocity at the new perigee becomes:

$$V_4 = V_3 + \Delta V_2 = 8.929 \text{ km/s.}$$

By substituting  $V_4$  in the equation, the new semimajor axis is:

$$a_3 = \frac{1}{\frac{2}{r_2} - \frac{V_4^2}{\mu}} = \frac{1}{\frac{2}{7628} - \frac{8.929^2}{398600}} = 16084 \text{ km.}$$



KEY: a - ignition time    b - ignition time plus 6h

The altitude at apogee is:

$$h_A = 2a_3 - 2r_E - h_p = 18\ 162 \text{ km.}$$

The orbital period becomes:

$$T = 2\pi \sqrt{\frac{a_3^3}{\mu}} = 5.639 \text{ h.}$$

After the second-stage engine of the carrier has burned out, the attitude control system of the carrier adjusts the satellite to a normal direction so that the momentum wheel is perpendicular to the orbit. Then two momentum wheels start spinning at the rated velocity, and the attitude control system of the carrier balances the reaction torque.

Thereafter, three explosive nuts are blasted and then ignite the carrier retro-rocket in order to separate the first-stage rocket from the satellite. When the carrier arrives at a safe direction, the two satellites separate from each other without losing their respective attitude relative to the earth and to the orbit. When the satellite member is aligned with one of the two positions of the marked targets at the perigee, the satellite prepares to enter its final orbit.

Assume that the launch time is one of the purposes (such as white target marker). At the time when the satellite first arrives at its perigee position, and assuming that the satellite still maintains its predetermined position in its parking orbit, then within the launch time of +6h, the satellite will approach the perigee in  $6-5.639=0.361$ h. Therefore, at the latest of its 17 orbits in the parking orbit, or after 4 days, the perigee position of the satellite will be consistent with one of two



KEY: a - altitude at apogee=26,556km    b - altitude at apogee=19,520km    c - satellite

target positions.

In this situation, one of the two satellites will be sent

directly into the nominal orbit by its on-board hydrazine propulsion system. The target semimajor axis  $a_5=26,556\text{km}$ ; the perigee velocity should be increased to

$$V_6 = \sqrt{398600 \cdot \left( \frac{2}{6378 + 1250} - \frac{1}{26556} \right)} = 9.460 \text{ km/s}$$

$$\Delta V_4 = 9.460 - 8.929 = 0.531 \text{ km/s}$$

The propellant consumption in this maneuver is:

$$m_p = m_s = (1 - e^{-\Delta V / v_s}) = 500 \cdot (1 - e^{-0.531 / 2.25}) = 105 \text{ km.}$$

Therefore, the satellite mass in its initial orbital operation is 395km.

In similar situations, the second satellite will be sent into a 6h parking orbit. The semimajor axis of this orbit is:

$$a_4 = \sqrt[3]{\mu \left( \frac{T}{2\pi} \right)^2} = 16763 \text{ km}$$

The altitude at apogee is:

$$h_A = 2.16763 - 2.6378 - 1250 = 19520 \text{ km}$$

After 6h, the second satellite will arrive at the perigee position of the nominal orbit. However, the first satellite will arrive at its perigee. In this situation, the second satellite will be sent into its nominal orbit. The overall velocity increment is the same as that of the first satellite.

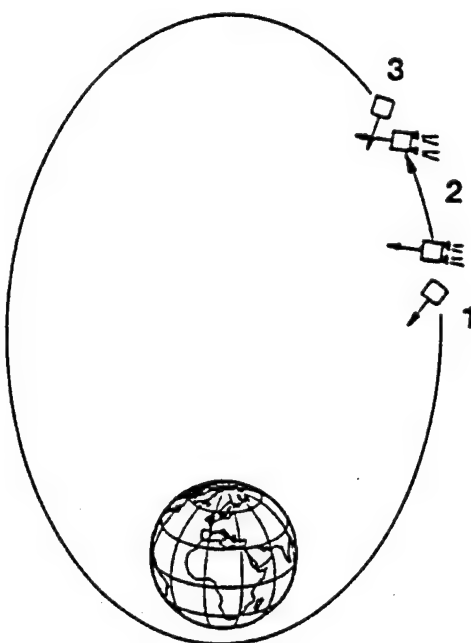
## 9. Orbital Control

As mentioned above the final orbit insertion and orbital control require in-plane maneuvering. These two situations

require to have predetermined the  $\Delta V$  vector generated by the determined orbital position in the direction of insertion of the predetermined orbital plane.

The satellite booster is used for in-plane maneuvering; this is the booster on a tripod opposite the antenna platform. The

#### In-Plane Maneuver



booster can provide the thrust vector in the direction of the antenna axis pointed toward the ground. The antenna axis will be readjusted to the predetermined  $\Delta V$  direction by the momentum wheel control circuit prior to maneuvering. The satellite rotational angle about its momentum wheel is controlled by a rate integration gyroscope. After maneuvering, the satellite immediately is restored to the attitude of earthward orientation.

If such maneuvering occurs over several adjacent orbits, the persistence time of each maneuver is relatively short because the required  $\Delta V$  for in-plane maneuvering is relatively low. Therefore, the interruption time can be limited to several minutes, or even less.

Out-of-plane maneuvering should be limited to once a year in order to minimize propellant consumption as much as possible. The persistence time of this maneuver is relatively long, because as high as 50m/s of velocity increment should be generated. For example, the time during which the booster should operate outside two planes with thrust  $T$  of 10N is:

$$t = m_s \cdot \Delta V / T = 395.50 / 20 = 987.5 \text{ s} = 16.5 \text{ min}$$

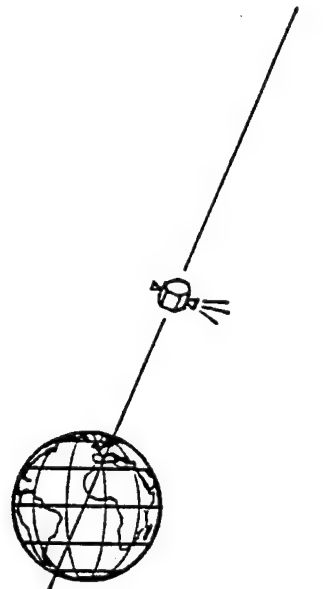
Since the satellite maintains a nominal direction during out-of-plane maneuvering, therefore in principle a single long-period operation can complete the maneuver. However, due to position variation of the satellite in orbit during the maneuver, methods of improving the efficiency is often adopted to distribute maneuvers over several adjacent orbits.

As determined by the assumed maneuver direction, two sets of boosters can be used in the direction opposite to that of the satellite. Once a booster malfunctions, each maneuver can be replaced with a maneuver in the opposite orbital plane for a pair of boosters in the reverse direction. Therefore, satellite velocity is higher in the position of opposite sides, and so the requirements on  $\Delta V$  are also higher.

## 10. In-orbit Standby

Required ground maintenance is the minimum for in-orbit standby. The main reason of potential complexity is the adoption of a direct-connection method between the momentum wheel and the

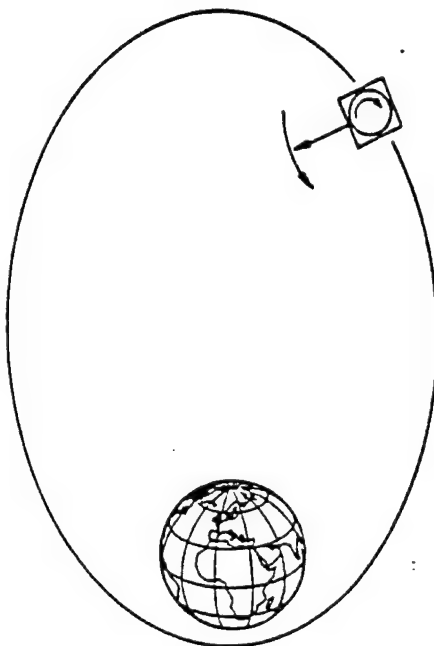
### Out-of-Plane Maneuver



main bus voltage, to switch the attitude control system to a stable safety mode. The momentum wheel restricts the counter potential of the wheel motor from overspeeding by about 10 to 20%. The satellite will rotate in the reverse direction. The entire dual spin system is passively stable, not related to the inertial ratio and the inherent fuel sloshing. The earth sensor and gyroscope can be disconnected from the power supply.

The TTC is switched to an omnidirectional receiving mode,

capable of receiving remote control command from the ground, for example, the command transmission of remote sensing data. The reaction control system does not operate, especially in the fact that the self-locking valve should be closed.

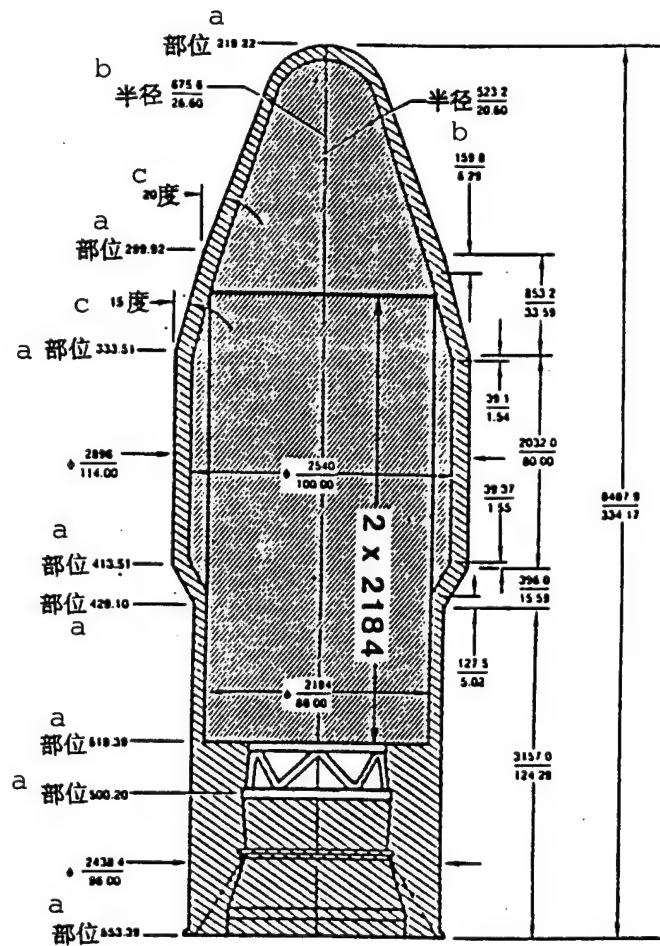


After several months, the satellite applies the pitch circuit mode with connection to the attitude control system. At the same time, we can determine and compensate for the fluctuating momentum vector.

#### 11. Effective Casing

The satellite casing is restricted by the cylindrical portion of the DELTA carrier rocket. The satellite casing

diameter is 2.18m, and its effective length is  $2 \times 2.184\text{m}$ , capable of accommodating two satellites. In other words, two satellites can fit in the casing, each 2m long and 2m in diameter. The margin in each direction is 9%.

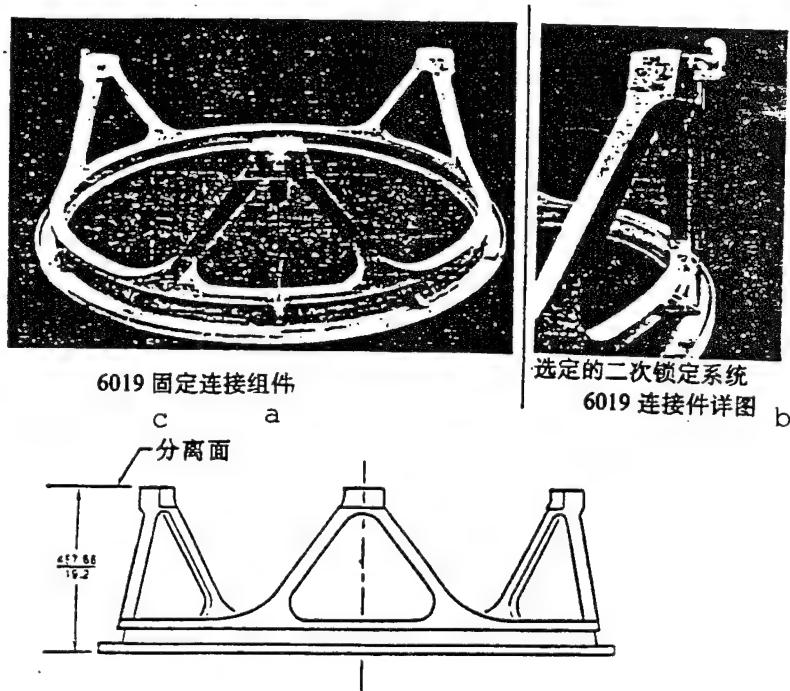


KEY: a - site   b - radius   c - degree

The middle part of the DELTA 7920 flow-rectifying cylindrical section is extended from 2.44 to 2.9m. What is the

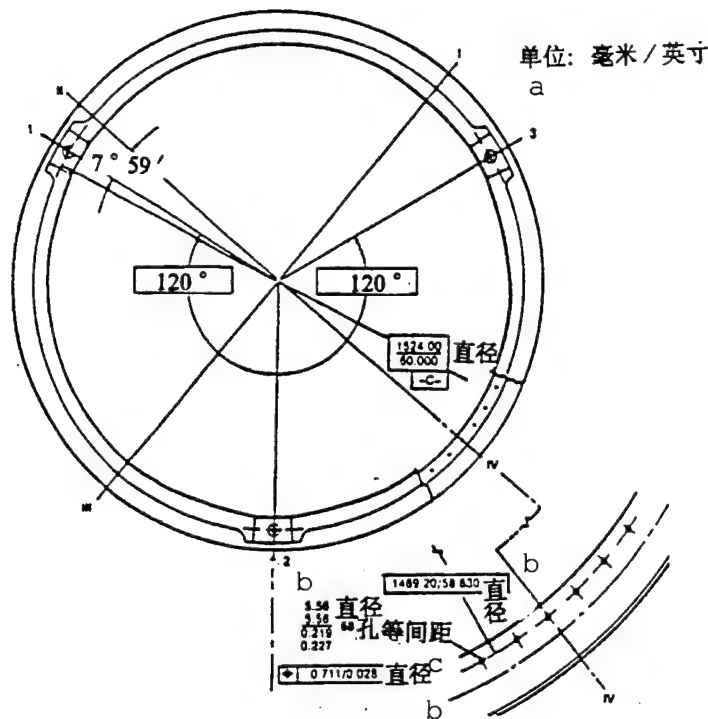
advantage of using such fairing (especially, if compatibility is to be maintained for launches with the H1 carrier rocket)? The Hughes Aircraft Manufacturing Corporation has requested McDonnell-Douglas to reduce the fairing to 2.44m, and to raise the same request about the HS 376 series product (2.16m in diameter). If the negotiations between these two companies are successful, the air resistance against the fairing can be reduced, even further possibly increase  $\Delta V$  of the second stage. Up to now, the 2.44-m scheme has been more expensive than the 2.9-m scheme (supported by GPS-NAVSTAR). Therefore, the latter scheme is still the fundamental scheme.

## 12. Fixed Connector Mount



KEY: a - mount-connector b - details of type 6019 connector of secondary locking system to be selected  
c - separation plane

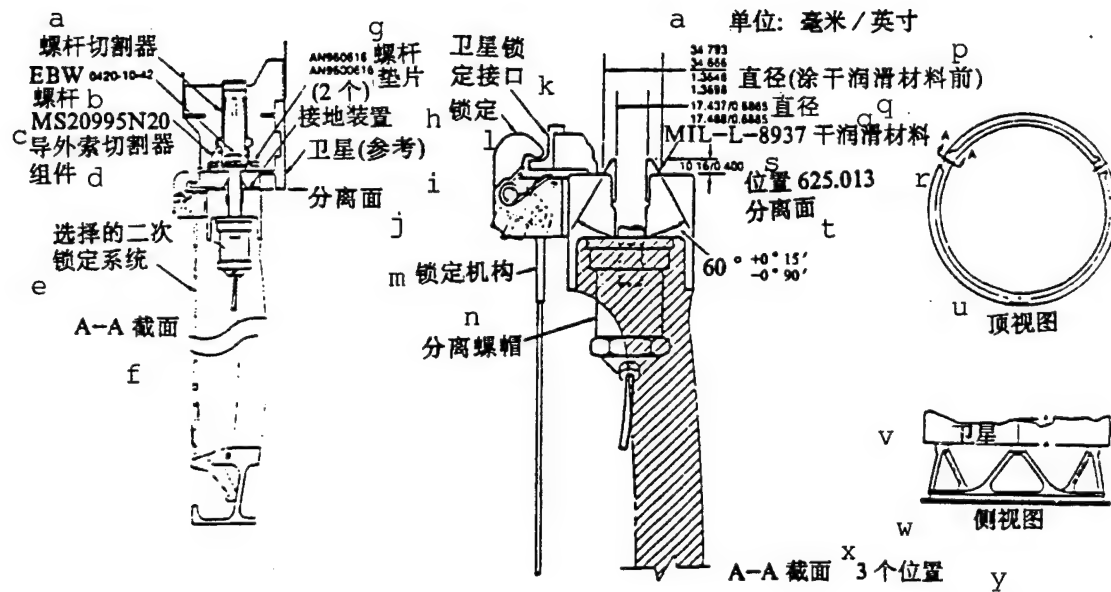
The second stage provides a three-point fixed connector mount. A selected secondary locking system can be used in this fixation. Under the fundamental scheme, this selection is abandoned.



KEY: a - unit: value in millimeters/value in inches  
 b - diameter    c - equal hole spacing

The fixed connector mount 6019 is 48.3m high, 152.4cm in diameter, and 47kg in mass. The structure of this component is processed with forged aluminum. The connecting member can support a satellite assembly of 2,177kg mass. The center of gravity distance is over the separation plane by 2.083m. The diametral center of gravity deviates by 5cm. The base seat of

the connecting member is fixed on the front frame of the second-stage rocket.



KEY: a - worm rod cutter b - worm rod c - cutter of rope leading to exterior d - component to be selected e - secondary locking system f - cross-section A-A g - worm rod cushions (2) h - grounding attachment i - satellite (reference) j - separation plane k - satellite locking l - locking m - locking mechanism n - separation nut cap o - unit: value in millimeters/value in inches p - diameter (before coating with dry lubricant) q - millimeters r - dry lubricant material s - position t - separation plane u - top view v - satellite w - side view x - cross-section A-A y - three locations

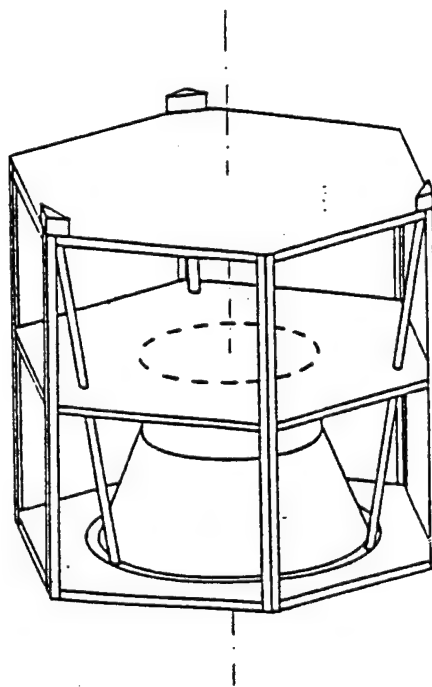
The mass of the connecting member constitutes part of the carrier rocket mass.

At three equidistant points, the satellite connector member

is fixed to a matching plane 1524mm in diameter by using a 15.9mm bolt and an explosive nut. When these three explosive nuts are fired, they separate from the carrier rocket. At the same time, the second-stage rocket was pushed in the reverse direction by the DELTA nitrogen retro-firing system.

We must note that DELTA requires that three fixed bolt cutter members be installed on the satellite side of the separation plane. During separation, the bolt and cutter members are retained in the satellite.

### 13. Main Structure

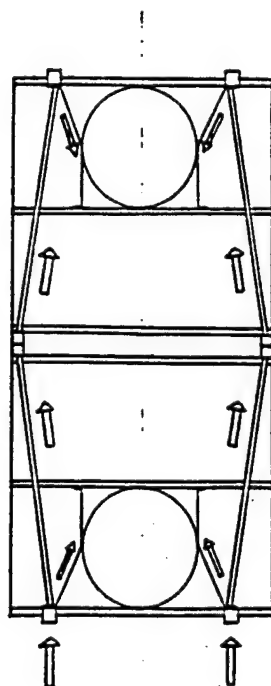


The main structure of the satellite consists of the following: (1) interface with carrier rocket, (2) interface with companion satellite, (3) hydrazine fuel tank support, (4) satellite equipment installation area (intermediate platform),

and (5) installation area for antenna and payload, that is, the upper platform.

By just removing the solar panel, it is very easy to access the satellite and the payload equipment. Three reinforcing rods provide hard connections between the upper and lower interface points.

#### 14. Dual-Satellite Launch Scheme



The main portion of the satellite mass during launch, that is, 380kg for each satellite, can be included in the hydrazine fuel tank. The load of the lower fuel tank can directly enter the carrier rocket interface point through the conical supporting skirt. A cylindrical segment connects the upper part of the fuel

tank support to the platform, and provides lateral direction rigidity to the satellite.

The load of the upper fuel tank cannot be transmitted through the satellite center because by so doing this will hinder the layout of the antenna platform phase control array. This load is supported by two sets of three reinforcing rods to be supported around the satellite circumference.

The structural members of the separation system between the satellites are the same as those of the separation system between the carrier rocket and the next satellite.

EXPERIMENTAL SCHEME OF USING TWO GEOSTATIONARY  
SATELLITES FOR COMMUNICATION AND POSITIONING  
IN JAPAN

written by Senchuan Rongjiu, et al.  
translated by Gao Zhengren, and  
edited by Li Guiqi

I. Introduction

Beginning in 1988, the Japanese Communication Integrated Research Institute cooperated with the Japanese Radio Wave System Development Center (RCR) in the development of a two geostationary satellite communication and positioning integrated system. Various experiments were also conducted.

In the dual satellite positioning integrated system, the distance between a vehicle and a satellite is determined based on the time delay of radio wave propagation. This positioning method determines the location of the vehicle by calculations. To proceed with this experiment, communication equipment was developed in order to simultaneously conduct positioning, and to obtain data or acoustic frequencies. In this method, positioning and communication performance properties are mastered; in addition, the integrated system of optimal communication and

positioning was also studied. The article describes the general situation of this system.

## II. Operating Features of the Communication and Positioning Integrated System

One of the important purposes of communication between a vehicle and its operating personnel, or between different vehicles is to manage the vehicles, and operating personnel and objects in the vehicle. This is also a necessary means in establishing a high level community circulation management system. At the present time, whether in the air, sea, or on the land, there is always crowded traffic. Management of these bodies aims at solving an important problem, thus relying on flexibly and effectively applying the radio wave system. Additionally, the development of systems with communication function and positioning function is very important to the management of materials, safe management, and navigation, as there are continuously increasing demands on navigation of vehicles.

The communication and positioning integrated system can provide users with simultaneously positioning of vehicles, their monitoring and control, as well as graphics and alphanumeric information. The following means of application are available.

### (1) Navigation

When determining the location of a moving vehicle, a navigation system can also receive such information as distance

to the destination, time required, and route recommended, among other information.

(2) Traffic control

Once a moving vehicle enters a specified region, the traffic control system can record and automatically position the vehicle. Additionally, control personnel can monitor the position of the moving vehicle, as well as receive and send all necessary information for traffic control.

(3) Operations management

Traffic control personnel of moving vehicles can monitor and control positions of moving vehicles in their region. With two-way communication, operations such as destination-changing can be done in order to raise operating efficiency.

(4) Communications in rescue

When a moving vehicle has a malfunction or has an accident, the situation of the position and events can be reported to the traffic control personnel or the appropriate units.

As mentioned above, the required communication and positioning properties can apply to different regions; in other words, communications can be used in the above-mentioned aspects, or whether it is used on the land, sea, or air. An investigation report must clearly include the following: upon positioning, the positioning accuracy has to be higher for navigation, traffic control, as well as emergency communication during disaster

relief. Positioning accuracy for operations and management services can be at a lower level. During communication, whether on land or at sea, data communication is sufficient. In the cases of traffic and operational control of aircraft, voice communication is the principal form.

### III. Experimental Systems

#### 1. System configuration

This experimental system is composed of fixed stations, mobile stations, and two geostationary satellites. The two satellites in operation are fixed over 150° E. Long., as the experimental technical experimental satellite V (ETS-V), and over 18° E. Long., as the Pacific Ocean region satellite (POR). On board the POR, there is a transponder (MCS-D) of the international Maritime Communication System. This experimental system executes two missions: bi- and unidirectional ranging. The following ranging methods are available.

##### 1.1. Bidirectional ranging

In bidirectional ranging, time comparisons between the fixed station and the mobile station are not required. The mobile station and the fixed station are used for positioning. In other words, with positioning by a fixed station, the operating personnel of the moving vehicle constitute the main system. Thus, the operating efficiency of the control level of the moving vehicle can be upgraded. When positioning with a mobile station,

the moving vehicle is the main system. This is adaptable to navigation systems.

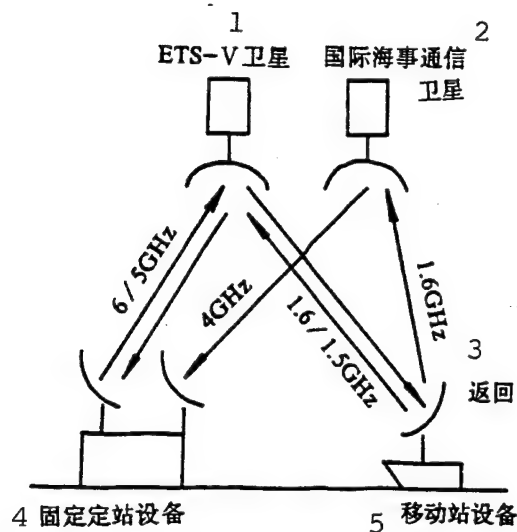


Fig. 1. Block diagram of experimental system with bidirectional ranging

KEY: 1 - ETS-V satellite 2 - International Maritime Communication Satellite 3 - return  
4 - fixed station equipment 5 - mobile station equipment

Fig. 1 shows the system configuration when using the bidirectional ranging mode for positioning with the fixed station. Through the L/C of the ETS-V (this is the circuit that the C-band is employed in uplinks and the L-band is used in the downlinks) to transmit the ranging signal to the moving station, which sends the signal back in the intermediate-frequency band or the fundamental frequency band, to return to the fixed station through the L/C circuit of the two satellites. The fixed station determines the time delay between the time when signals were received that were sent by this station, and through the two geostationary satellites. Based on the time delay, as well as the known satellite position and the position of the fixed

station, a personal computer is used to compute the distance between the moving vehicle and the satellite.

### 1.2. Unidirectional ranging

In unidirectional ranging, time comparisons have to be made between the fixed station and the mobile station prior to ranging. However, all circuits from the execution positioning station to those stations not executing the positioning can be used as communication circuits. When positioning with the fixed station, this is a system involving mainly control personnel, as in the case of bidirectional ranging. However, when positioning with a mobile station, the fixed station sends a signal to the mobile station only via one geostationary satellite; therefore, a subcarrier of the ranging signal can be sent via broadcasting. So circuitry in a geostationary satellite does not have to be multiple-element-connected. In this way, the occupation rate of transponders can be reduced. Fig. 2 shows the configuration of an experimental station in unidirectional ranging with a fixed station for positioning.

Prior to ranging, only one geostationary satellite is used by the fixed and the mobile stations. With time comparisons from a highly stable clock in the fixed station, the time drift between the two stations can be determined. Then the mobile station applies a positioning method synchronized with the clock of this station to send the ranging signal to the mobile station through two geostationary satellites. Based on the time datum of

this station, the fixed station determines the reception time. Based on these data and the time comparison data, a fixed station

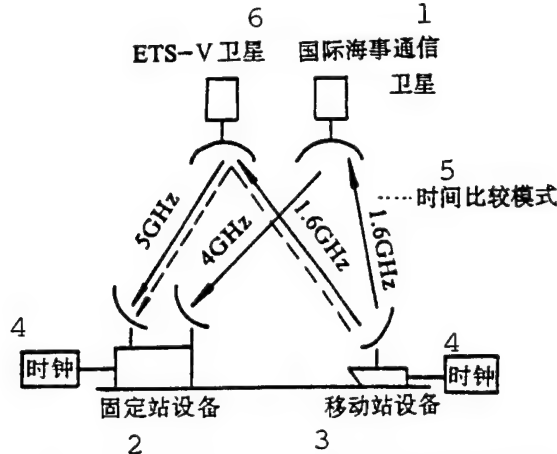


Fig. 2. Block diagram of experimental system during unidirectional ranging  
KEY: 1 - International Maritime Communication satellite 2 - fixed station equipment  
3 - mobile station equipment 4 - clock  
5 - time comparison mode 6 - ETS-V satellite

determines the distance between the mobile station and the satellite. Then based on these distance data and the satellite positional data, the position of this station is calculated. When positioning with a fixed and a mobile station, in principle the data indicators that are obtained are consistent. Therefore, a fixed station is used for positioning experiments.

## 2. Communication ranging integrated equipment for experiments

The following methods of communication and ranging integrated systems were developed as the experimental installation.

(a) Single channel per carrier (SCPC) communication channel is used for ranging signals, and

(b) The communication ranging method involves low-power spectrum density superimposed on the expanded frequency spectrum.

In the following, method (a) is called the SCPC, and method b is called the SS method. The main advantage of the SCPC method is that only simple equipment added to the satellite system of the presently-used SCPC method is able to be employed in ranging. However, there are also disadvantages, since it is unable to increase the frequency of the ranging signal, thus lowering its accuracy. However, the SS method can raise the ranging signal frequency higher with high ranging accuracy, but the instability in determining the time delay should cancel out, and a compander should be added to cancel out the instability of the time delay determination, thus adding to equipment complexity. This experiment was conducted with two modes of installations with the above-mentioned features, but also comparative studies were made on the experimental installations.

In both modes, digital modulation and demodulation equipment was used. Communication and positioning were conducted with the same demodulation mode. In addition, the ranging signal was transmitted with the M series pseudo-random noise (PN) code to transmit the ranging signal, thus exhibiting the ranging function. Table 1 lists the ranging signal parameters.

### 2.1. SCPC mode

Fig. 3 is a block diagram showing the operation of an SCPC mode fixed station in IF status. To allow the fixed station to

simultaneously receive signals from two geostationary satellites

TABLE 1. Modulation-Demodulation Mode and Ranging Signal Parameters

		SCPC	SS
调制解调方式	a	24kb/s OQPSK	5kb/s BPSK
PN 码速 率	b	12kb/s	e 位固定 5kb/s f 扩展 1.275Mb/s
PN 码长	c	1 000 个芯片 d 83.33ms	g 位固定 500 个芯片 100ms h 扩展 255 个芯片 0.2ms

KEY: a - modulation-demodulation mode  
b - PN code rate c - PN code duration  
d - 1000 chips e - bit stationary at  
5kb/s f - expanded to 1.275Mb/s  
g - bit stationary of 500 chips  
h - expanded by 255 chips

the dual-reception system was adopted. At the mobile station, besides receiving the system data as well as the return signals from the intermediate-frequency band and the fundamental frequency band with functions that differ from those of the fixed station, but the configuration is basically the same as the fixed station. Now, 1000 of the 1023 chips of the PN code are used in ranging to send the ranging signal. The modulation and demodulation mode is QPSK [quadrature phase-shift keying] of 24kB/s.

In the I.Q channel, the Q channel is the ranging channel, and the I channel is the data communication channel. So the I channel executes data communication of 24kB/s for ranging through the delay locked loop. Synchronism of the received signal is maintained. The DLL began a matched mode pulse detector MPD of a

digital correlator. Thus, a high rate can be realized at the

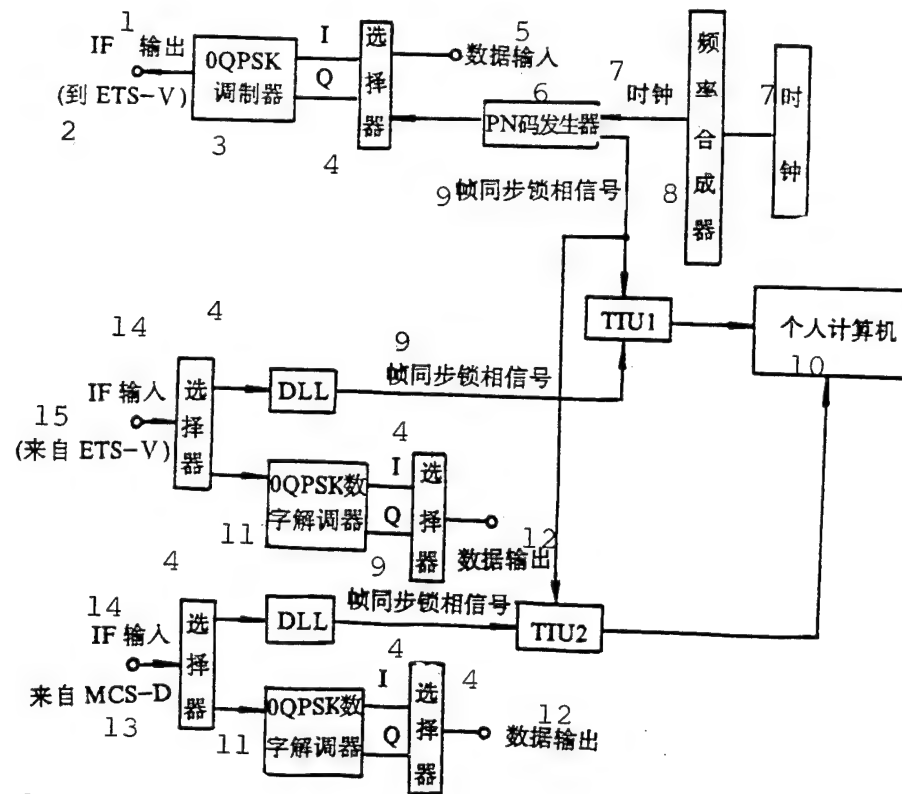


Fig. 3. Block diagram of location positioning terminal in fixed station (SCPC mode)

KEY: 1 - IF output 2 - (to ETS-V) 3 - modulator  
 4 - selector 5 - data input 6 - PN code generator  
 7 - clock 8 - frequency synthesizer 9 - frame  
 synchronizer phase-locked signal 10 - personal  
 computer 11 - OQPSK digital demodulator 12 - data  
 output 13 - from MCS-D 14 - IF input 15 - from  
 ETS-V

beginning capture of the PN receiving signal. Also, to reduce the number of bits of the MPD correlator and to simplify the hardware structure, 31 receiving signal chips and at the receiving site were employed to accomplish the correlation check. Now, a threshold value determination is made with the correlator. When some chips (31) were used, it may be possible to have an unchecked correlation value (when the correlation value is lower than the threshold value for checking, this is a case of not

being checked), or checking mistakes (checking done on the correlation value higher than the threshold value, means that checking is not required), or a problem of mistaken checking.

Fig. 4 shows the probability of not checking and the probability of mistakes in checking from calculations.

From the calculation results in the figure, even if the bit error rate (BER) is  $1 \times 10^{-2}$ , only by appropriately selecting and determining the threshold value can the probability of not requiring checking and the mistaken rate of checking be controlled to within a very low range.

In the time surveying unit (TIU), when the sending frame pulse is considered as the start of count signal for beginning the count, this is synchronized with the receiving PN signal. When the frame pulse of the PN code generator in DLL is used as the end-of-count signal, the counter is used to determine the time delay, and a personal computer serves in processing the time delay, thus determining in order to calculate the mobile station's position.

## 2.2. SS mode

Fig. 5 is a block diagram showing the SS mode fixed station operating in the IF mode. To enable the fixed station to simultaneously receive signals transmitted from two geostationary satellites, two receiving systems should be set up. In addition to different numbers of receiving systems, as well as the

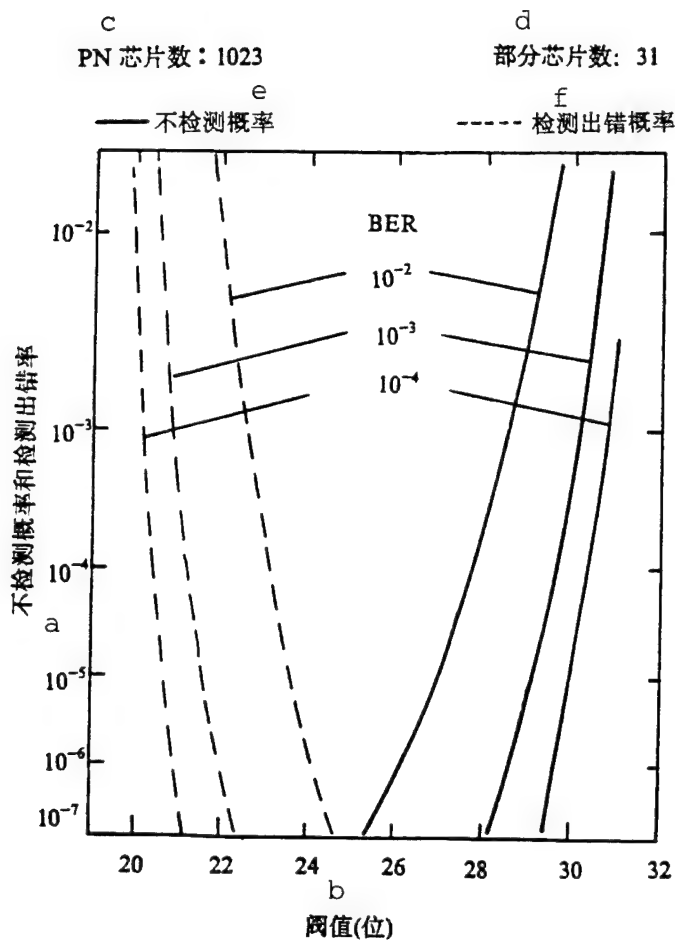


Fig. 4. Detected and undetected-error probabilities of matched clocks during partial correlations  
 KEY: a - undetected and detected-error probabilities  
 b - threshold value (in bits) c - number of PN chips (1023) d - number of some of the chips (31)  
 e - undetected-error probability f - detected-error probability

returning functions of the intermediate and fundamental frequency bands in the mobile station as differing from those of the fixed station, all the basic structures of the mobile station are the same as in the fixed stations. By using PN code of 1.275MHz in frequency to extend the signal of the 5kb/s fundamental band, the signal is transmitted after demodulated with BPSK [binary phase-shift keying] control. Especially, the mobile station employs

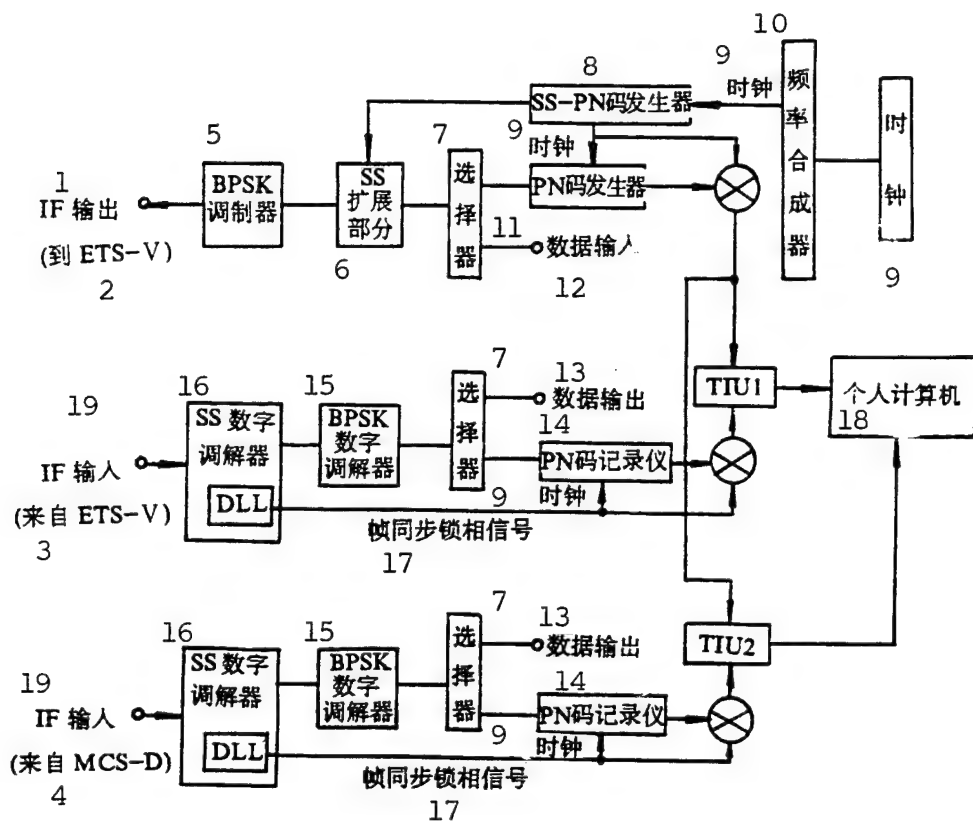


Fig. 5. Structure of communication positioning terminals in fixed station (SS mode)

KEY: 1 - IF output 2 - ETS-V 3 - from ETS-V  
 4 - from MCS-D 5 - BPSK modulator 6 - expansion portion of SS  
 7 - selector 8 - SS-PN code generator 9 - clock 10 - frequency synthesizer  
 11 - PN code generator 12 - data input 13 - data output 14 - PN code recorder 15 - BPSK digital modulator 16 - SS digital modulator 17 - frame synchronizing phase-locked signals 18 - personal computer 19 - IF input

the nonlinear C-category amplifier as the high-frequency amplifier of the transmission system, generally the conventional BPSK mode is applied. Therefore, the post-amplification frequency band is expanded. To avoid this situation, the frequency band is controlled within a limited range, and then the fixed envelope line type BPSK modulation method is adopted. For frequency expansion, the PN code employs 255 chips with 0.2ms as

the frame duration. Since the delay time with satellite transmission also varies with the frame amplitude of the PN code for frequency expansion, the longer the frame, the longer is the delay time. Thus, instability will occur when determining the time delay. To prevent this from happening, it is necessary to adopt the instability cancellation. The fundamental band signal of the frame amplitude is processed with the PN code with bit fixing. After cancelling the uncertainty of the receiving side, data or voice can be sent to replace this bit stationary PN code. At the receiving site, measurements can be made on the time delay between the transmitted signal and the received signal of the bit stationary PN code, as well as the transmission signal and received signal of the PN code for frequency expansion. These time delay determinations can be processed with a personal computer to calculate the mobile station positions.

#### IV. Distribution of Surveying Accuracy

##### 1. Ranging accuracy

Consideration should be given to ranging error, as coming from varying radio wave propagation routes due to refraction in the atmospheric and ionospheric layers, and the error due to varying electronic properties of the equipment. The article considers only the errors due to the equipment proper and due to varying electronic properties. The key problem of the experimental installation of the system is the phase-jitter problem due to DLL input noise used for tracking-ranging.

In the SCPC mode, the synchronizing DLL is applied. In the SS mode, the nonsynchronizing mode DAL is employed. The relationship between the deviation from the phase-jitter standard and the input noise is given by the following equations:

$$\frac{\delta}{f_0} = \sqrt{\frac{B_L N_0}{2P}} \quad (SCPC\text{方式})^1$$

$$\frac{\delta}{f_0} = \sqrt{\frac{B_L N_0}{2P} \left(1 + \frac{BN_0}{P}\right)} \quad (SS\text{方式})^2$$

KEY: 1 - (SCPC mode) 2 - (SS mode)

$\Delta y$  = deviation from phase-jitter standard

$f_0$  = clock pulse frequency of ranging signal

$B_L$  = DLL-equivalent frequency bandwidth of environmental noise

$N_0$  = noise power density

$P$  = signal power

$B$  = BPF frequency band.

Fig. 6 gives the calculation results. The abscissa is the  $C/N_0$  (signal power/noise power density) at the DLL input terminal. The values on the right side of the ordinate are the standard deviations of the ranging error obtained based on phase-jitter standard deviation. Table 2 values were calculated from the C/L and C/C circuits of the ETS-V, and the L/C circuits--from MCS-D. The experimental circuit predicts the  $C/N_0$  value. However, the circuit design has a prerequisite condition that the

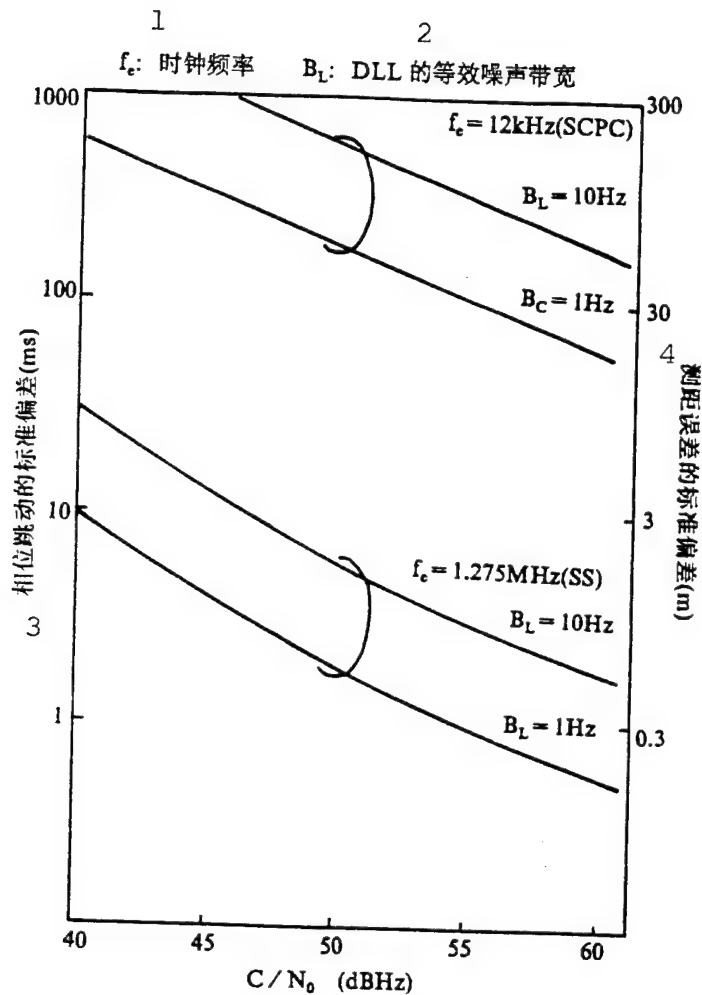


Fig. 6. Received  $C/N_0$  and phase error (ranging accuracy of DLL)  
 KEY: 1 - clock frequency 2 - equivalent noise bandwidth of DLL 3 - standard deviation (ms) of phase jitter 4 - standard deviation (m) of ranging error

mobile station antenna is a 40-cm diameter, short reflector antenna (SBF) used in ETS-V shipboard experiment. Also, during the shipboard experiment, since it cannot sufficiently ensure the space required for antenna installation, therefore the mobile station antenna should simultaneously track two satellites

TABLE 2. Examples of Circuit Design

1 C / L 线路(ETS-V)		6 SES 位置	7 N 鹿岛	8 N 中心	9 N 最差 <sup>(1)</sup>	8 S 中心	9 S 最差 <sup>(2)</sup>
上行链路 2	4 SES.HPA 发射(dBm)	42.0	←	←	←	←	←
	EIRP(dBm)	93.2	←	←	←	←	←
	5 传输损耗(dB)	199.6	←	←	←	←	←
	SAT G / T (dBk)	-8.1	←	←	←	←	←
	C / N <sub>0</sub> 上行链路(dBHz) 2	84.1	←	←	←	←	←
下行链路 3	SAT EIRP(dBm)	59.7	61.1	55.7	61.0	55.7	
	5 传输损耗(dB)	187.7	187.8	188.5	187.4	188.0	
	SES G / T <sup>(3)</sup> (dBk)	-15.2	←	-15.5	-15.2	←	
	C / N <sub>0</sub> 下行链路(dBHz) 3	55.4	56.7	50.3	57.0	51.1	
C / N <sub>0</sub> 总计(dBHz) 10		55.4	56.7	50.3	57.0	51.1	
L / C 线路(ETS-V) 1		6 SES 位置	7 N 鹿岛	8 N 中心	9 N 最差 <sup>(1)</sup>	8 S 中心	9 S 最差 <sup>(2)</sup>
上行链路 2	4 SES.HPA 发射(dBm)	48.5	←	←	←	←	←
	EIRP <sup>(3)</sup> (dBm)	55.2	←	←	←	←	←
	5 传输损耗(dB)	188.3	188.3	189.0	188.0	188.4	
	SAT G / T (dBk)	-4.5	-2.8	-8.6	-3.9	-9.7	
	C / N <sub>0</sub> 上行链路(dBHz) 2	61.0	62.7	56.2	61.9	56.1	
下行链路 3	SAT EIRP(dBm)	32.9	34.6	28.1	34.1	28.2	
	5 传输损耗(dB)	198.4	←	←	←	←	
	SES G / T <sup>(3)</sup> (dBk)	32.7	←	←	←	←	
	C / N <sub>0</sub> 下行链路(dBHz) 3	60.4	62.1	55.6	61.6	55.7	
C / N <sub>0</sub> 总计(dBHz) 10		57.1	59.4	52.9	58.7	52.9	

TABLE 2 [concluded]

L / C 线路(搭载 MCS-D)		SES 位置 6	波束中心 7	鹿岛 11	12 仰角 10°
上行链路 2		4 SES.HPA 发射(dBm)	48.5	←	←
		EIRP <sup>(1)</sup> (dBm)	55.2	←	←
		5 传输损耗(dB)	188.0	188.3	189.1
		SAT G / A (dBk)	-12.7	-14.3	-14.9
		C / N <sub>0</sub> 上行链路(dBHz) 2	53.1	51.2	49.8
下行链路 3		SAT EIRP(dBm)	22.8	20.9	19.5
		5 传输损耗(dB)	197.0	←	←
		SES G / T <sup>(3)</sup> (dBk)	30.0	←	←
		C / N <sub>0</sub> 下行链路(dBHz) 3	54.4	52.5	51.1
C / N <sub>0</sub> 总计(dBHz)		10	50.7	48.8	47.7

(1) (38° N, 143.8° W)

(2) (17° S, 102.0° E)

(3) SES antenna, 40cmSBF (pointing to the center of  
the line connected the two satellites)

	gain	tracking loss	polarization loss
T <sub>X</sub>	15.2dB <sub>i</sub>	4.0dB	3.0dB
R <sub>X</sub>	14.7dB <sub>i</sub>	3.6dB	

(4) (0° N, 180° E.)

KEY: 1 - C/L circuit (ETS-V) 2 - uplink 3 - downlink  
 4 - sending 5 - transmission losses 6 - SES position  
 7 - Ludao [Chinese transliteration of Japanese place  
 name] 8 - center 9 - worse case 10 - total  
 11 - center of wave beam 12 - elevation angle  
 13 - L/C circuit (carrying MCS-D)

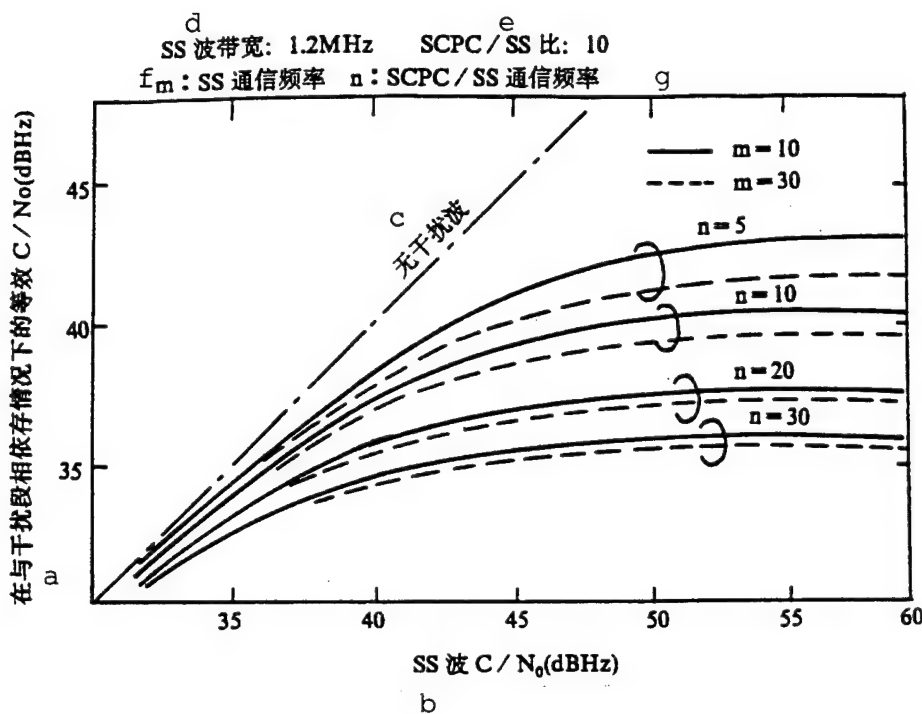


Fig. 7. Deterioration situation of  $C/N_0$  related to interference wave with SS mode  
 KEY: a - equivalent  $C/N_0$  (dBHz) related to interference segment  
 b - SS wave  $C/N_0$  (dBHz) c - without  
 interference wave d - bandwidth of SS wave: 1.2MHz  
 e - SCPC/SS ratio: 10 f - m:SS communication  
 frequency g - n: SCPC communication frequency

can be determined. When two geostationary satellites are used in positioning, the location of the moving object can be obtained from the point of intersection of two spheres with radius equal to the distance between the satellite and the moving object, and three spheres including the earth. Therefore, the positioning accuracy is limited by the ranging data accuracy and the satellite position accuracy.

Fig. 8 cites an example of the accuracy that can be obtained by two-satellite positioning with one satellite carrying the

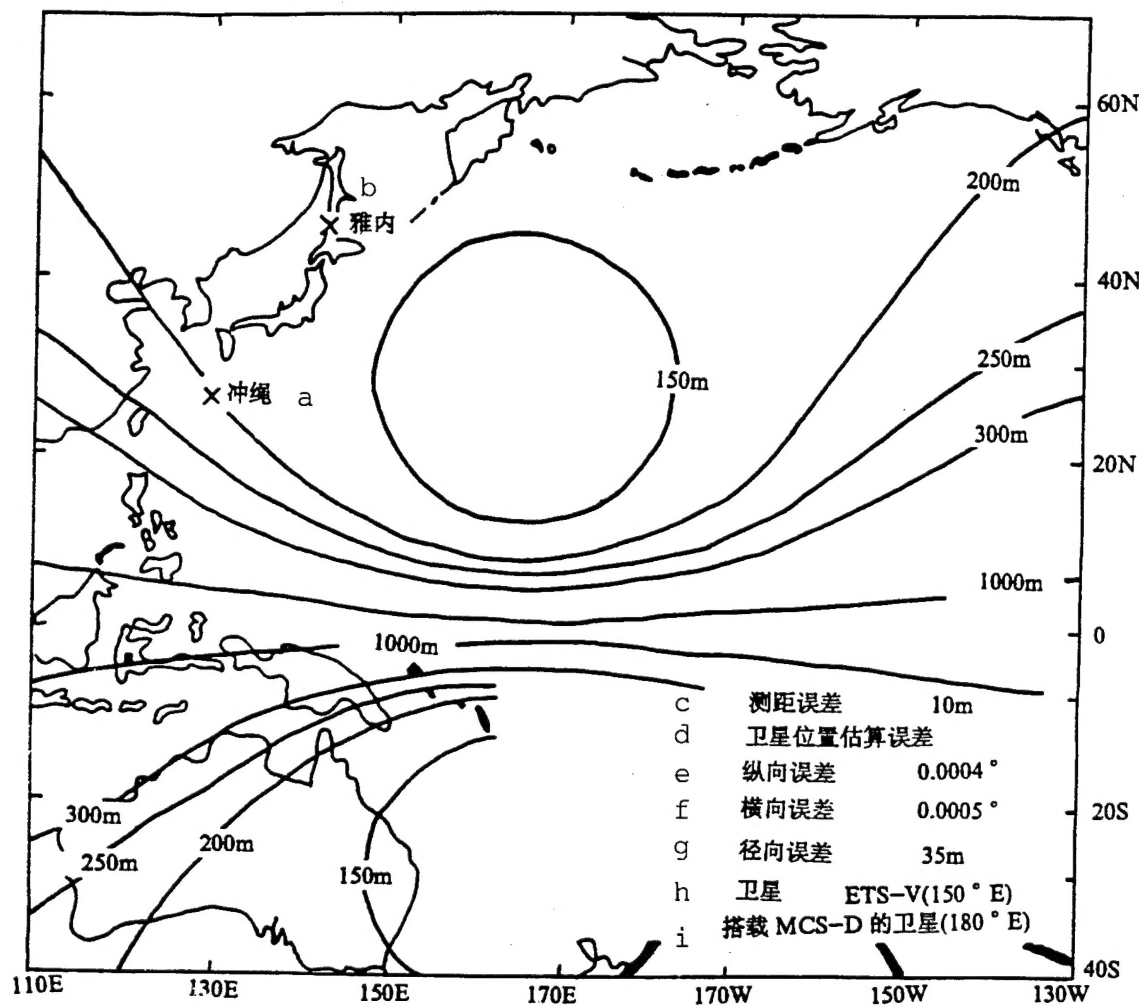


Fig. 8. Example of evaluation of positioning error

KEY: a - Okinawa    b - Yanei [Chinese transliteration of Japanese place name]    c - ranging error    d - error in estimating satellite position    e - error in longitudinal direction    f - error in latitudinal direction    g - diametral error    h - satellite    i - satellite carrying MCS-D

MCS-D, and the other satellite is the ETS-V satellite. In this

example, the positioning accuracy of the longitudinal direction is  $0.0004^{\circ}$ ; the accuracy in the latitudinal direction is  $0.0005^{\circ}$ ; the diametral positioning accuracy is 35m; and the ranging accuracy is 10m. The above-mentioned results are the absolute positioning accuracy not using the datum station with very high positioning accuracy. Additionally, for positioning using a datum station whose position is known, the error in position estimation of the mobile station should be subtracted from the absolute error of the datum station. Through the relative positioning, the ideal positioning accuracy can be obtained.

## V. Conclusions

The article briefly describes a communication and positioning experimental scheme based on two geostationary satellites. In 1989, development of the experimental equipment was basically accomplished through the maintenance and repair of the C-band receiver of the MCS-D circuits, and the positioning software. The formal experiments were conducted between the end of 1989 to 1990. There were two stages in the experiment. In the first stage, the mobile station and the fixed station were placed at the same location to determine and check the system delay, thus mastering the two functions of communication and ranging and their fundamental features. In the same stage, the mobile station was deployed at the correct position, in which ranging accuracy was evaluated. In the final stage, the mobile station was carried by ship and or vehicle for various experiments.

This article was translated from a Japanese journal,  
Quarterly Journal of Communication Integrated Research Institute,  
Vol. 36, No.1, 1990, pp. 119-126.

DISTRIBUTION LIST

---

DISTRIBUTION DIRECT TO RECIPIENT

---

ORGANIZATION	MICROFICHE
B085 DIA/RTS-2FI	1
C509 BALLOC509 BALLISTIC RES LAB	1
C510 R&T LABS/AVEADCOM	1
C513 ARRADCOM	1
C535 AVRADCOM/TSARCOM	1
C539 TRASANA	1
Q592 FSTC	4
Q619 MSIC REDSTONE	1
Q008 NTIC	1
Q043 AFMIC-IS	1
E404 AEDC/DOF	1
E410 AFDIC/IN	1
E429 SD/IND	1
P005 DOE/ISA/DDI	1
1051 AFIT/LDE	1
PO90 NSA/CDB	1

Microfiche Nbr: FTD95C000649  
NAIC-ID(RS)T-0326-95